ACAM Instrument Characterization and Trace Gas Retrievals

Xiong Liu[1], Matthew Kowalewski[2,3], Scott Janz[3], Cheng Liu[1], Pawan K. Bhartia[3], Nickolay Krotkov[3], Kelly Chance[1], Kenneth Pickering[3], James Crawford[4]

[1]Harvard-Smithsonian CFA [2]GESTAR [3]GSFC [4]LaRC

DISCOVER-AQ Science Team Meeting

February 15, 2012

Outline

- **Motivation**
- **Instrument characterization**
- **Trace gas retrievals**
- **Summary and future work**

Motivation

- **ACAM: UV/Visible spectrometers**
  - **304-520 nm at 0.8 nm FWHM, 460-900 nm at 1.5 nm FWHM**
  - **Nadir spatial resolution of ~1.5×0.75 km^2, zenith view**
- **Develop advanced operational algorithms for trace gases & aerosols from ACAM and similar airborne instruments**
  - **Radiative transfer models, ozone profiles/trace gas VCD, averaging kernels**
  - **Accurate characterization (wavelength and radiometric calibration, noise estimate, slit function) is more critical relative to typical DOAS methods**
  - **TOA solar irradiance reference would be very useful.**
- **A Surrogate for UV/Visible part of GEO-CAPE**
  - **Can ACAM trace gas measurements meet GEO-CAPE requirements?**
  - **How well can ACAM capture spatial temporal variation of trace gases?**
  - **Can we improve near-surface ozone retrievals from ACAM Chappuis bands?**
- **Work in progress about ACAM wavelength/slit function calibration and trace gas fittings from ACAM measurements**
  - **Use one day of ACAM data (July 21, 2011) to improve our understanding of instrument characterization and optimize retrieval algorithm**
  - **Use ACAM data without much spatial (step-pair) and spectral co-adding to explore ACAM's maximum capability.**

Wavelength/Slit Function Characterization

- **Satellite observation: cross-correlate high resolution solar Fraunhofer lines with TOA solar irradiance`**
- **Develop an improved algorithm for ACAM: derive slit function (Asymmetric Gaussian) & perform wavelength registration accounting for gas absorption and ring effect (critical for Huggins bands)**

$$Y(x) = \exp\left\{-\left[\frac{x}{hw1e \times \left(1 + asy \times sign(x)\right)}\right]^2\right\}$$

hw1e: half width at 1/e

asy: asymmetric factor

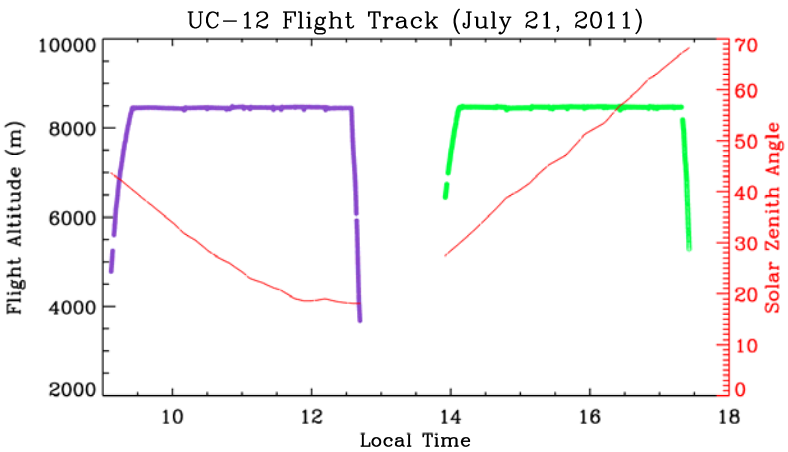

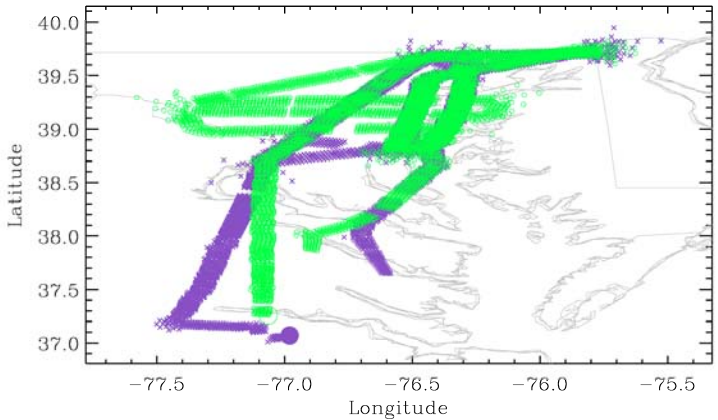

Wavelength/Slit Function Characterization

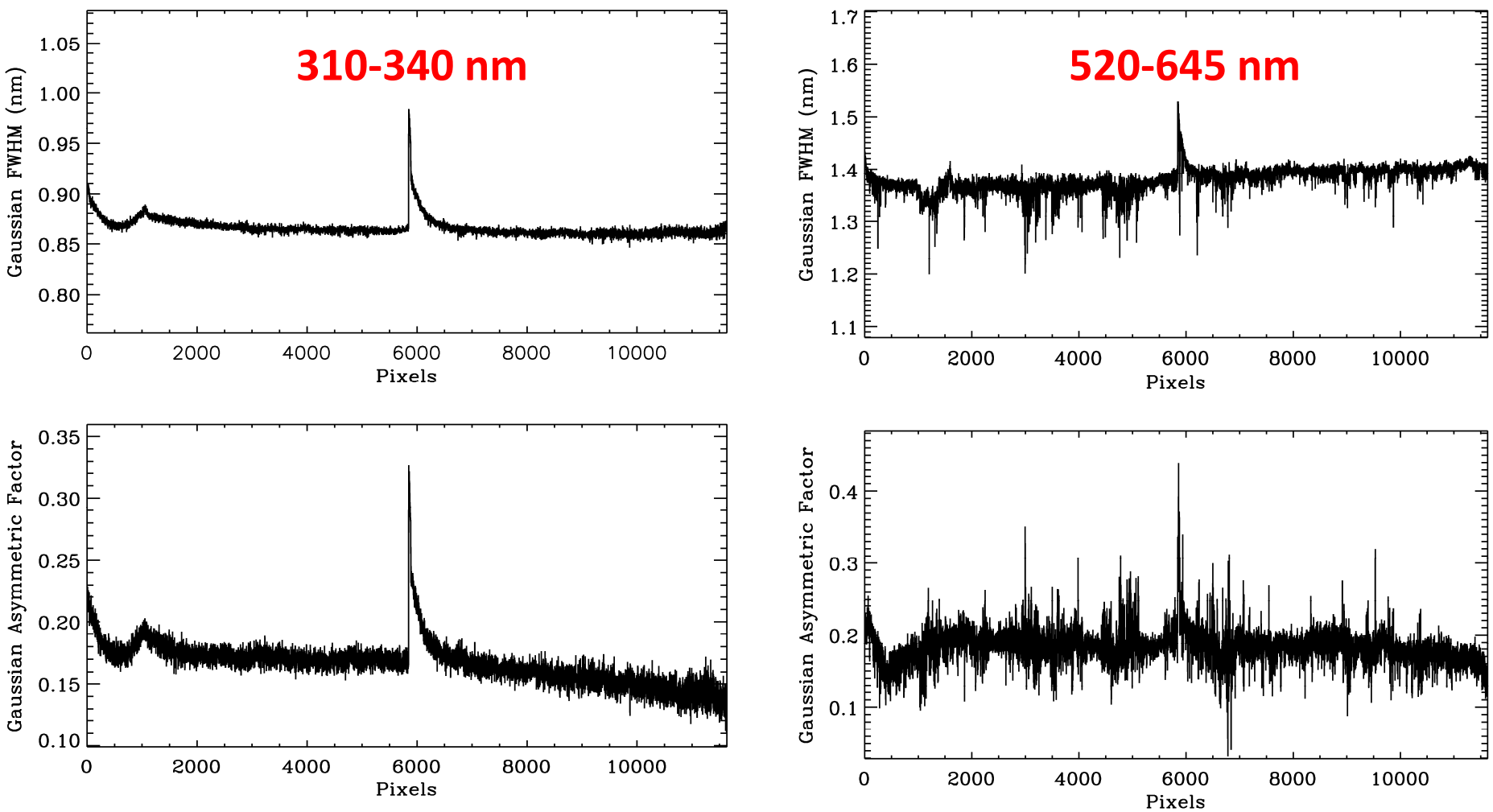

- **Instrument less stable during taking off especially in aq channel because temperature variation.**

SNR Characterization and Identification of Bad Pixels

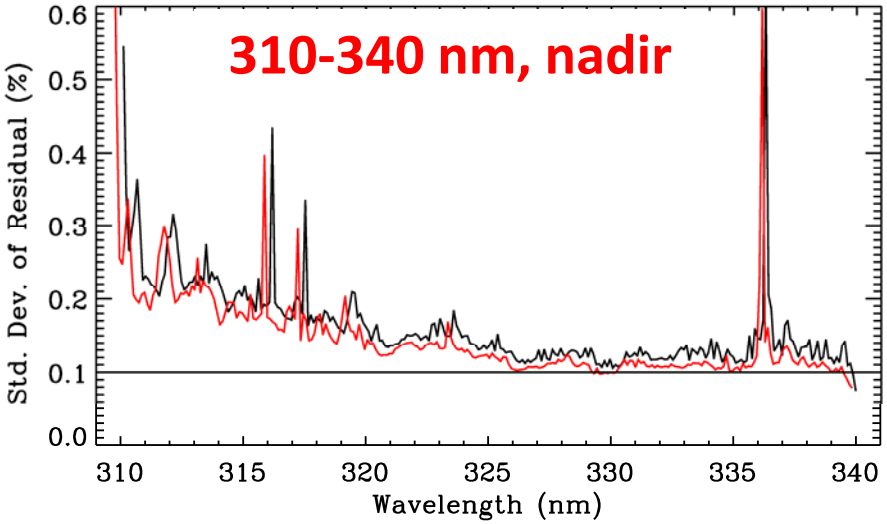

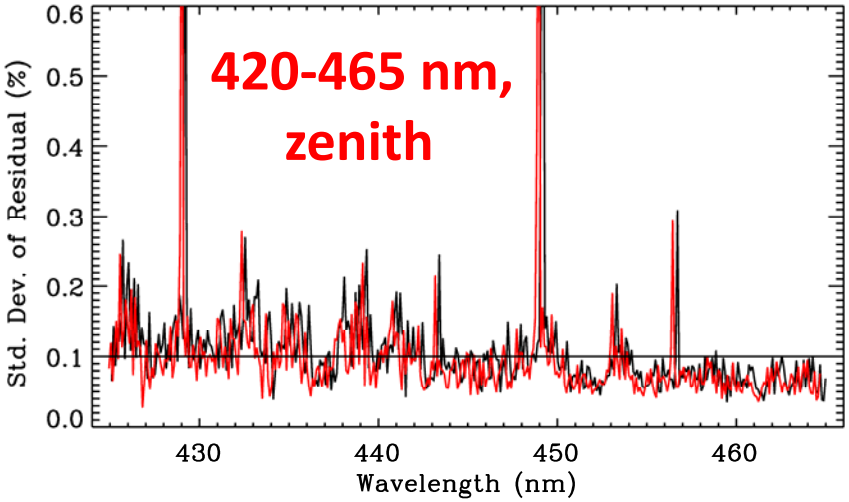

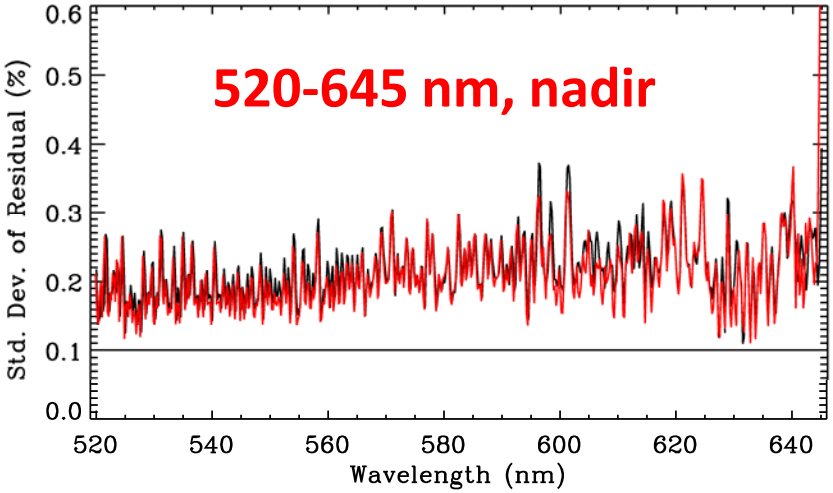

- **Standard deviation of fitting residuals indicates SNR**
  - **~1000 at 340 nm and in blue**
  - **~700 in visible**
  - **Note: ACAM has 8 pixels/FWHM**
- **Spikes in mean/std. dev. Of fitting residuals indicate problematic pixels in the spectrum**

Wavelength/Slit Function Characterization

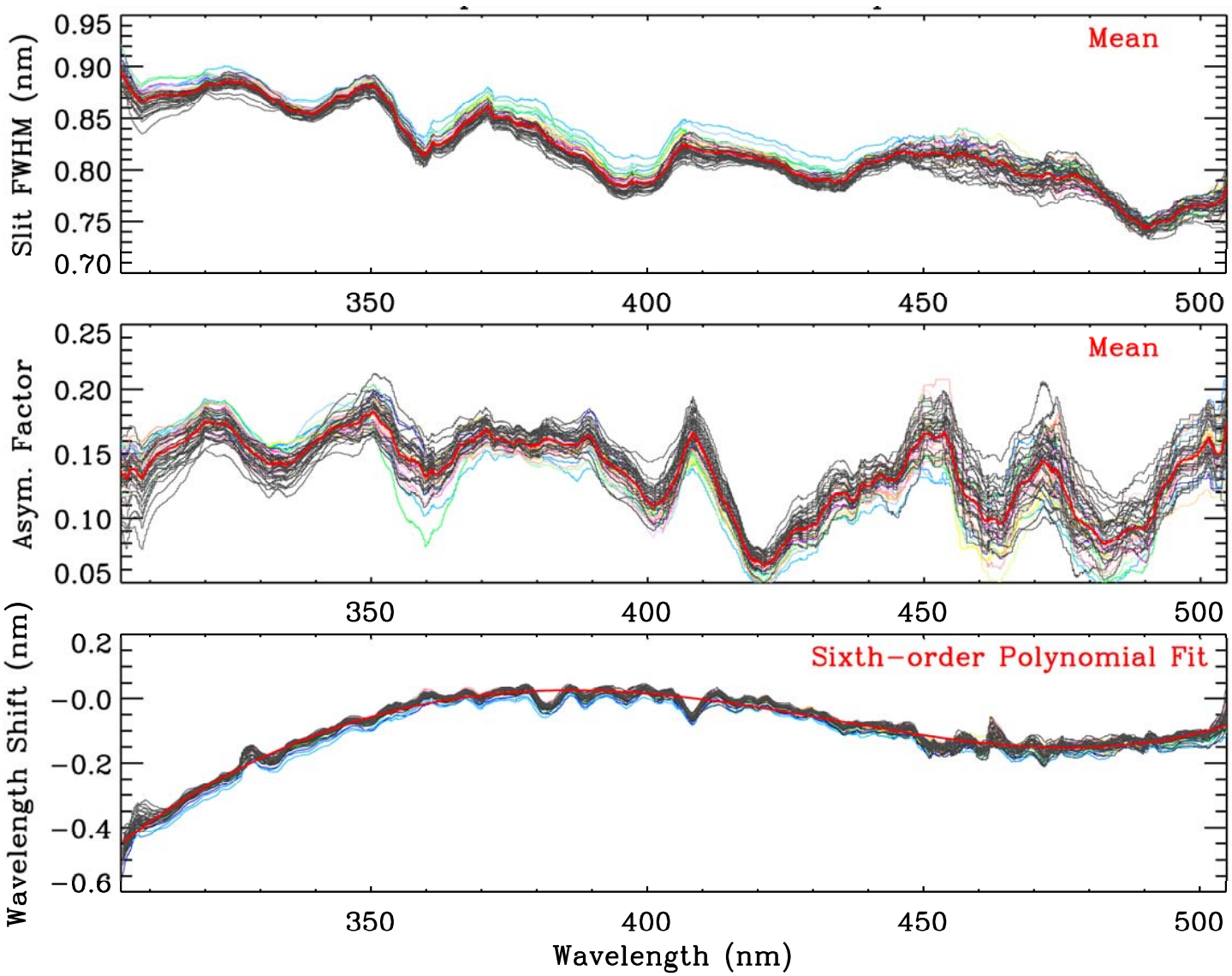

- **Wavelength dependent slit functions and shift in aq channel**

Preliminary Comparison with RTM Calculation

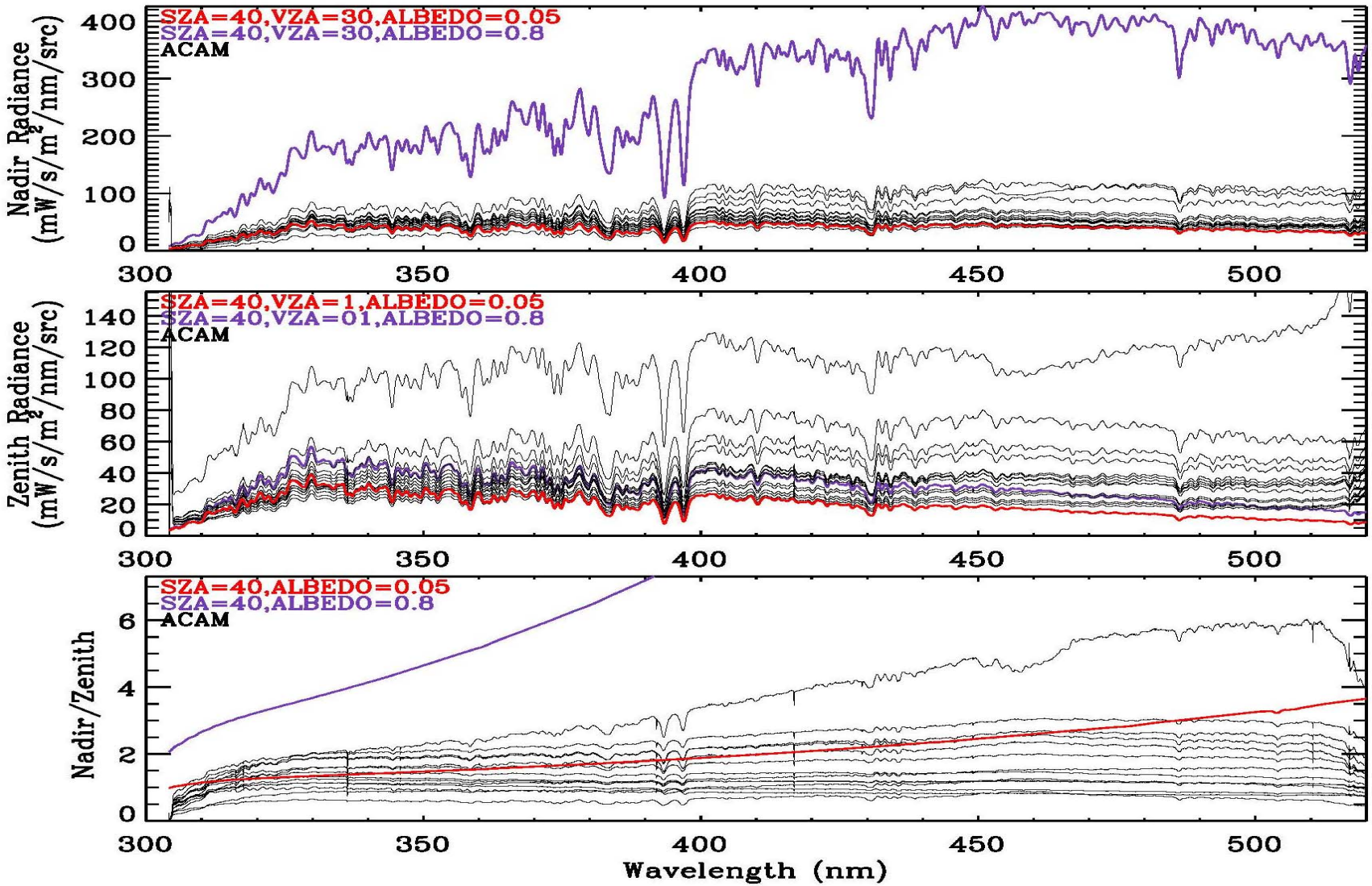

- **It is probably very important to include aerosols/clouds to simulate zenith-sky measurements.**

Preliminary Comparison with RTM Calculation

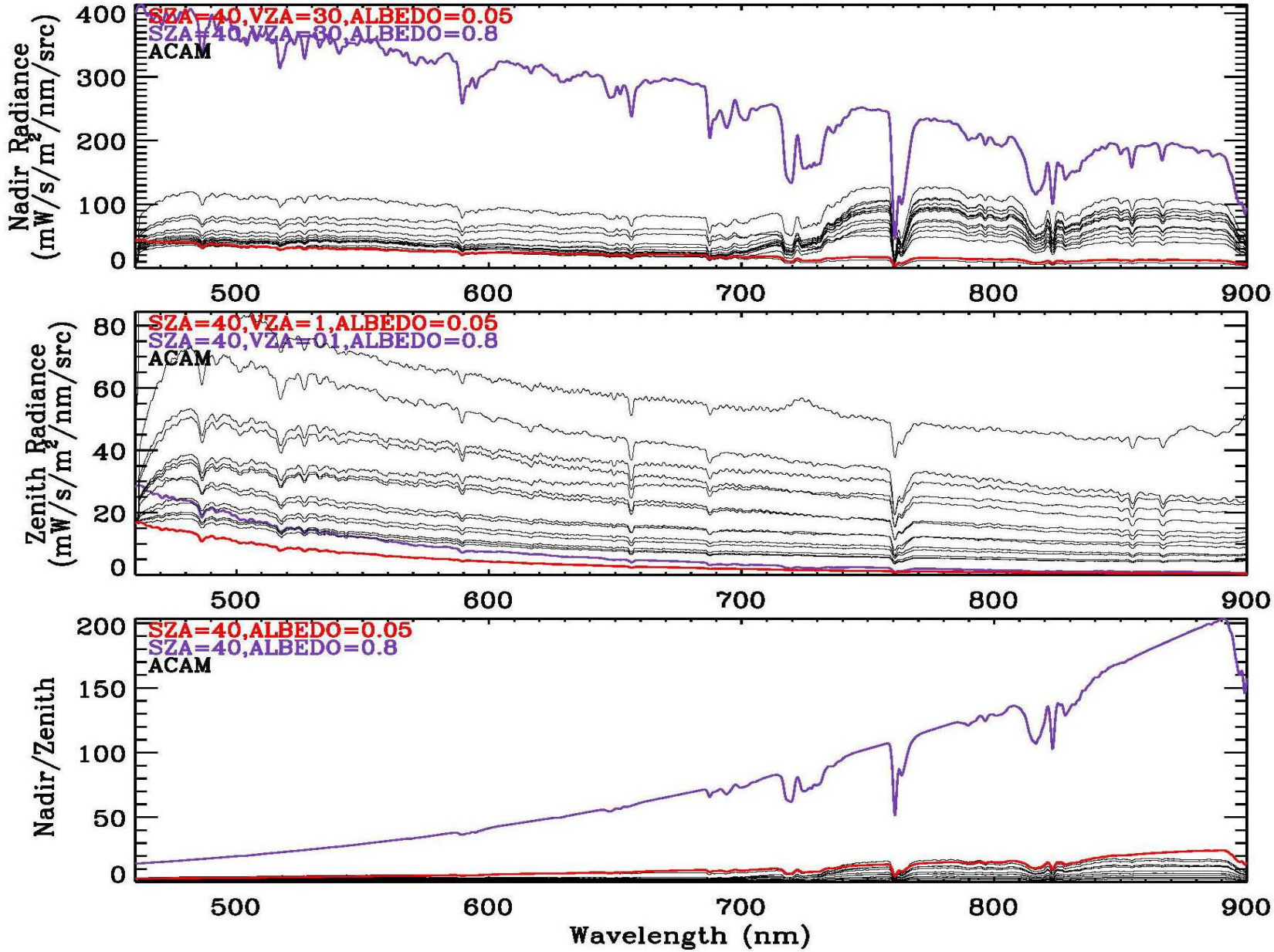

Derivation of TOA Solar Reference

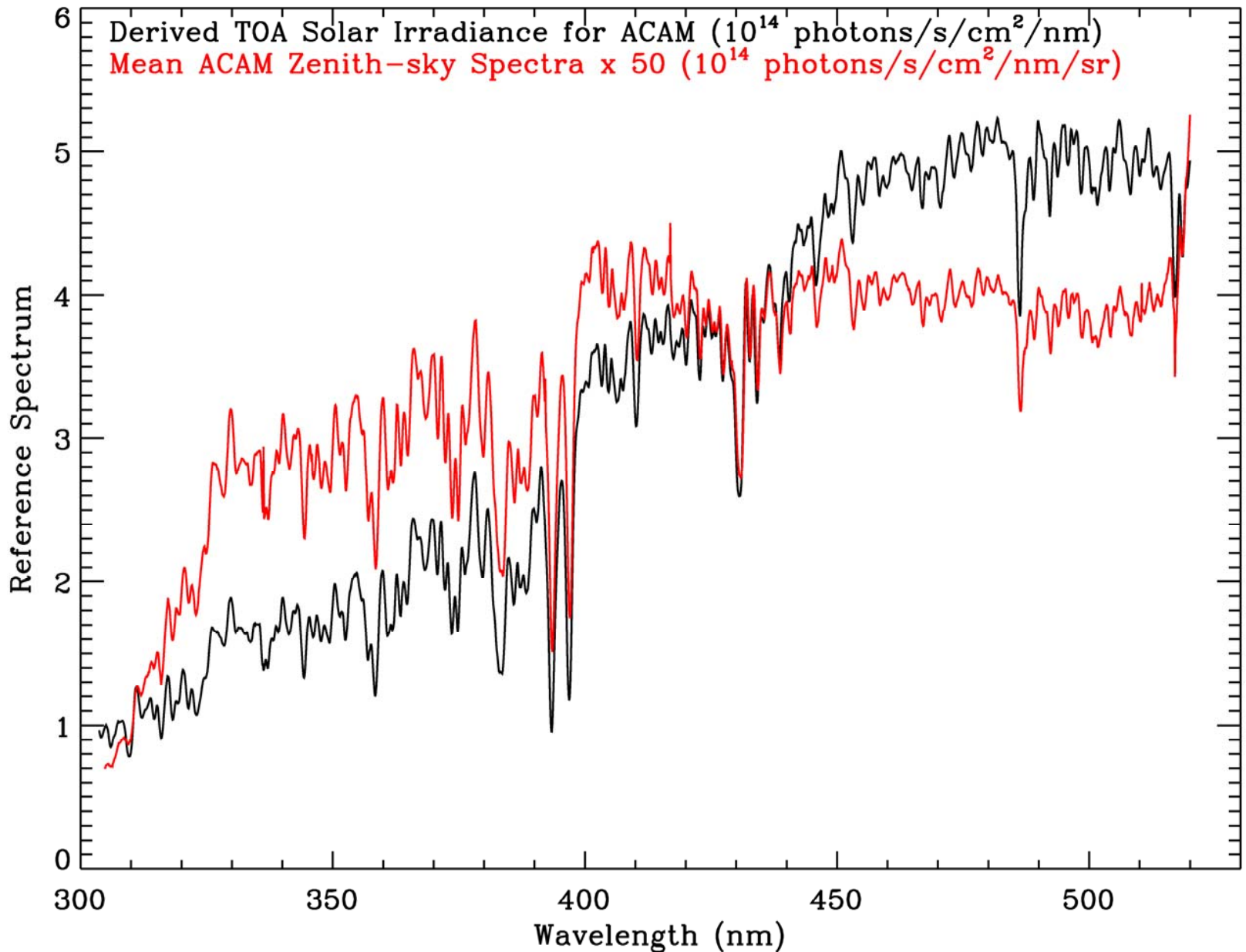

O_3 SCD Retrieval (318-335 nm)

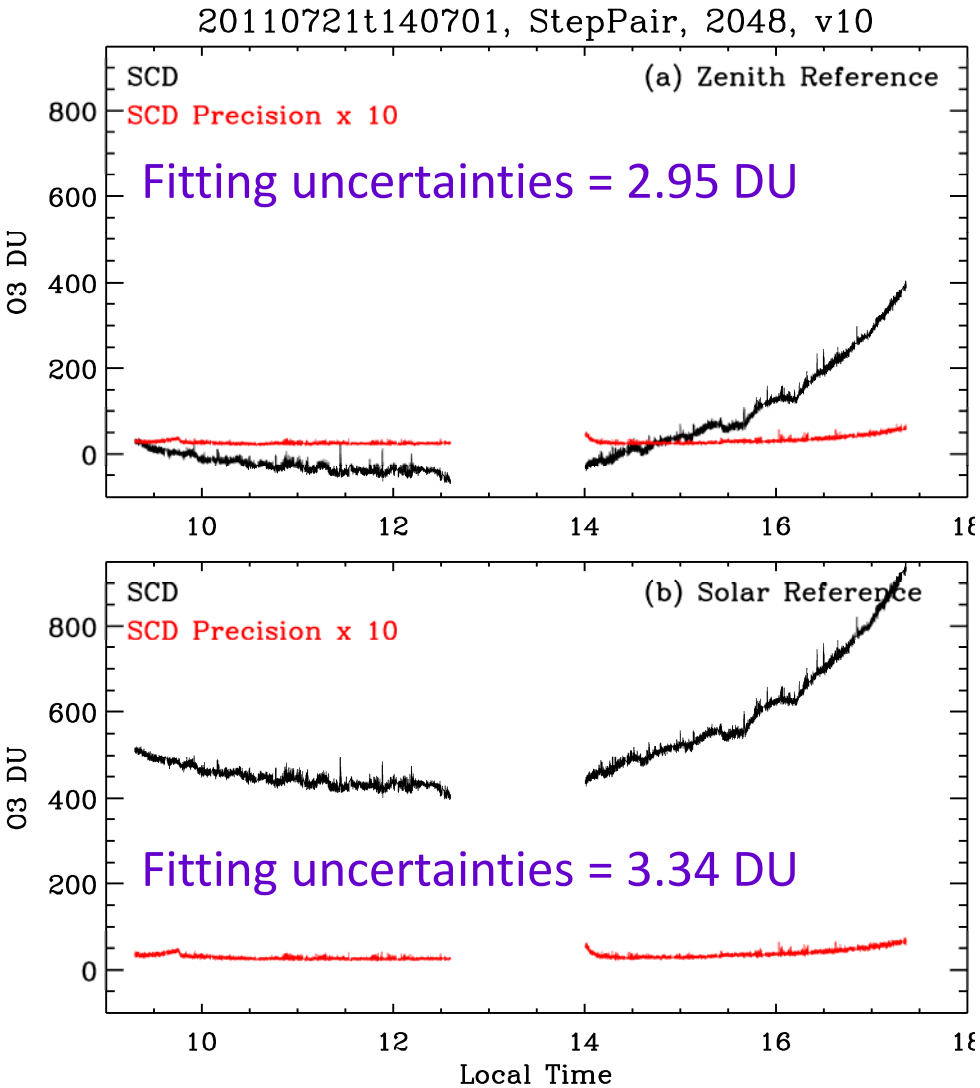

- **Both reference works**
- **Zenith ref. → relative SCD**
- **Solar ref. → absolute SCD, can be used for both nadir and zenith.**

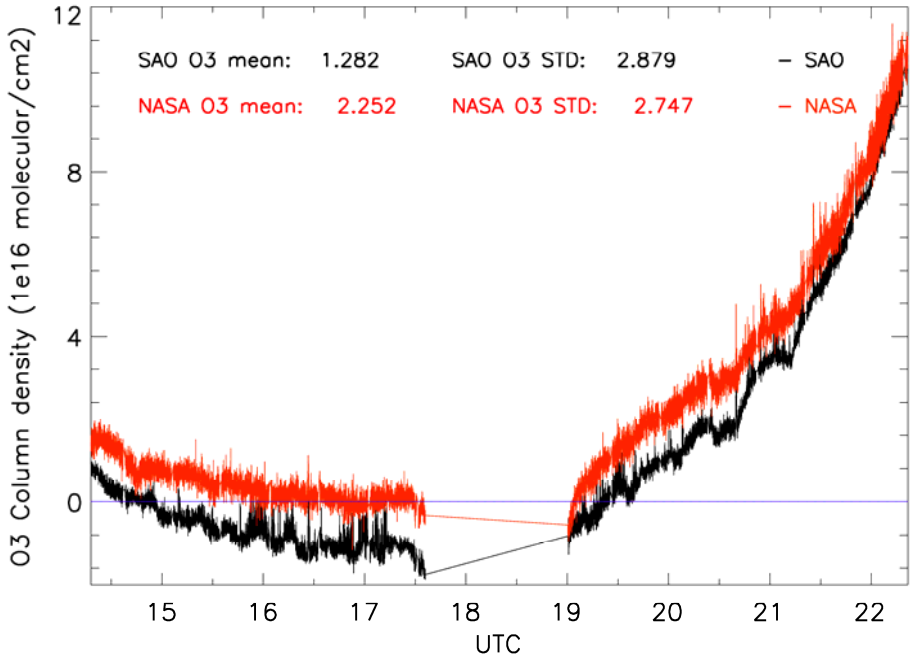

NO_2 SCD Retrieval (420-465 nm)

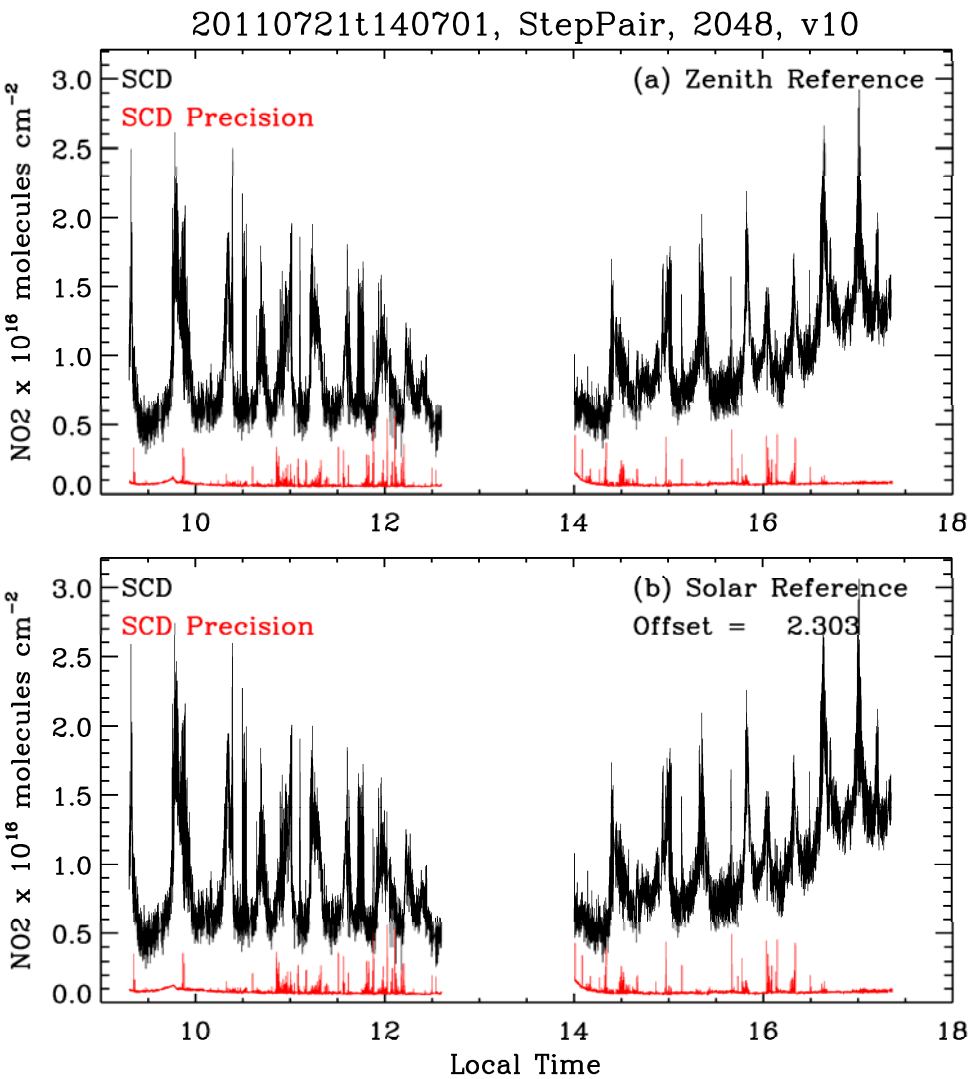

- **Both show similarly large spatiotemporal NO_2 variation.**
- **Fitting uncertainty: 7.4E14 molecules cm^{-2} for zenith ref. & 8.1E14 molecules cm^{-2} for solar ref.**
- **Solar reference produces a large systematic offset (can be removed).**

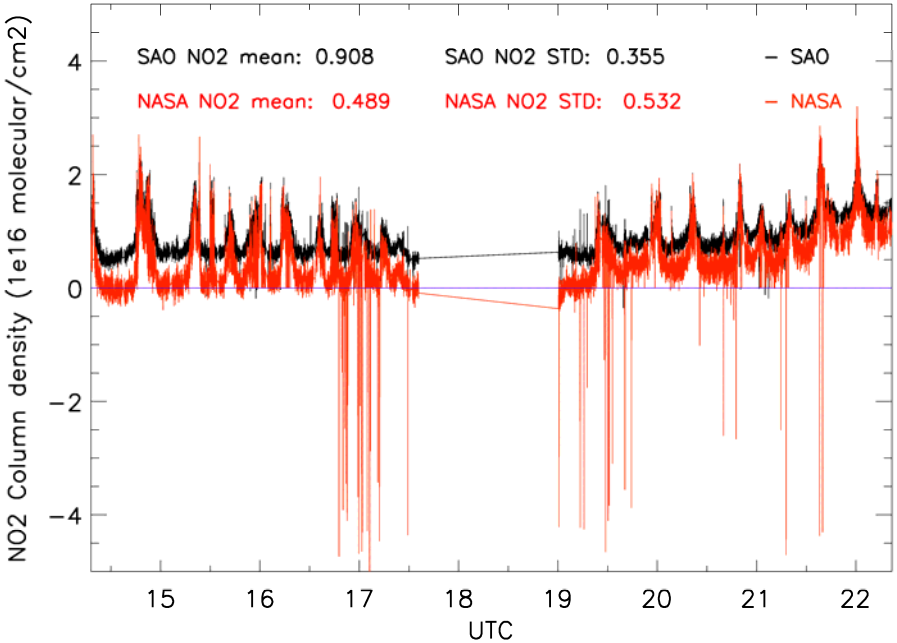

H_2O SCD Retrieval (420-465 nm)

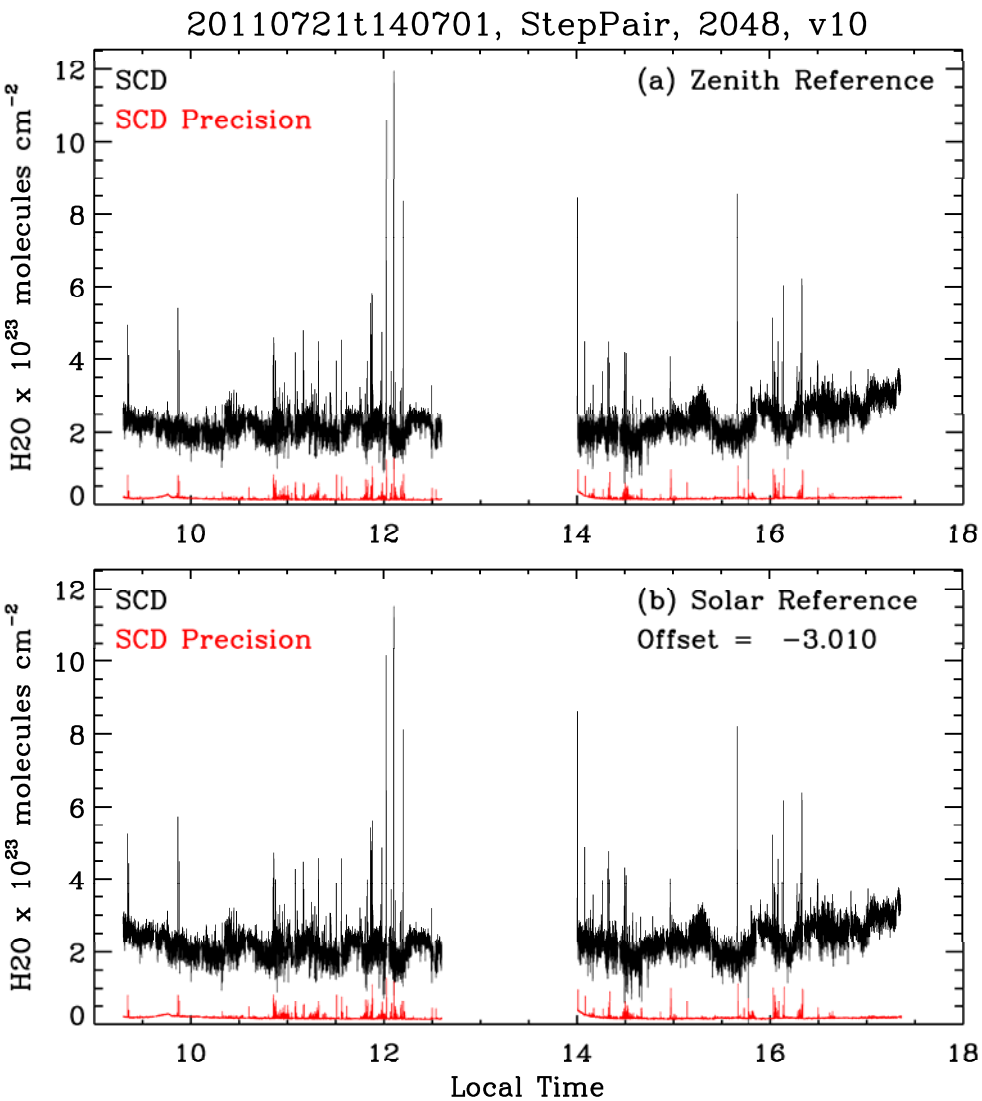

- **Both zenith and solar references show similar spatiotemporal variation**
- **Fitting uncertainty: 1.7E22 molecules cm^{-2} for zenith reference & 1.8E20 molecules cm^{-2} for solar reference**
- **Solar reference produces a large systematic offset**

HCHO SCD Retrieval (327-358 nm)

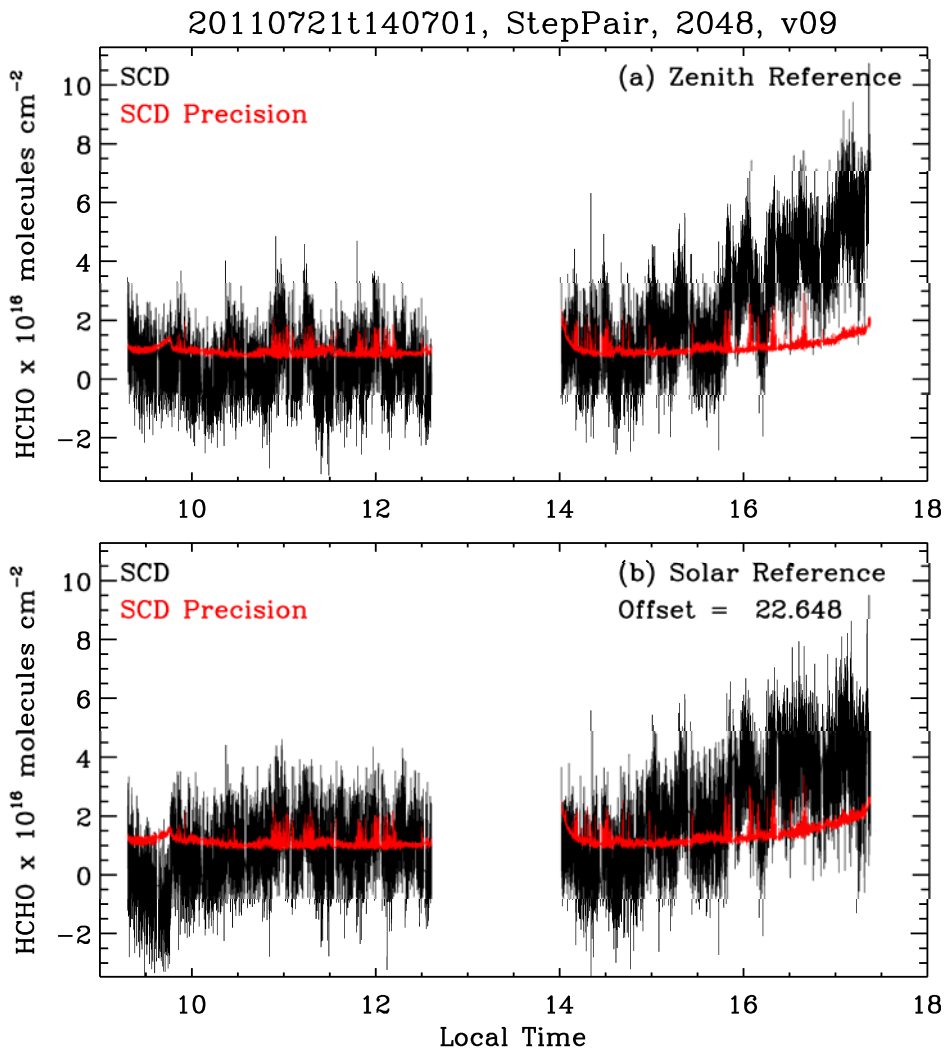

- **Relatively noise, can still clearly see spatiotemporal variation**
- **Zenith-sky reference less noisy.**
- **Uncertainty: 1.06E16 molecules cm^{-2} for zenith ref. & 1.27E16 molecules cm^{-2} for solar ref.**
- **Solar reference produces a large systematic offset.**

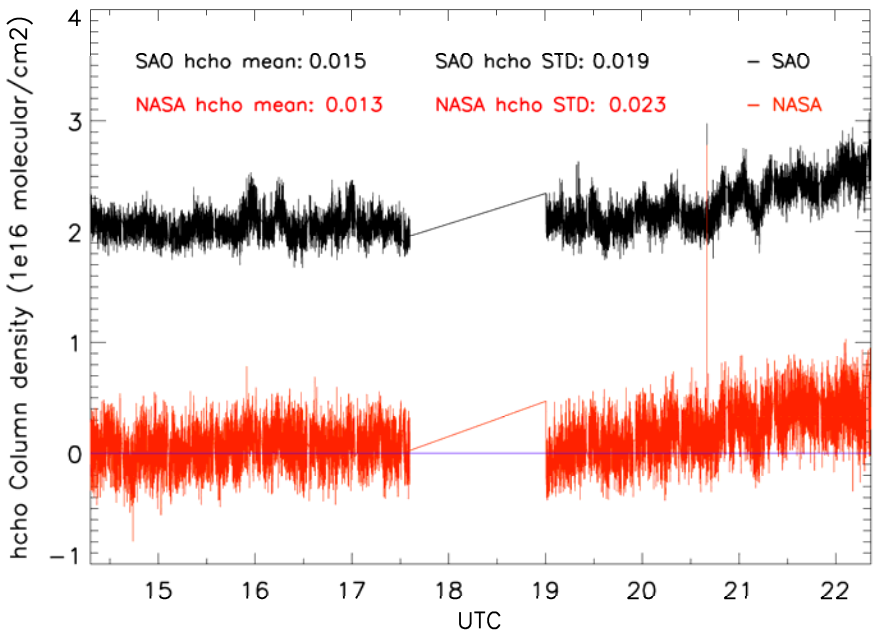

CHOCHO SCD Retrieval (433-462 nm)

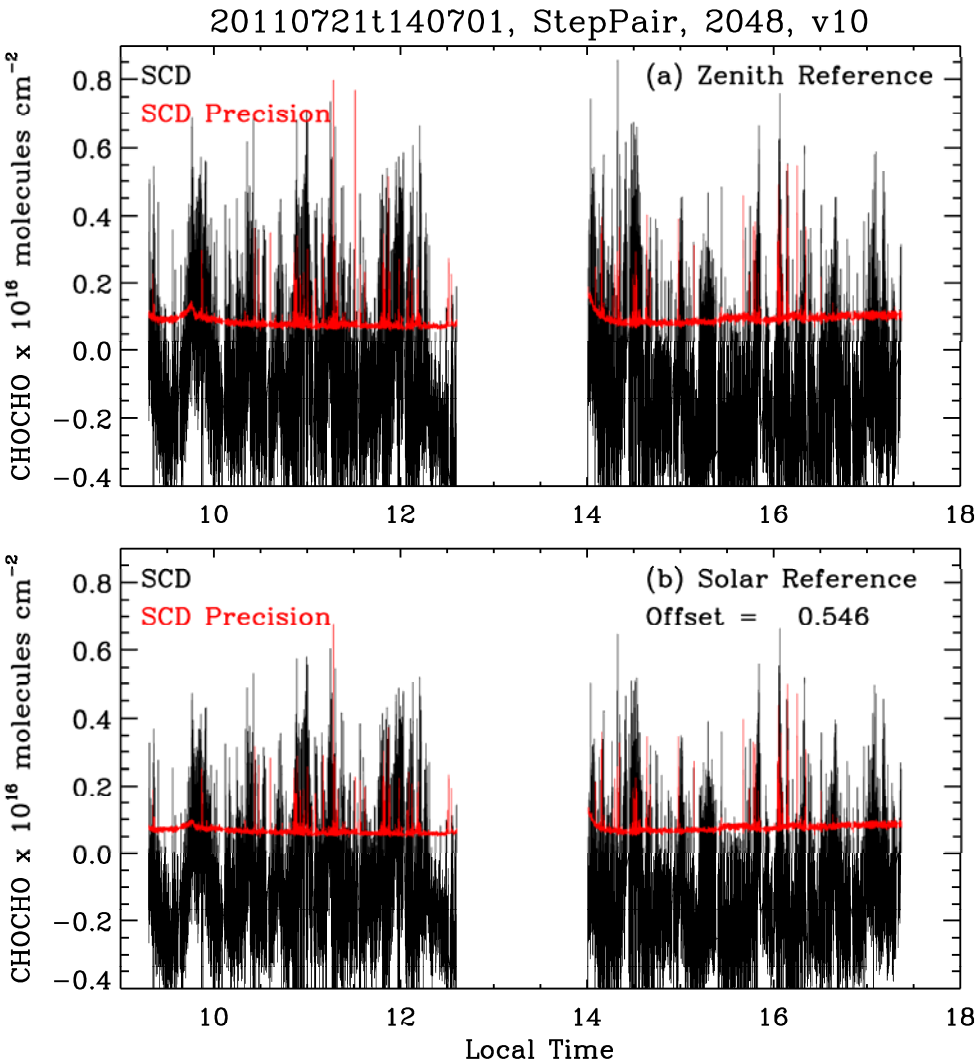

- **Relatively noise, can see clearly spatiotemporal variation**
- **Fitting uncertainty: 9.1E14 molecules cm^{-2} for zenith reference & 7.3E14 molecules cm^{-2} for solar reference**
- **Solar reference produces a large systematic offset.**

SO_2 SCD Retrieval (305-330 nm)

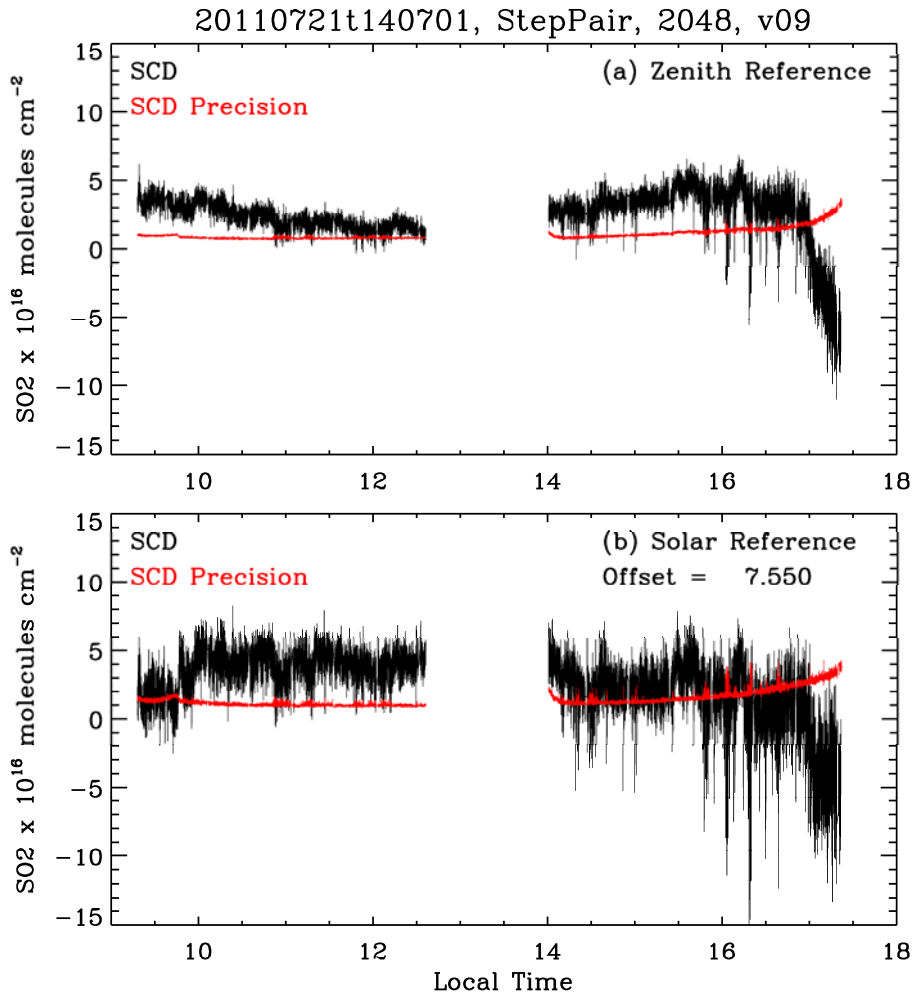

- Zenith and solar references show different patterns.
- Fitting uncertainty: 1.06E16 molecules cm^{-2} for zenith reference & 1.44 E16 molecules cm^{-2} for solar reference
- Solar reference produces a large systematic offset.

Summary

- **Develop alternative methods to perform wavelength and slit function calibration of ACAM measurements.**
- **Derive TOA solar irradiance using slit functions for trace gases retrievals**
- **Perform retrievals of SCDs for several trace gases (O_3, NO_2, H_2O, HCHO, CHOCHO, SO_2) with both zenith-sky and derived TOA solar irradiance.**
- **Retrievals of some species (NO_2, H_2O, HCHO, CHOCHO) seem to be capable of capturing spatiotemporal variation with fitting uncertainties that meet the GEO-CAPE requirements.**
- **The use of derived TOA solar irradiance work quite well for O_3, NO_2, H_2O, CHOCHO, although producing a systematic offset (can be removed).**

Future Work

- **Use collocated DISCOVER-AQ measurements of trace gases and aerosols to check the radiometric calibration of the ACAM instrument.**
- **Develop algorithms to retrieve VCDs of trace gases directly with on-line radiative transfer calculations, initially focusing on clear-sky conditions.**
- **Develop algorithms to retrieve ozone profiles (including aerosol index, first UV, then UV+Visible) with on-line radiative transfer calculations.**
- **Develop methods to account for clouds in the retrievals.**
- **Develop methods to retrieve/account for aerosols.**

How to prove our retrieval abilities for gases when particles modify the radiation field ?

An example of plots for choice

– O_3 profiles, clean and dirty,

– aerosol profiles, clean,

“dirty” – i.e., scattering, or somewhat absorbing

There was variation in scattering and some variation in absorbing particles in D-AQ measurements

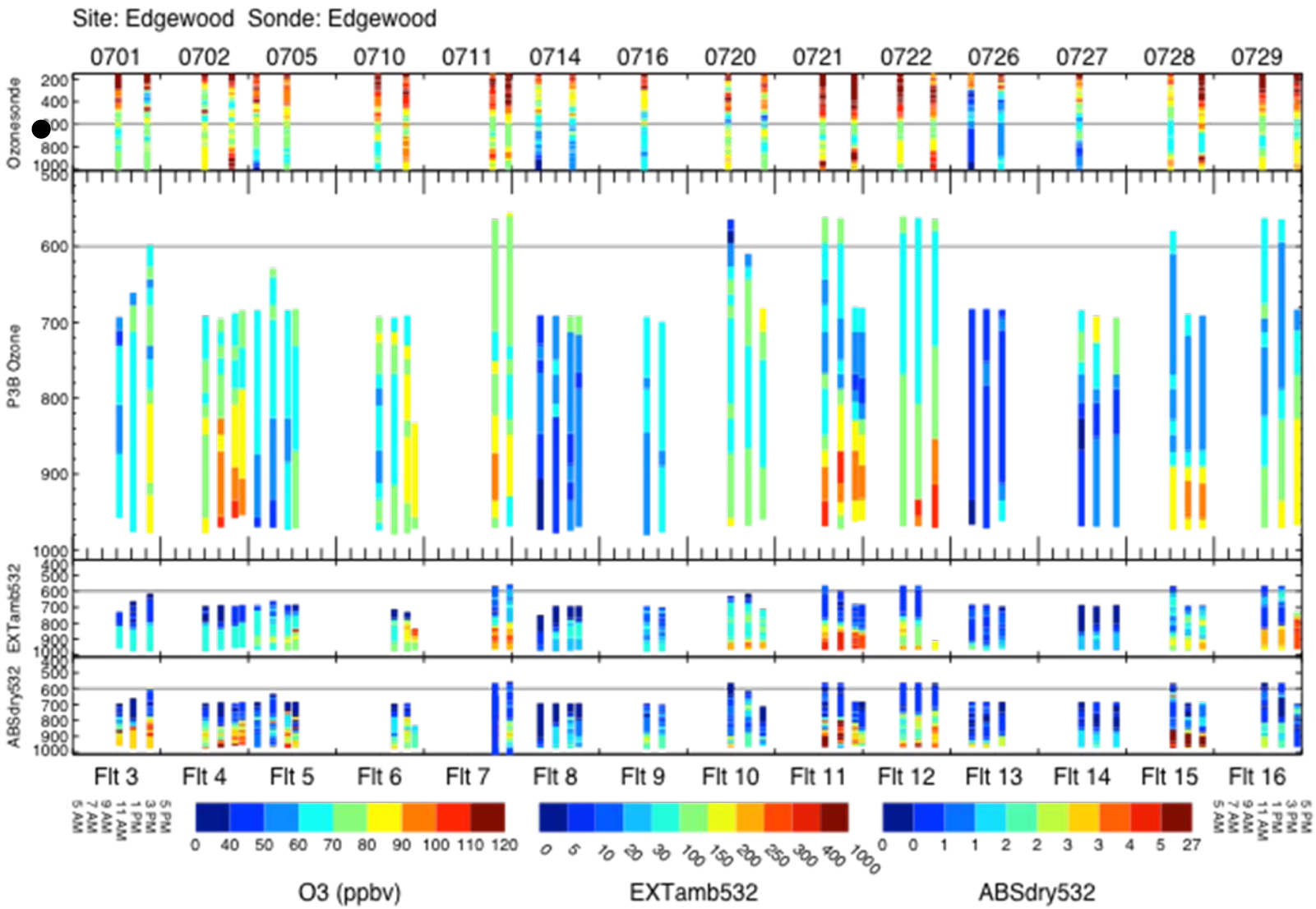

There was also a large variation in hygroscopicity in D-AQ measurements

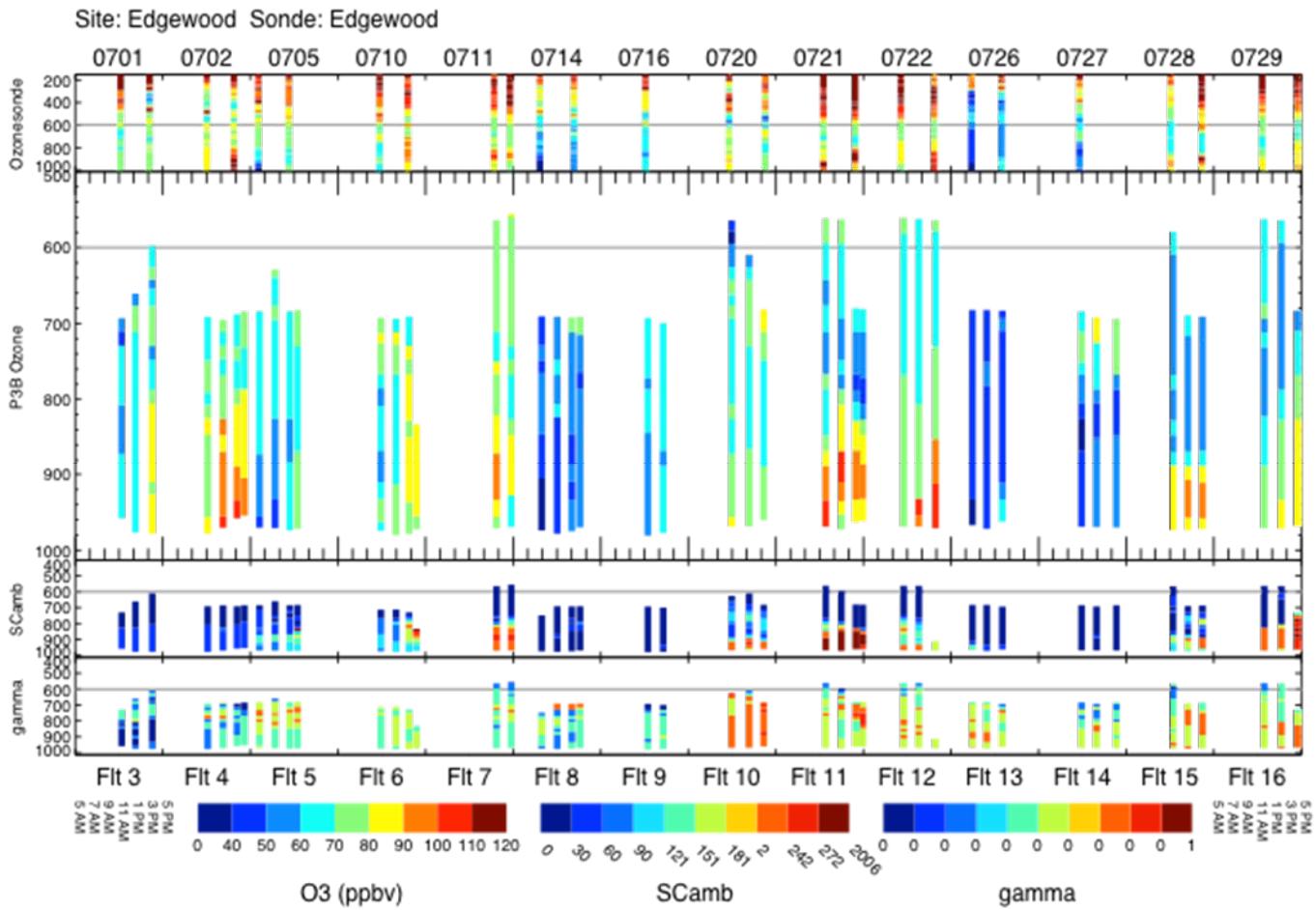

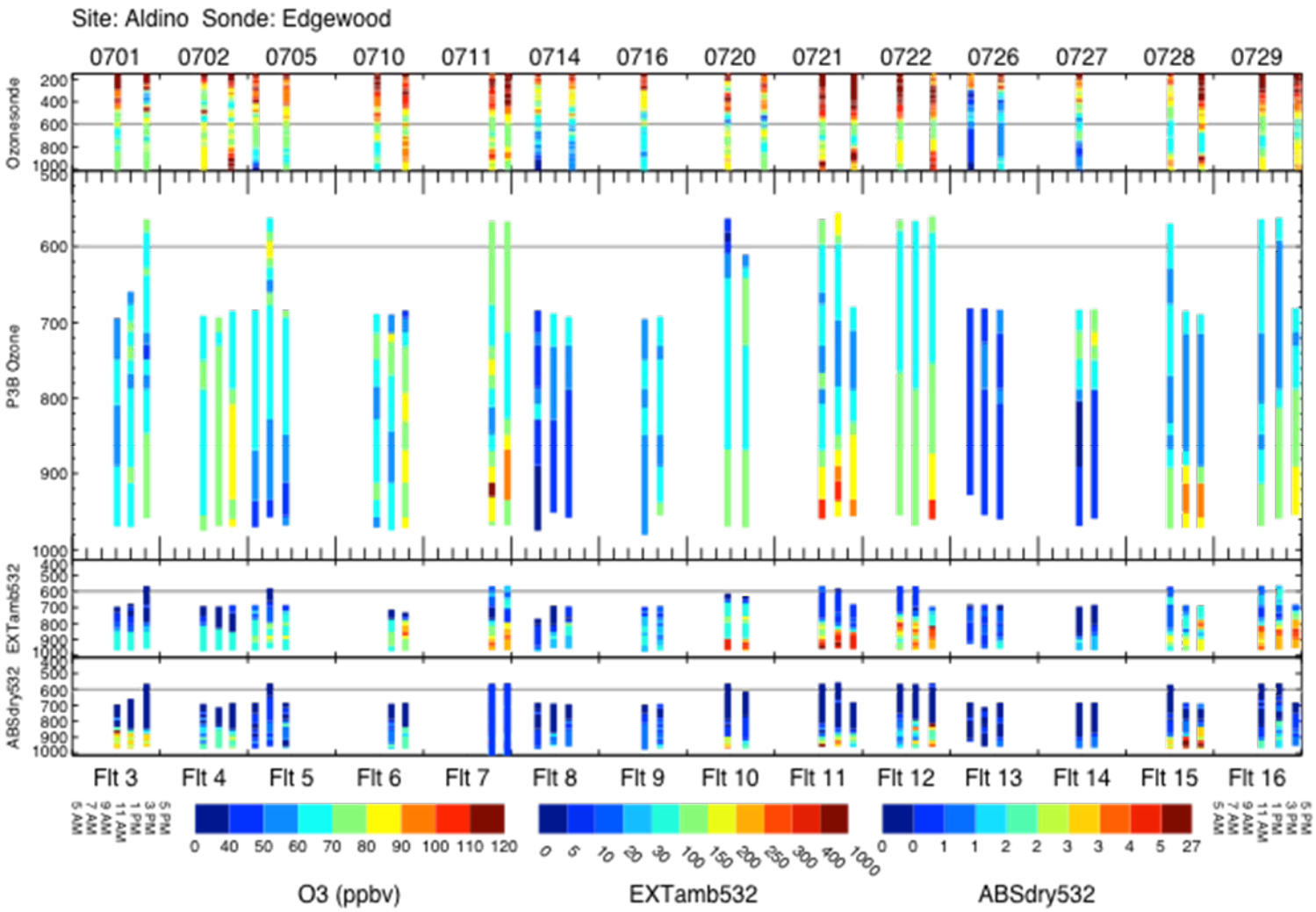
Site: Aldino Sonde: Edgewood
0701
0702
0705
0710
0711
0714
0716
0720
0721
0722
0726
0727
0728
0729
Ozonesonde
P3B Ozone
EXTamb532
ABSdry532
Flt 3
Flt 4
Flt 5
Flt 6
Flt 7
Flt 8
Flt 9
Flt 10
Flt 11
Flt 12
Flt 13
Flt 14
Flt 15
Flt 16
5 AM
7 AM
9 AM
11 AM
1 PM
3 PM
5 PM
0 40 50 60 70 80 90 100 110 120
O3 (ppbv)
0 5 10 20 30 100 150 200 250 300 400 1000
EXTamb532
0 0 1 1 2 2 3 3 4 5 27
ABSdry532

Sondes show much less O_3 variation above P-3 altitude

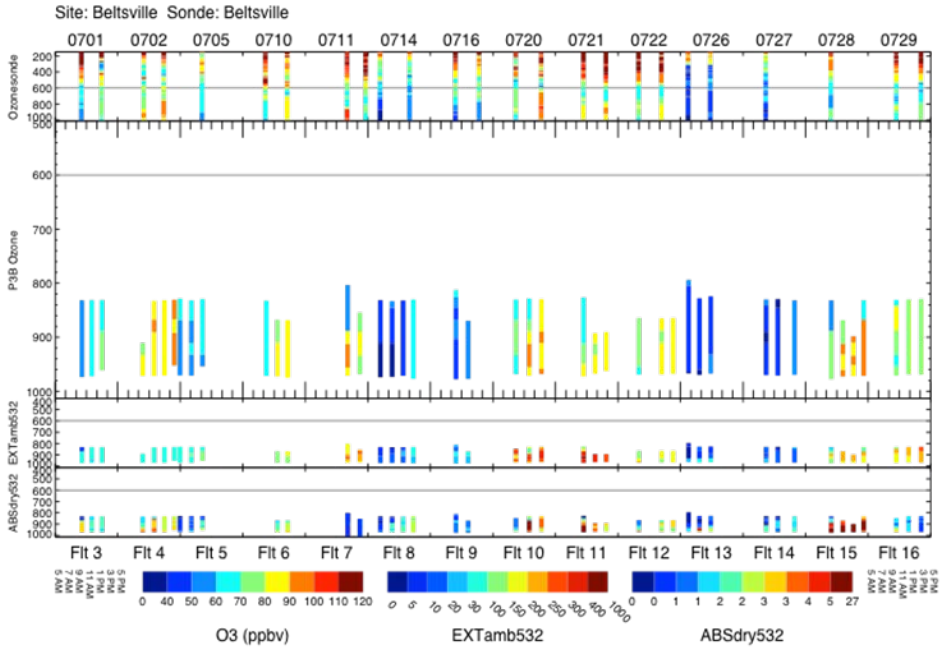

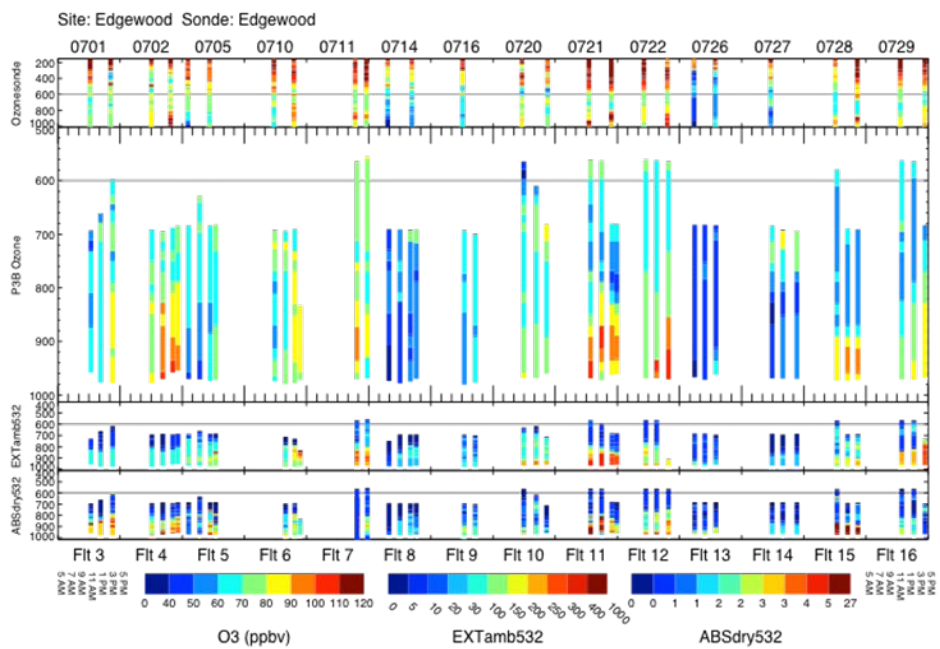

Essex also has good O_3 pollution samples

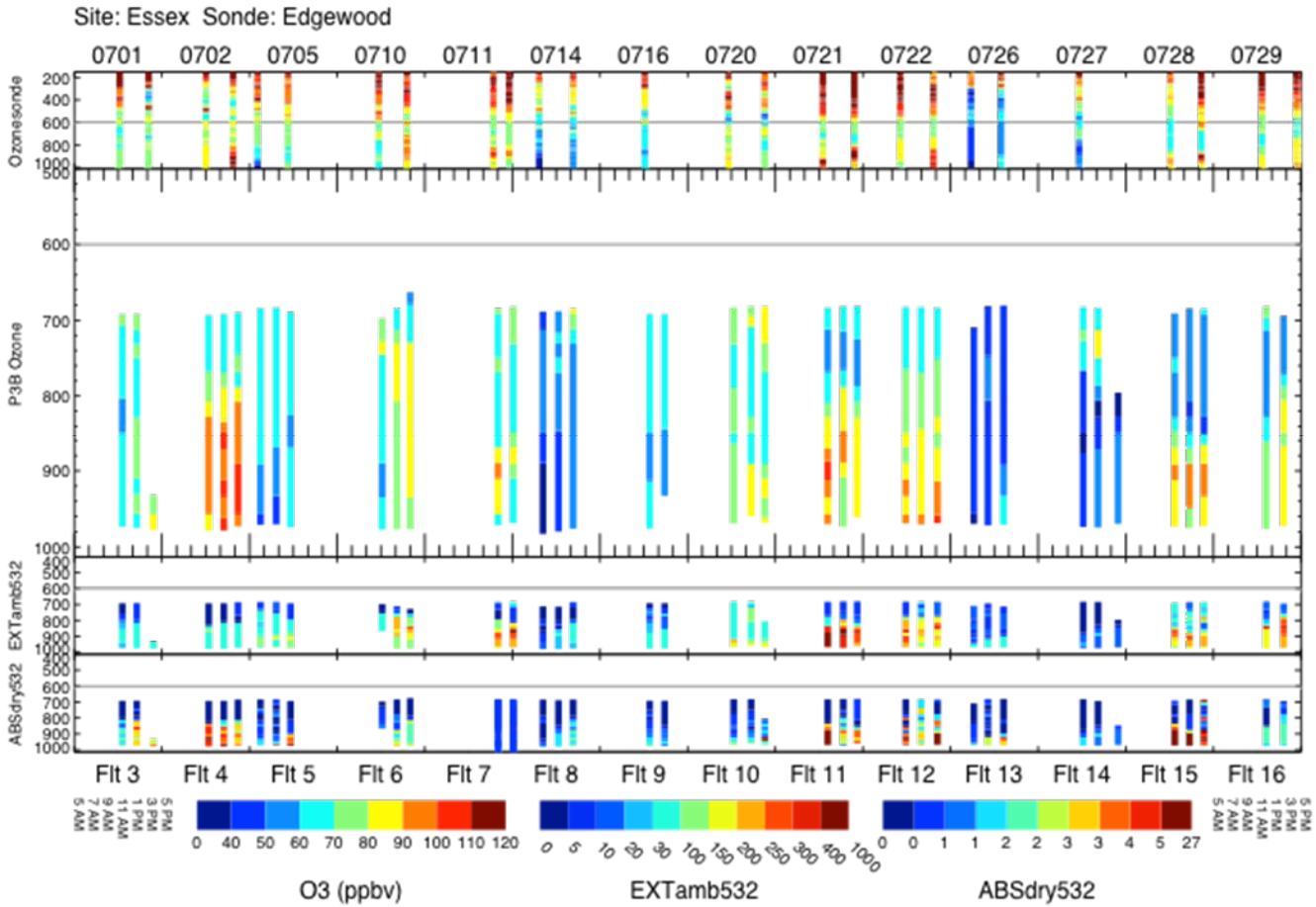

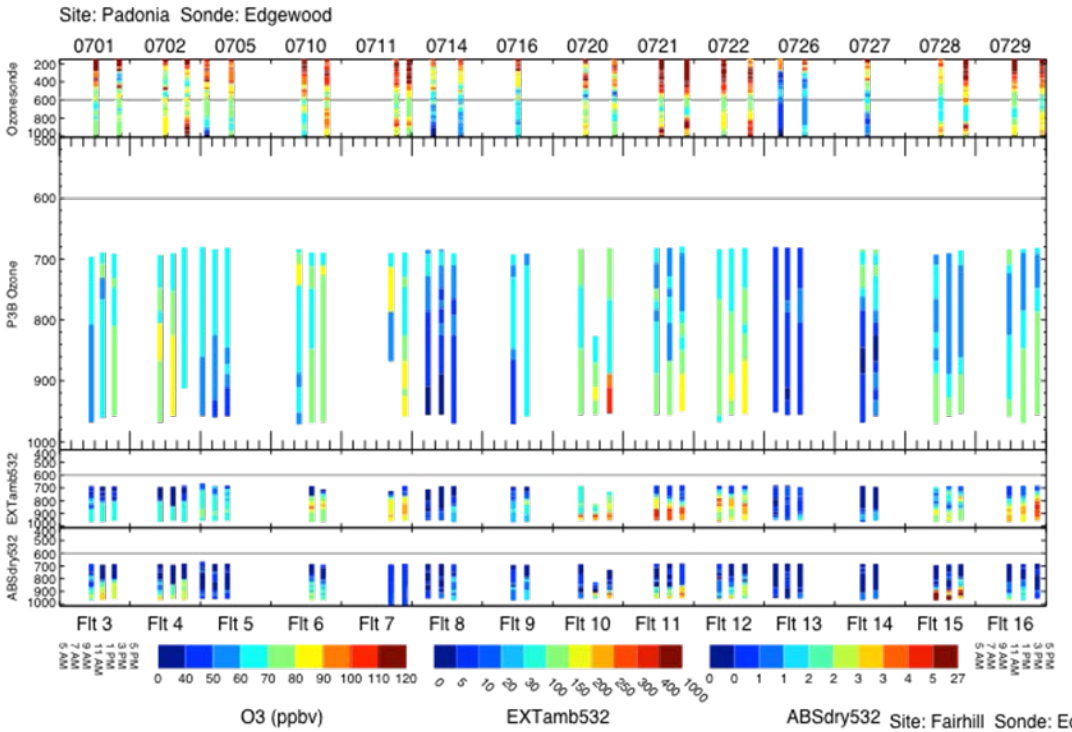
Site: Padonia Sonde: Edgewood
0701 0702 0705 0710 0711 0714 0716 0720 0721 0722 0726 0727 0728 0729
Ozonesonde
P3B Ozone
EXTamb532
ABSdry532
Flt 3 Flt 4 Flt 5 Flt 6 Flt 7 Flt 8 Flt 9 Flt 10 Flt 11 Flt 12 Flt 13 Flt 14 Flt 15 Flt 16
O3 (ppbv)
EXTamb532
ABSdry532

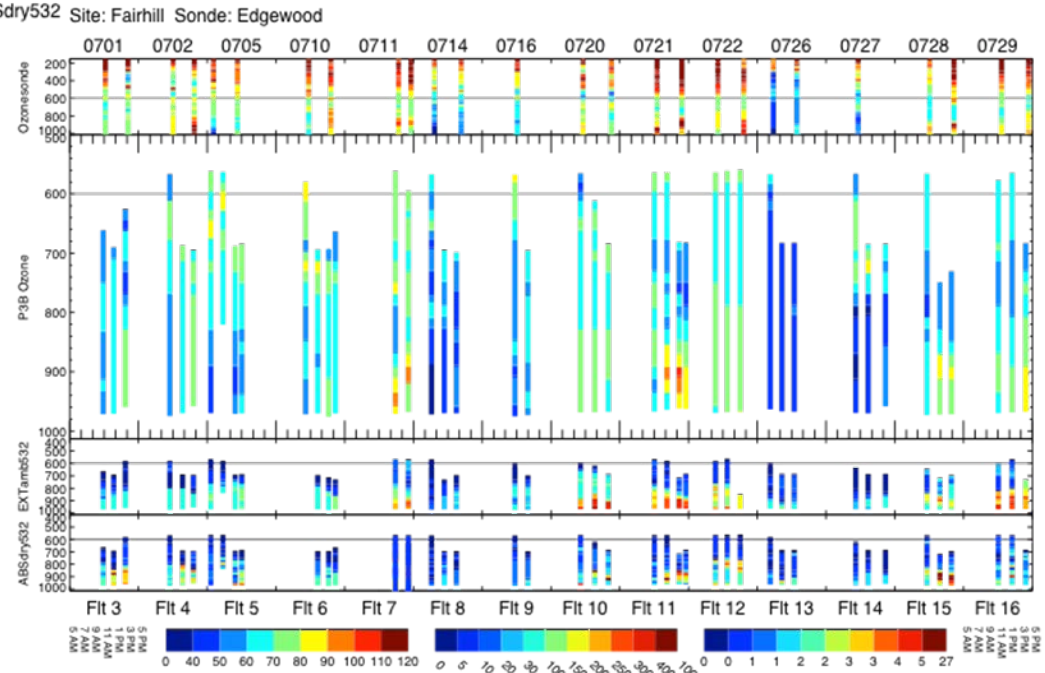
Site: Fairhill Sonde: Edgewood
0701 0702 0705 0710 0711 0714 0716 0720 0721 0722 0726 0727 0728 0729
Ozonesonde
P3B Ozone
EXTamb532
ABSdry532
Flt 3 Flt 4 Flt 5 Flt 6 Flt 7 Flt 8 Flt 9 Flt 10 Flt 11 Flt 12 Flt 13 Flt 14 Flt 15 Flt 16

UAHuntsville
The University of Alabama in Huntsville

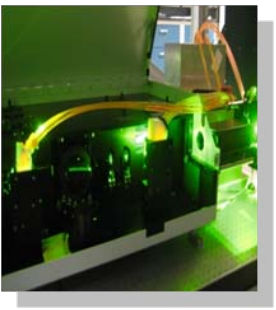

Boundary Layer and Free Tropospheric Ozone Spatio-Temporal Variability - UAH Lidar Measurements and Model Simulations

UAHuntsville/ATS Seminar, Oct. 19, 2011

Michael J. Newchurch[1], Shi Kuang[1], John Burris[2], Guanyu Huang[1], Wesley Cantrell[1], Lihua Wang[1], Arastoo Pour-Biazar[1], Kevin Knupp[1], Brad Pierce[3]

[1] Atmospheric Science Department, University of Alabama in Huntsville
[2]Goddard Space Flight Center, NASA
[3]University of Wisconsin

NASA

NOAA
NATIONAL OCEANIC AND ATMOSPHERIC ADMINISTRATION
U.S. DEPARTMENT OF COMMERCE

RAPCD
Regional Atmospheric Profiling Center for Discovery

Outline

- 1. Why is tropospheric O3 important?
- 2. Tropospheric O3, formation, removal, and budget
- 3. O3 climatology
- 4. Comparison of the techniques for ozone observation
- 5. Model improvement by using satellite boundary condition
- 6. LNO_x Influence on Trop. O3
- 7. DIfferential Absorption Lidar (DIAL) concept
- 8. UAH ozone DIAL system
- 9. Lidar observations used for atmospheric modeling, satellite validation, and air quality studies
- 10. O3 laminar detection
- 11. Wesley: Micro-scale Horizontal Variability
- 12. Ozone Variation in Near-Surface Layer
- 13. O3 Lidar Network
- 14. Future plans
- 15. Summary

1. Why is tropospheric O3 important?

- O3 is a precursor of the hydroxyl radical (OH), which controls the lifetime of many gases.
- O3 is a strong greenhouse gas influencing the climate by its radiative forcing.
- O3 is an important pollutant in the surface air.

2. Tropospheric O3, formation, removing and budget

Table 11-4 Present-day global budget of tropospheric ozone

	$Tg\ O_3\ yr^{-1}$
SOURCES	3400-5700
Chemical production	3000-4600
$HO_2 + NO$	(70%)
$CH_3O_2 + NO$	(20%)
$RO_2 + NO$	(10%)
Transport from stratosphere	400-1100
SINKS	3400-5700
Chemical loss	3000-4200
$O(^1D) + H_2O$	(40%)
$HO_2 + O_3$	(40%)
$OH + O_3$	(10%)
others	(10%)
Dry deposition	500-1500

Tropospheric O3 is largely controlled by the *in situ* photochemistry although the transport from stratosphere contributes significantly.

Causes strong vertical gradients at the surface

Daniel Jacob, Introduction to Atmospheric Chemistry, P216

3. O3 climatology

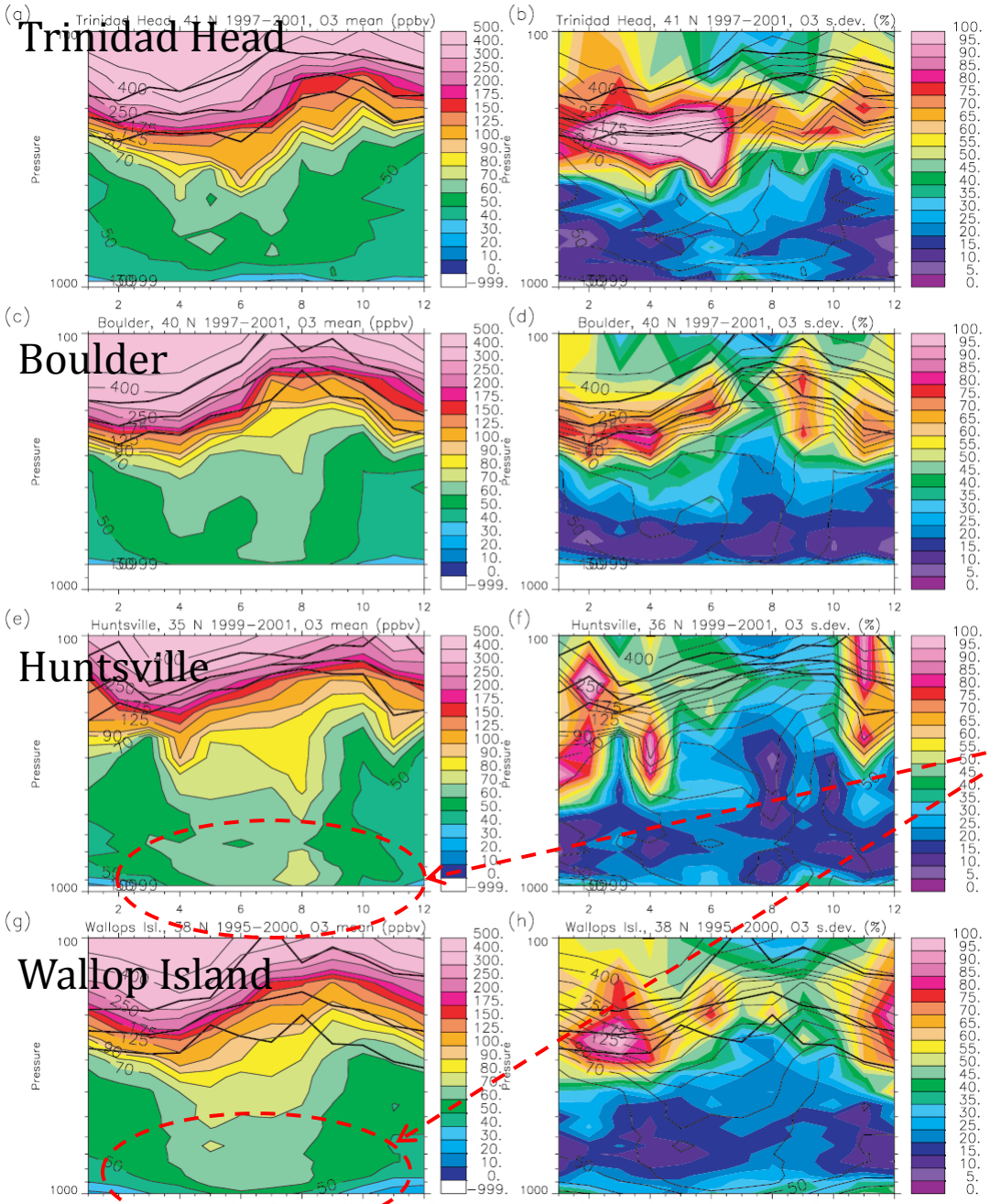

- Strong upper-tropospheric and lower-stratospheric variations in winter and spring due to the stratosphere-troposphere exchange (STE).
- All stations show variability in the PBL pollution sources.
- Middle troposphere is the least variable region.
- Eastern stations exhibit higher tropospheric ozone as a result of local pollution effects.

[Newchurch et al., 2003]

Figure 4. Vertical profiles of the annual cycle of monthly mean ozone mixing ratios (ppbv, left-hand panels) and coefficient of variation (right-hand panels) for (a, b) Trinidad Head, California; (c, d) Boulder, Colorado; (e, f) Huntsville, Alabama; and (g, h) Wallops Island, Virginia.

4. Comparison of the techniques for ozone observation

	Ozonesonde	Ground-based lidar	Sun-synchronous Satellite (OMI) [a]	Geostationary satellite (GEO-CAPE)[e]
Vertical resolution	~100m	100-1000m	10-14km	
Spatial coverage	Point	Point [b]	Global	Land and coastlines over 10-60ºN band
Spatial resolution	N/A	N/A [b]	13X48km at nadir	8km
Temporal resolution	Typically 1 week, max 4 hr	2-30 min [c]	Typically 1 day	1 hr
Meas. uncertainty	10%	Typically 10% at the near range and 20% at the far range	6%-35%	
Cost	Typically $40k/year, max $1,752k/year [d]	~$200-300k/year for fixed station	high	high
Major strength	well-characterized, low up-front cost, good vertical resolution,	High temporal resolution, low cost for frequent routine measurement	global coverage , high accuracy on total column retrieval	High spatio-temporal resolution relative to sun-sny satellite
Major weakness	Low temporal resolution	Unable to measure ozone above thick cloud, higher up-front cost relative to sonde	Low vertical resolution (particularly limited to resolve PBL)	

[a] For OMI tropospheric ozone retrieval [*Liu et al.* 2010], [*Worden et al.* 2007].
[b] For ground-based only. The airborne lidar system can measure ozone with a 600-m spatial resolution, e.g., [*Langford et al.* 2011].
[c] For ground-base system, e.g., *Sunnesson et al.*1994; *Proffitt and Langford* 1997; *Kuang et al.* 2011. The temporal resolution is strongly related to the retrieval uncertainty. Generally longer integration time will reduce the uncertainty arising from statistical error.
[d] The estimated cost is based on $800/launch and launching 6 sondes every day.
[e] Fishman J. et al. manuscript, in prep.

5. Model improvement by using space-borne observations of lateral boundary conditions

Boundary Conditions of O_3 (Aug. 1, 2006)

-----Predefined boundary conditions cannot represent real atmosphere;

-----Satellite / global model provide better boundary conditions.

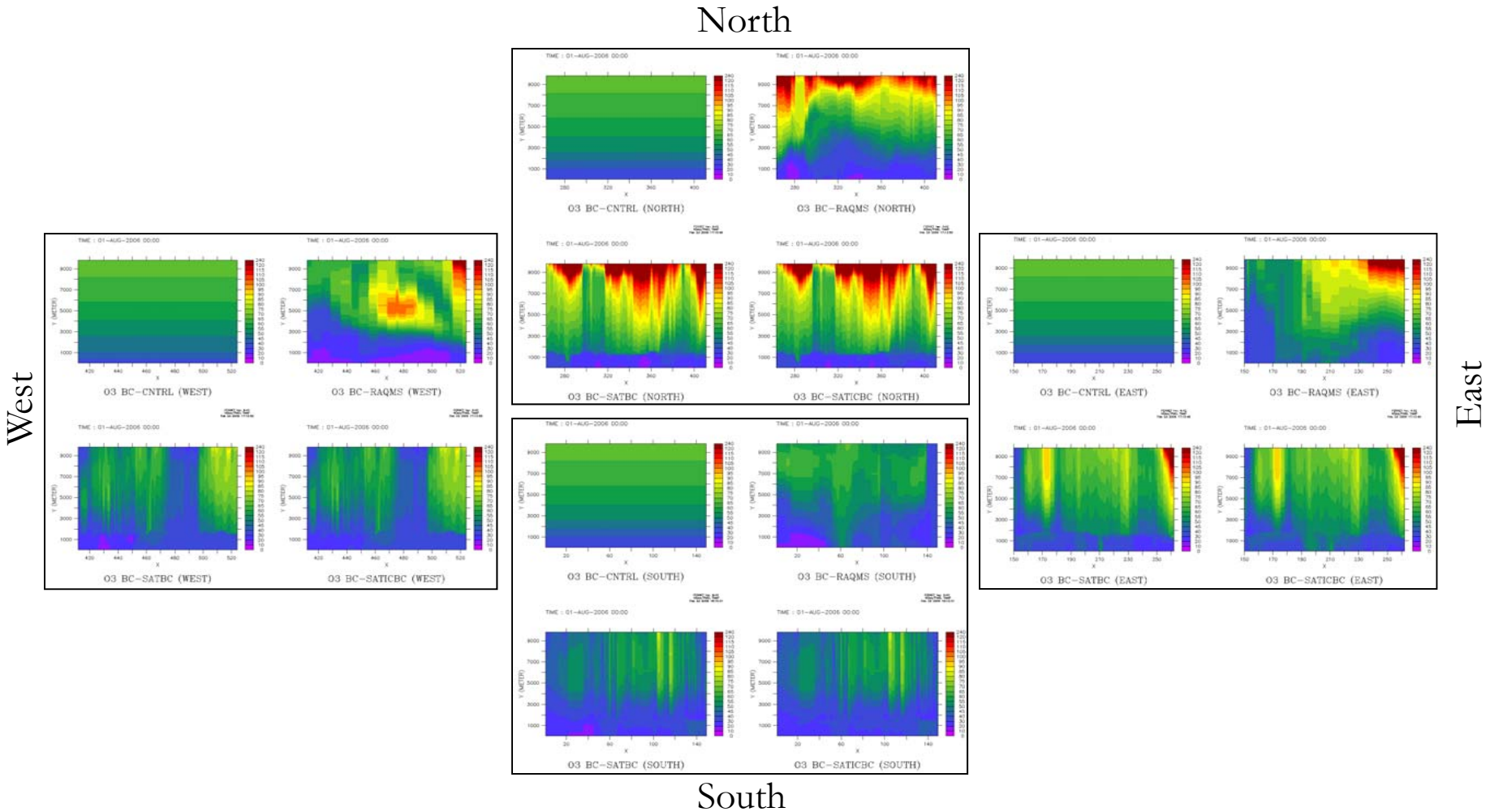

Figure 4 - Ozone (ppbv) BC at south, east, north, and west boundaries for August 1, 2006. Each panel contains BCs for CNTRL (top left), RAQMS_BC (top right), SAT_BC (lower left), SAT_ICBC (lower right) simulations, respectively.

Lateral boundary transport is important

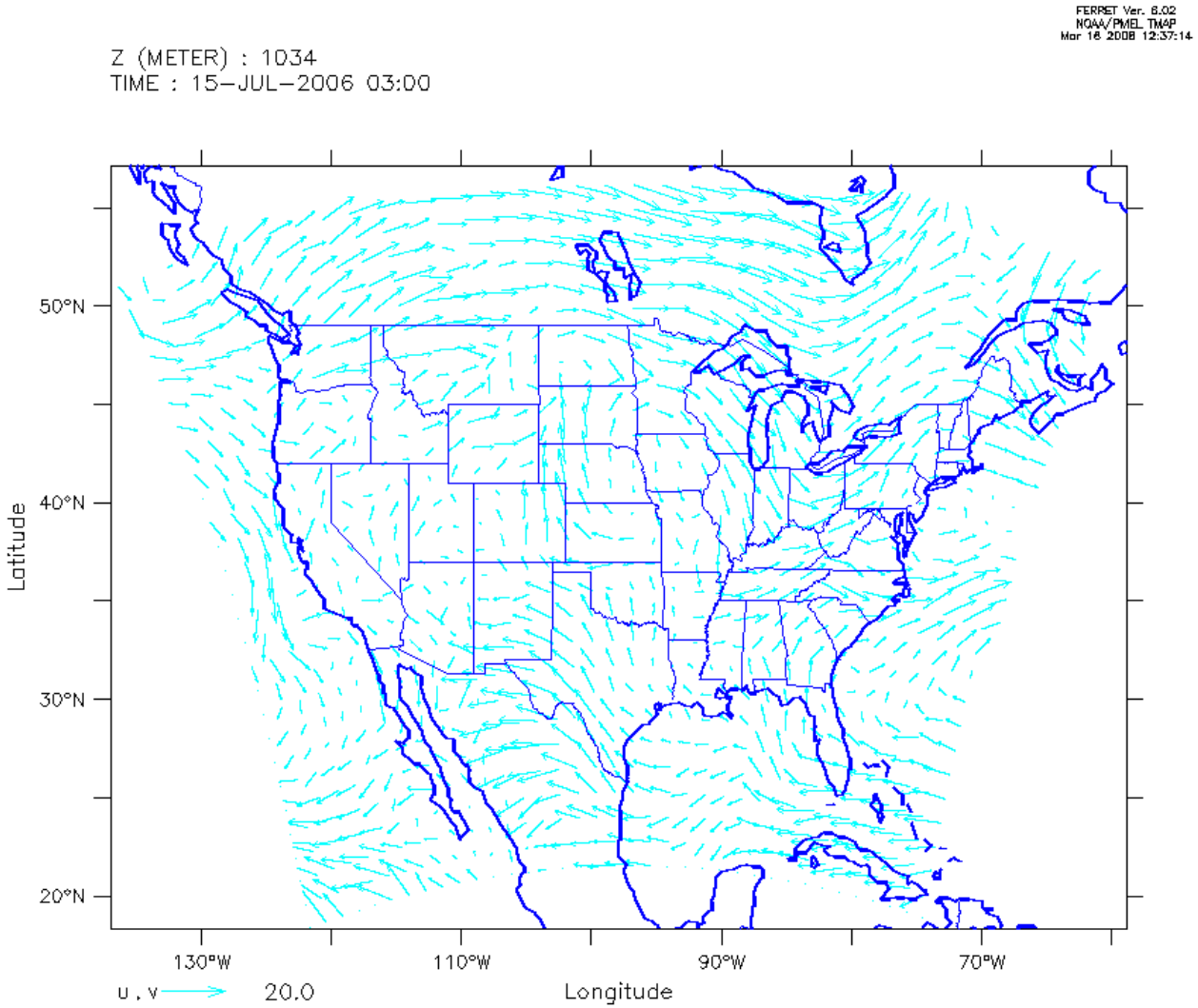

Ozone Diff (SATBC−CNTRL) (ppb)

Figure 12. Difference in ozone concentrations between SAT_BC and CNTRL simulations in the boundary layer for August 16, 2006. The plot clearly shows the role of transport in advecting ozone from the lateral boundaries

Better boundary/initial conditions improve CMAQ O3 prediction (evaluated with ozonesondes)

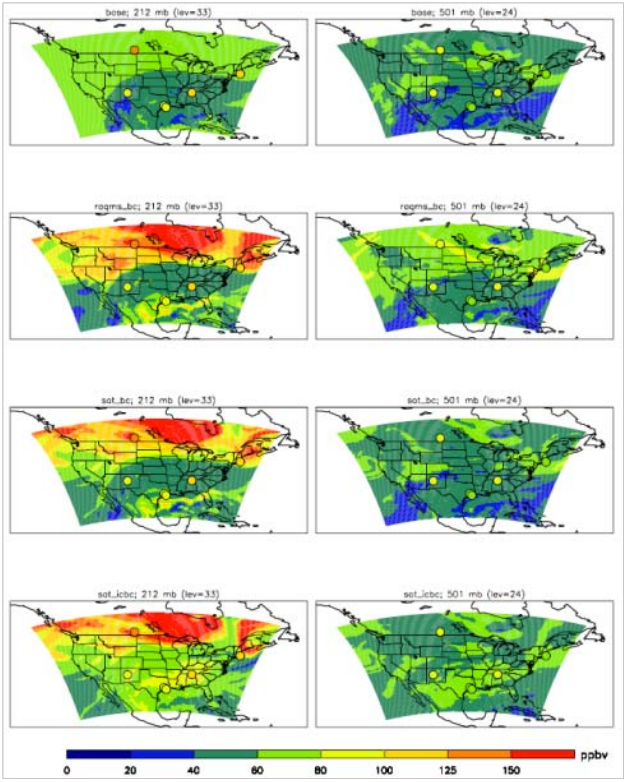

Figure 5 - O_3 (ppbv) at 19:00 GMT, Aug. 21, 2006 simulated by 4 CMAQ runs; over plotted with 6 ozonesondes launched between 15:00~23:00 GMT. Left panels represent CMAQ level 33 (212 hPa; 10km). Right panels represent level 24 (501 hPa; 5km).

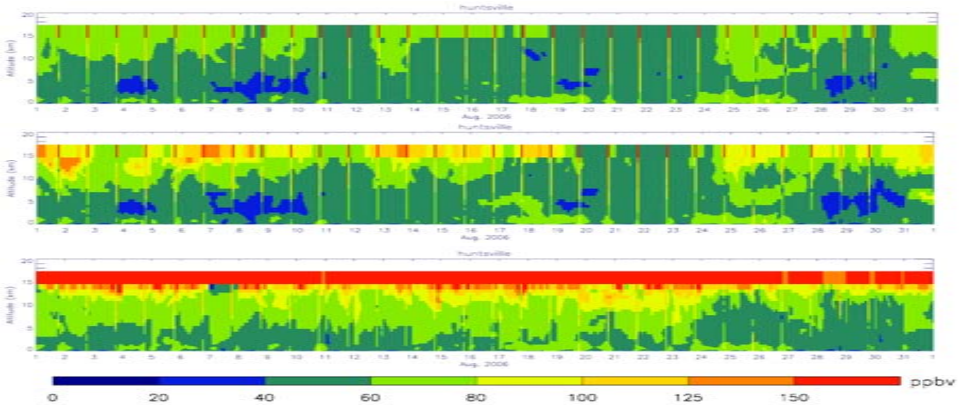

Figure 6 - SAT_ICBC further improves ozone prediction at Huntsville, AL.

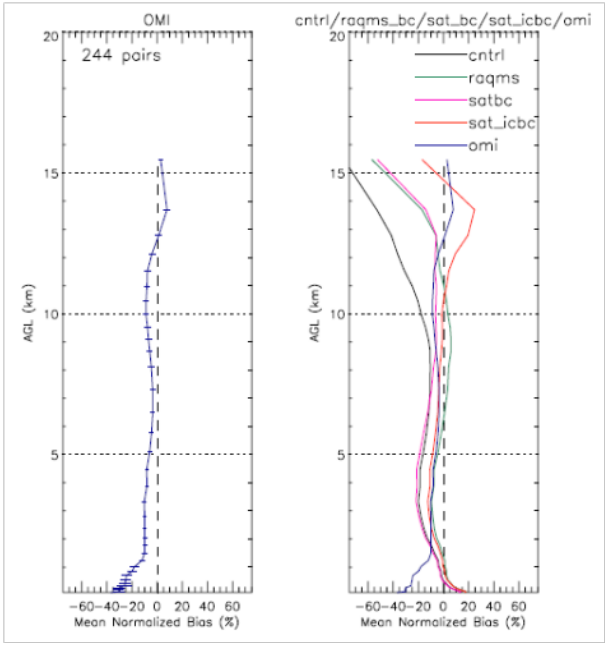

Figure 7 – Mean normalized bias (%) as model predicted O3/ OMI O3 are evaluated by ozonesonde measurements.

- **Using OMI ozone profiles as the boundary conditions for CMAQ calculations significantly improves the agreement of the model prediction of ozone with ozonesonde observations during IONS 2006 period. This improvement results from both representing the free-tropospheric ozone amounts more accurately and representing recirculating air masses more accurately.**
- **A simultaneous assessment of the OMI ozone profiles directly with the sondes indicates agreement to better than 10% throughout the free troposphere with 10-20% differences in the PBL.**
- **By modifying modeled O_3 with OMI O_3 throughout the model domain once a model-day, further improvement occurs, especially in the interior region where influences from the boundary condition are small.**

6. LNO_x Influence on Trop. O3

(1) Lightning is a particularly significant NOx source (LNOx) in the middle and upper troposphere. Current CMAQ model does not account for NOx emission from lightning.

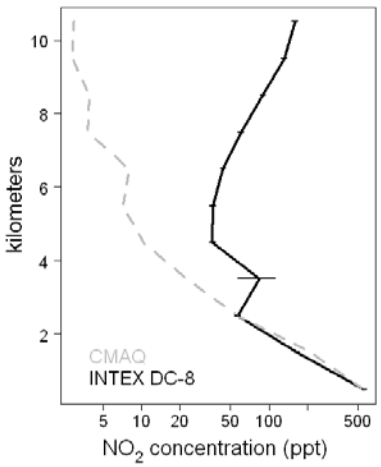

Figure 1 - Vertical distribution of NO2 concentrations observed by NASA INTEX DC-8 flights over the eastern United States compared to model predictions matched in space and time. Error bars denote 99% confidence interval of the mean, assuming the observations are drawn from a normally distributed population [Napelepenok et al., 2008].

(2) Include LNOx emission to the NOx emission inventory:

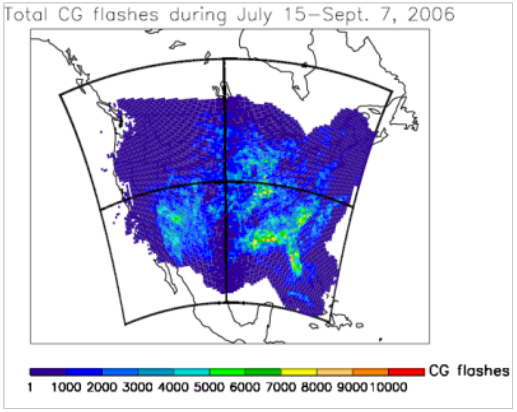

Figure 8 - Total CG flashes (7/15-9/7,2006) observed by NLDN; LNOx emission accounts for 27% total NOx emission averaged over the entire model domain, and 37.9% (SW), 32.1% (SE), 16.6% (NE), and 15.6% (NW) for the four sub-regions, respectively.

- **NLDN CG detection efficiency of ~95%**
- **assuming IC:CG ratio is 3**
- **assuming a 500 moles (~ 3.011x1026 molecules) N per CG/IC flash production rate.**
- **Vertically-distribute onto 39 model layers following the mid-latitude continental LNOx distribution profiles Pickering et al. [1998] developed.**
- **Add LNOx emission to SMOKE estimated NOx emissions.**
- **Make a CMAQ run including LNOx (CNTRL_LNOx)**

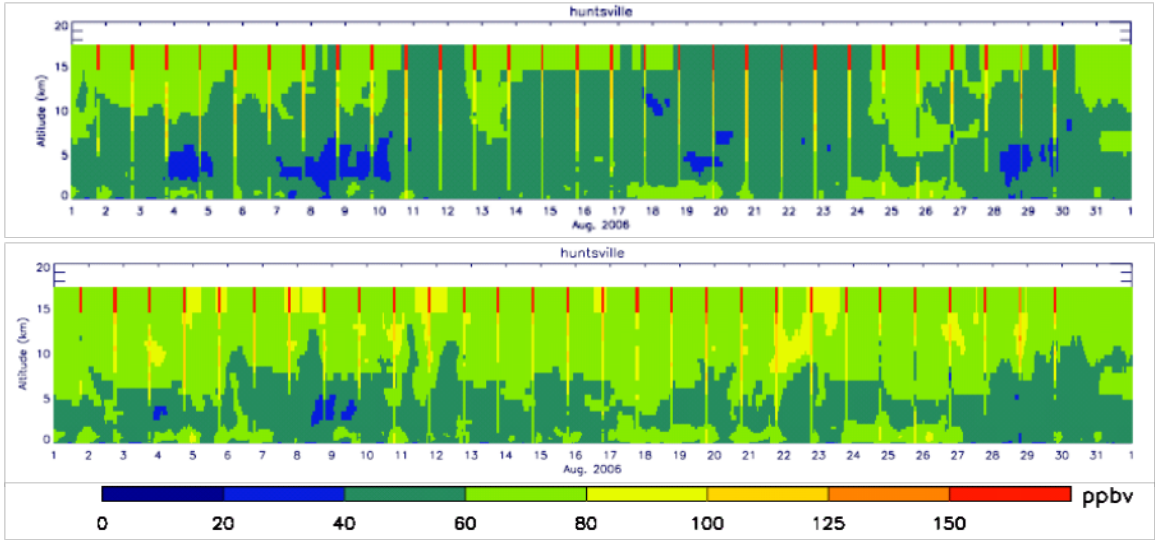

Figure 13 - Model predictions of ozone concentration at Huntsville, AL during August 2006, with 29 ozonesonde profiles (interpolated onto CMAQ vertical resolution) overplotted. Top: CNTRL; Bottom: CNTRL_LNO$_x$

Figure 14 – Mean of 29 ozonesondes measured between 17:00 ~19:00 GMT during August 2006, as well as mean of model predictions (CNTRL and CNTRL_LNO$_x$) at 19:00 GMT.

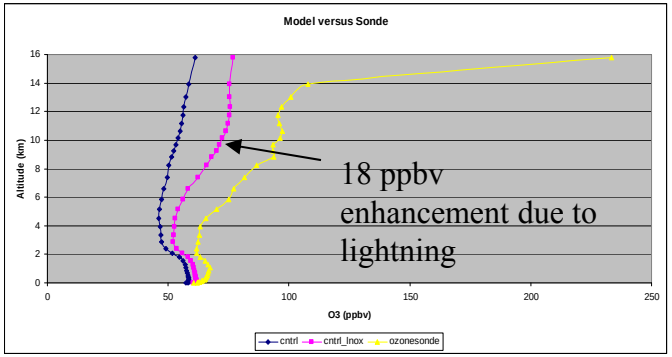

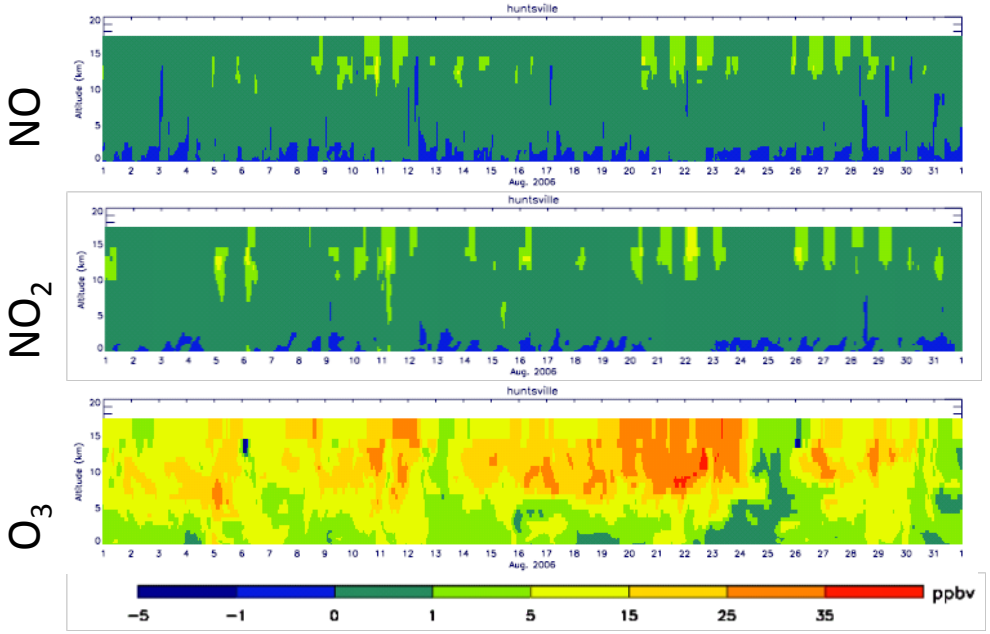

Figure 15 – Differences in NO, NO_2 and O_3 between CNTRL_LNO$_x$ and CNTRL for Huntsville, AL during August 2006, due to lightning influence.

A case study in Huntsville, AL during August 2006 shows increased NOx in upper troposphere due to lightning-NOx injection, and finds corresponding ozone enhancement around same altitude (~10 km), but still 20 ppbv lower than ozonesonde measurement

Consistent with Cooper et al., 2009

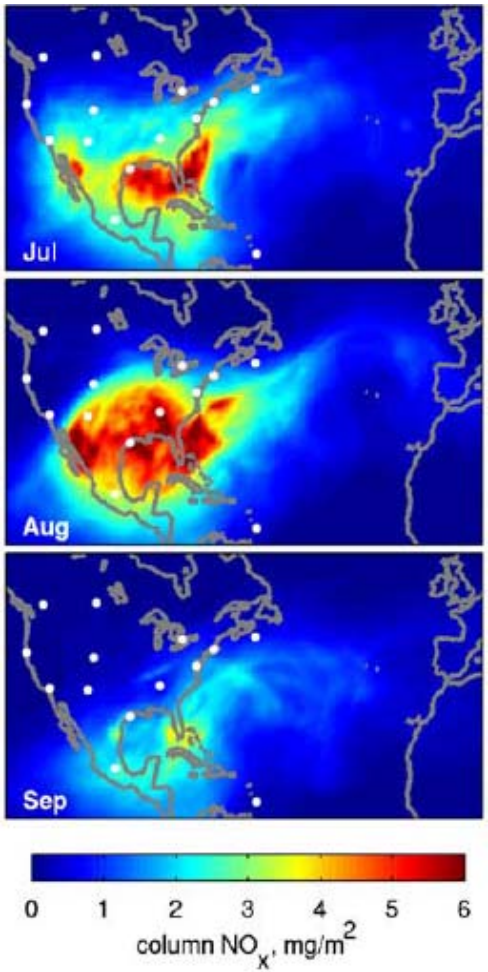

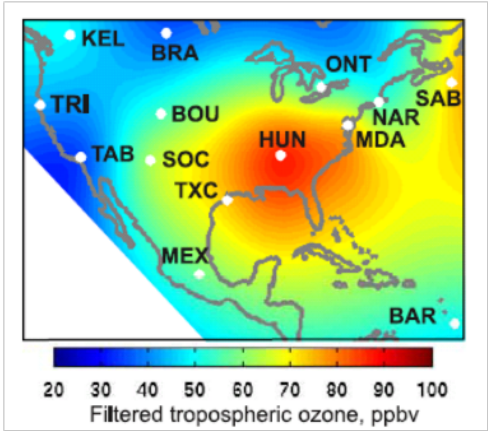

Figure 16 - Left: Monthly average location of a 20-day passive LNOx tracer that has been allowed to decay with a 4-day e-folding lifetime, indicating the regions where LNOx would most likely be found, as well as the regions where ozone production would most likely occur, for July through September 2006 [Cooper et al., 2009]. Right: Median filtered tropospheric ozone (FTO3) mixing ratios during August 2006 at all 14 IONS06 measurement sites between 10 and 11 km. FTO3 is the measured ozone within the troposphere with the model calculated stratospheric ozone contribution removed [Cooper et al., 2007].

O3 measurement with a 4-hour temporal resolution

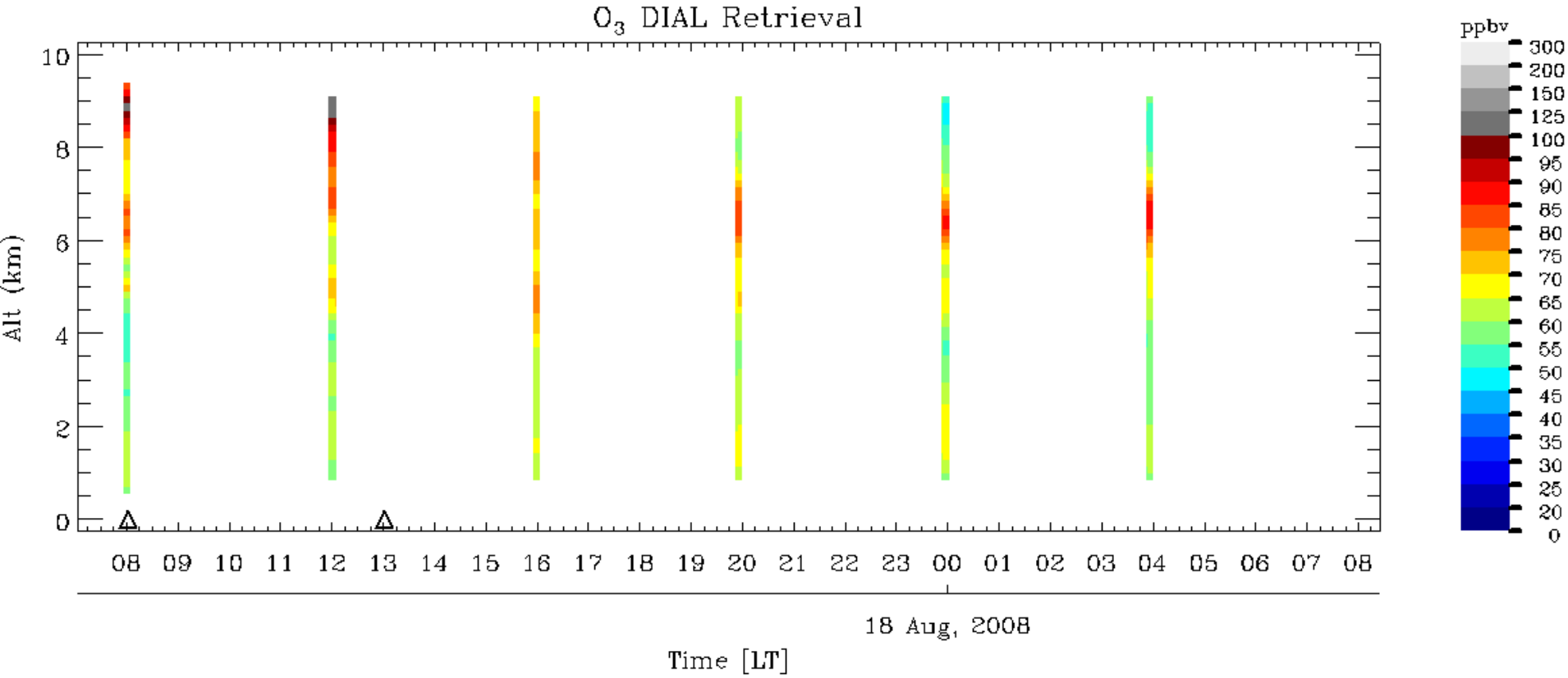

Lidar ozone curtain with10-minute resolution

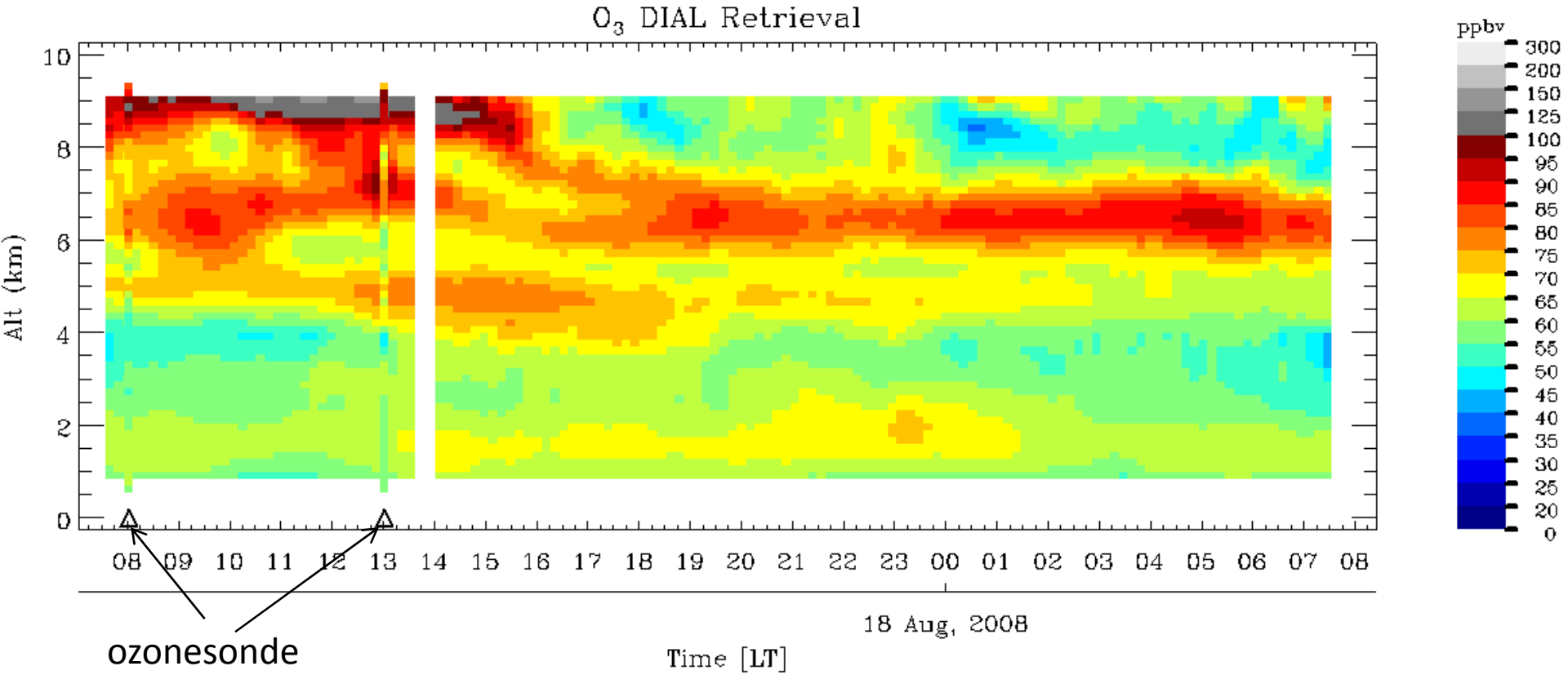

7. DIfferential Absorption Lidar (DIAL) concept

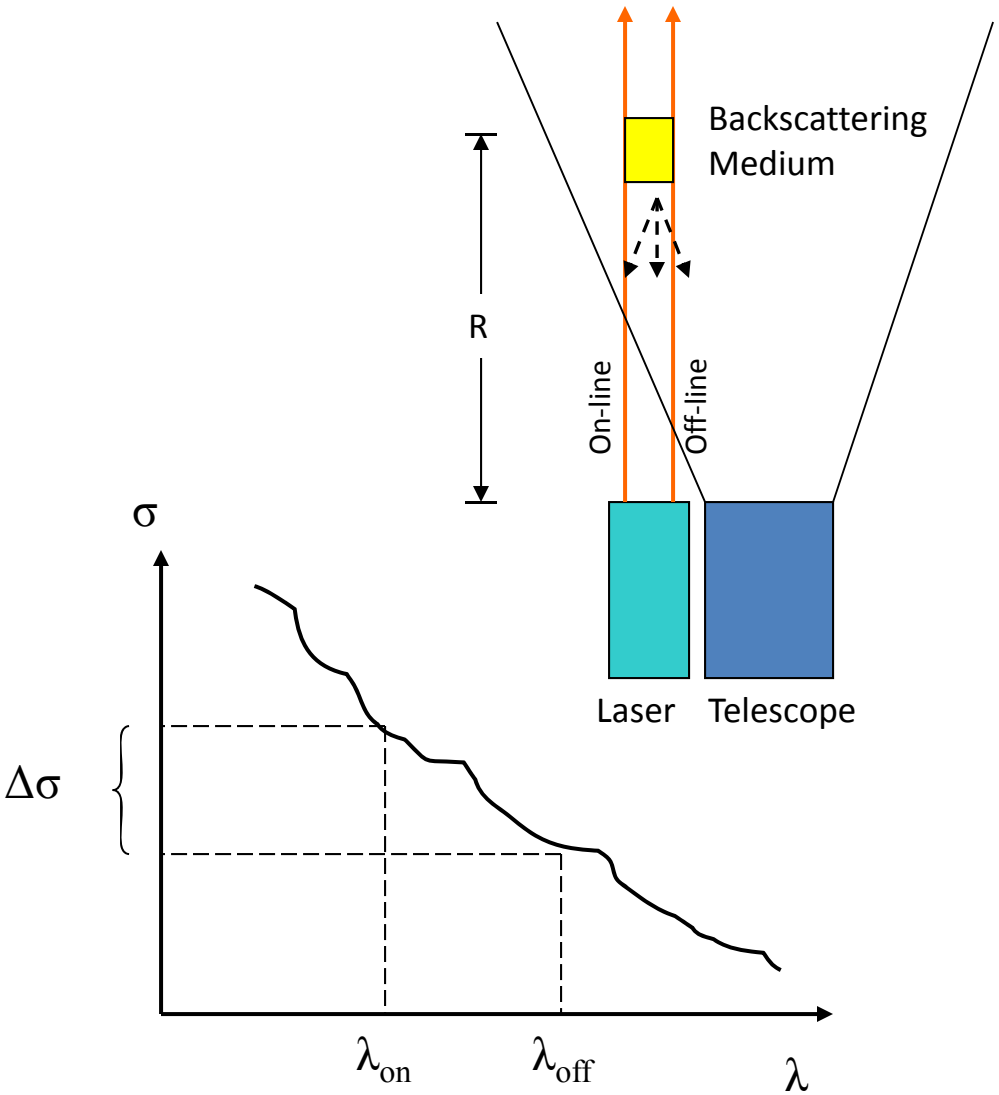

$$O3_{(r)} = \frac{-1}{2\Delta\sigma_{O3}} \frac{d}{dr} \ln \frac{P_{on(r)}}{P_{off(r)}}$$

O3 DIAL Equation

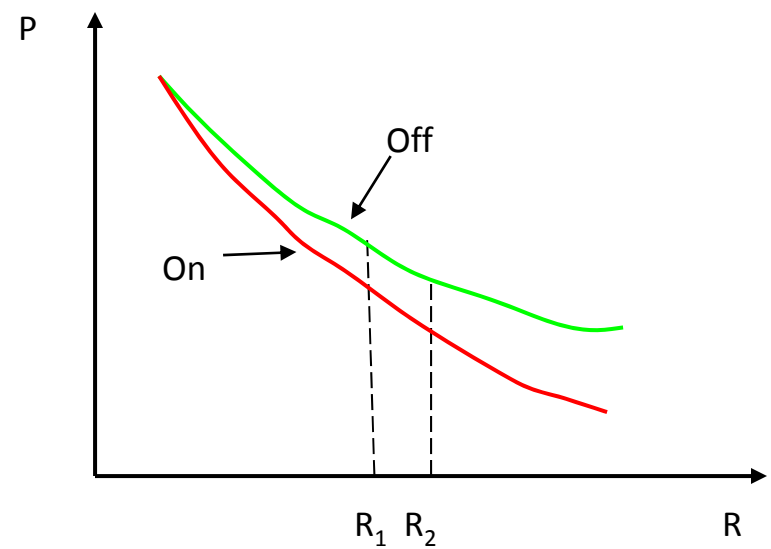

8. UAH ozone DIAL system

Two wavelengths and two receivers to measure 0.5-10 km

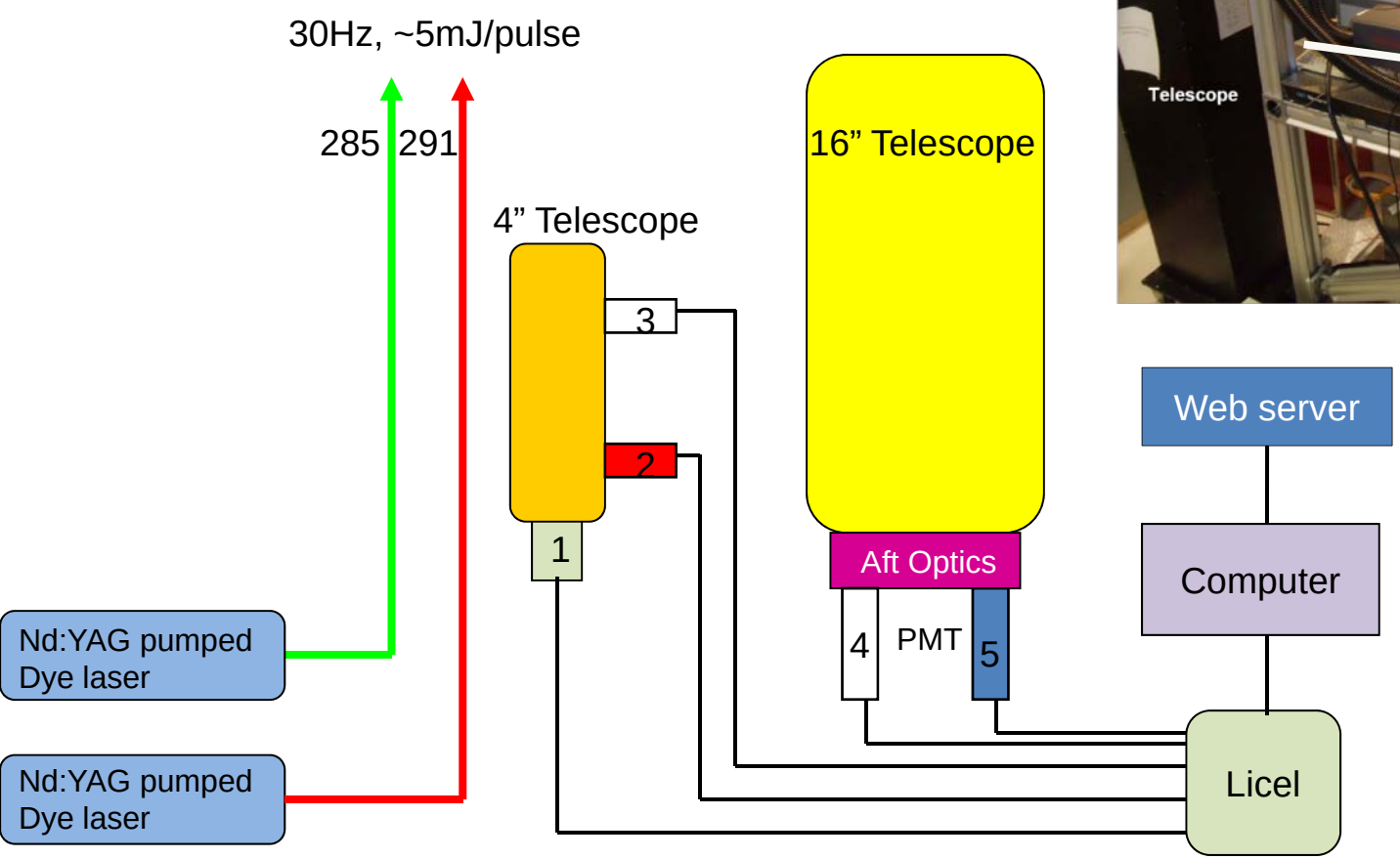

RAPCD-DIAL configuration

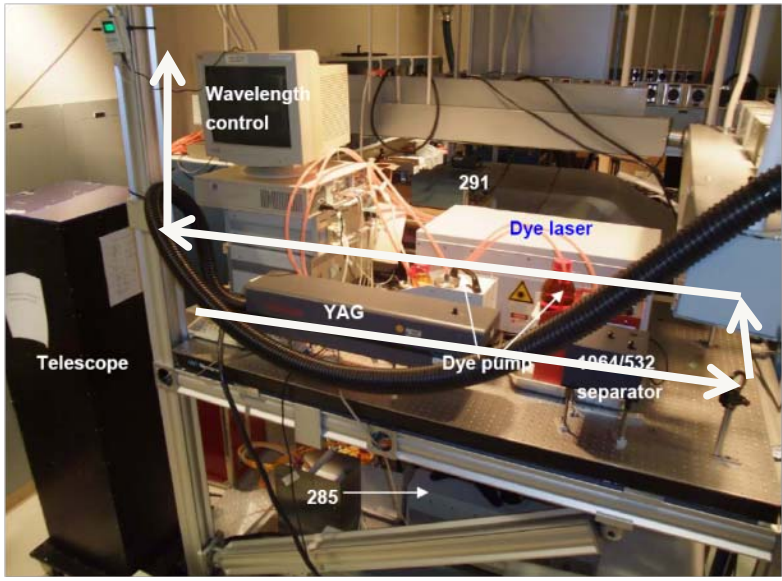

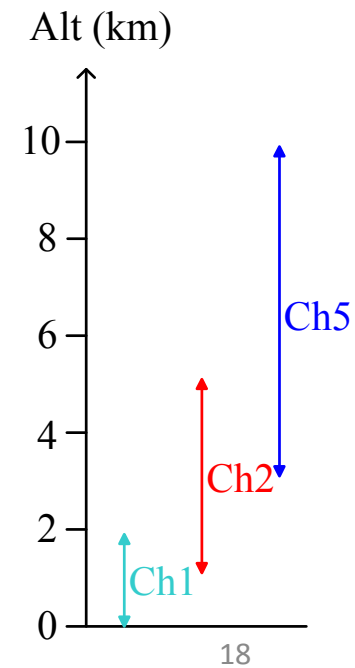

Measurement range

9. Lidar observations used for atmospheric modeling, satellite validation, and air-quality studies

Stratosphere-to-troposphere transport and its CMAQ Model simulation, Nov. 5, 2010

GOME total O_3 Nov. 5

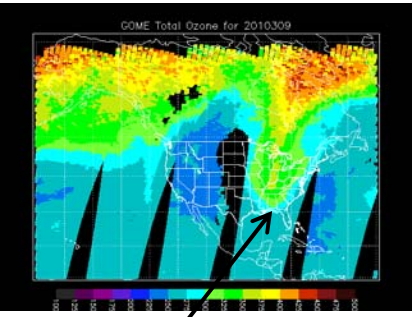

Huntsville

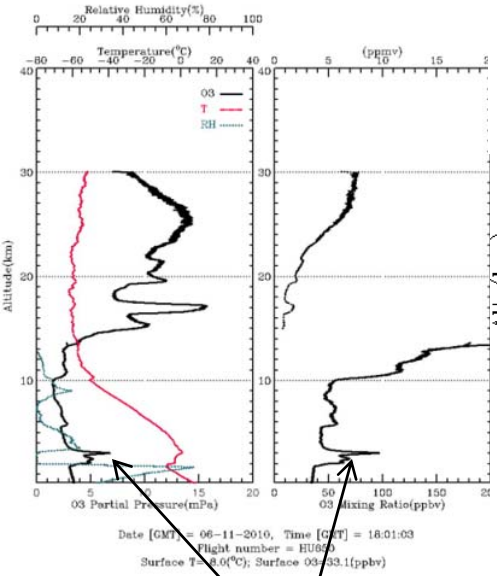

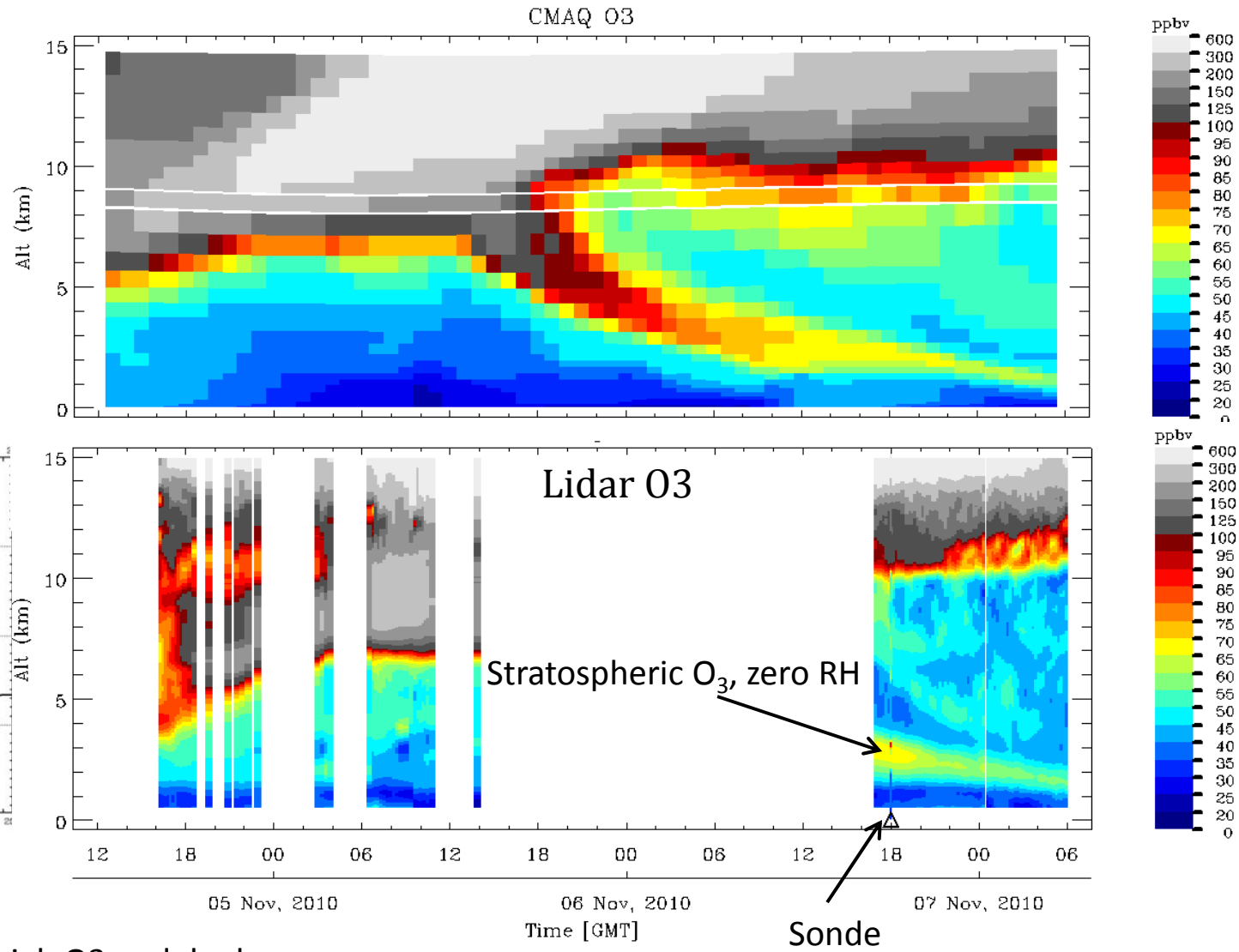

Ozonesonde showing the high O3 and dry layer

Local time

Stratosphere-to-troposphere transport, lidar O3 observation and NAM model derived PV, Apr. 27, 2010

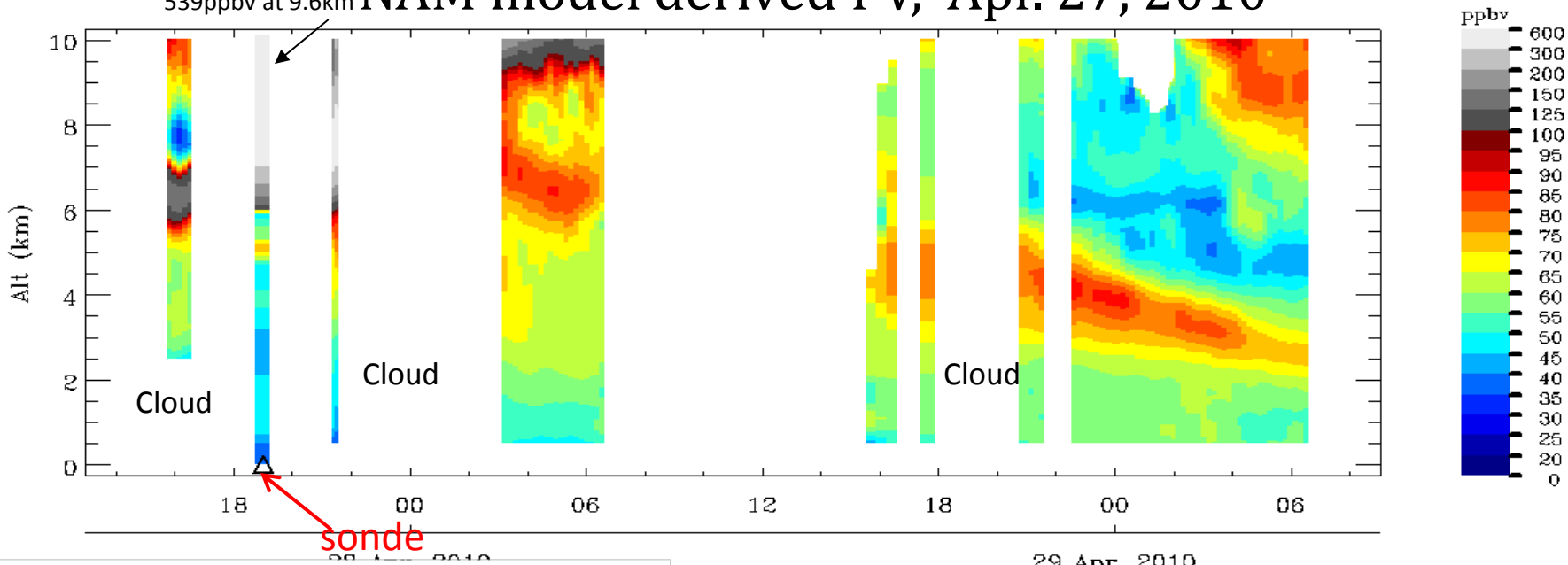

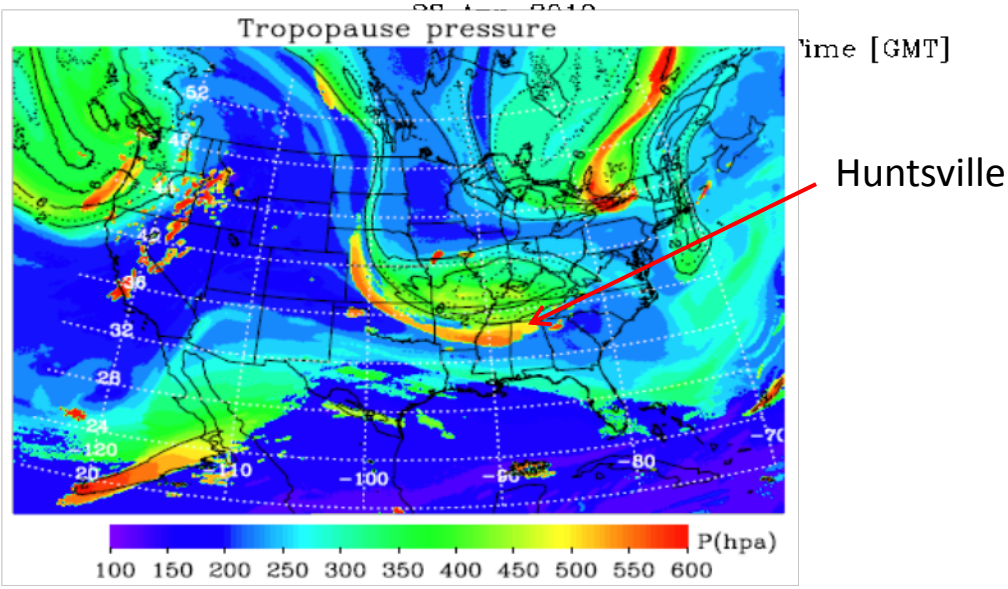

NCEP NAM reanalysis derived tropopause pressure (color) and potential vorticity (PV, solid), 12Z Apr. 27

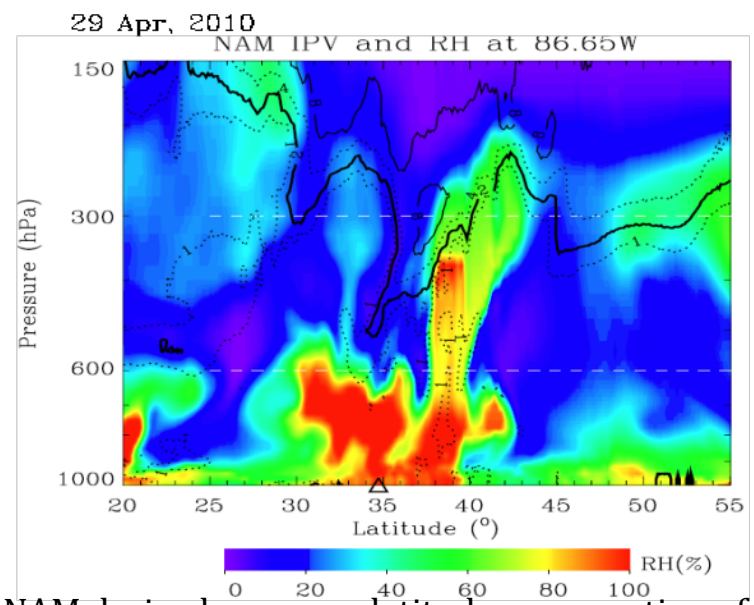

NAM derived pressure-latitude cross section of PV (solid) and RH (color) at 86.65°W

Stratosphere-to-troposphere transport O3 structure, Apr. 5, 2011

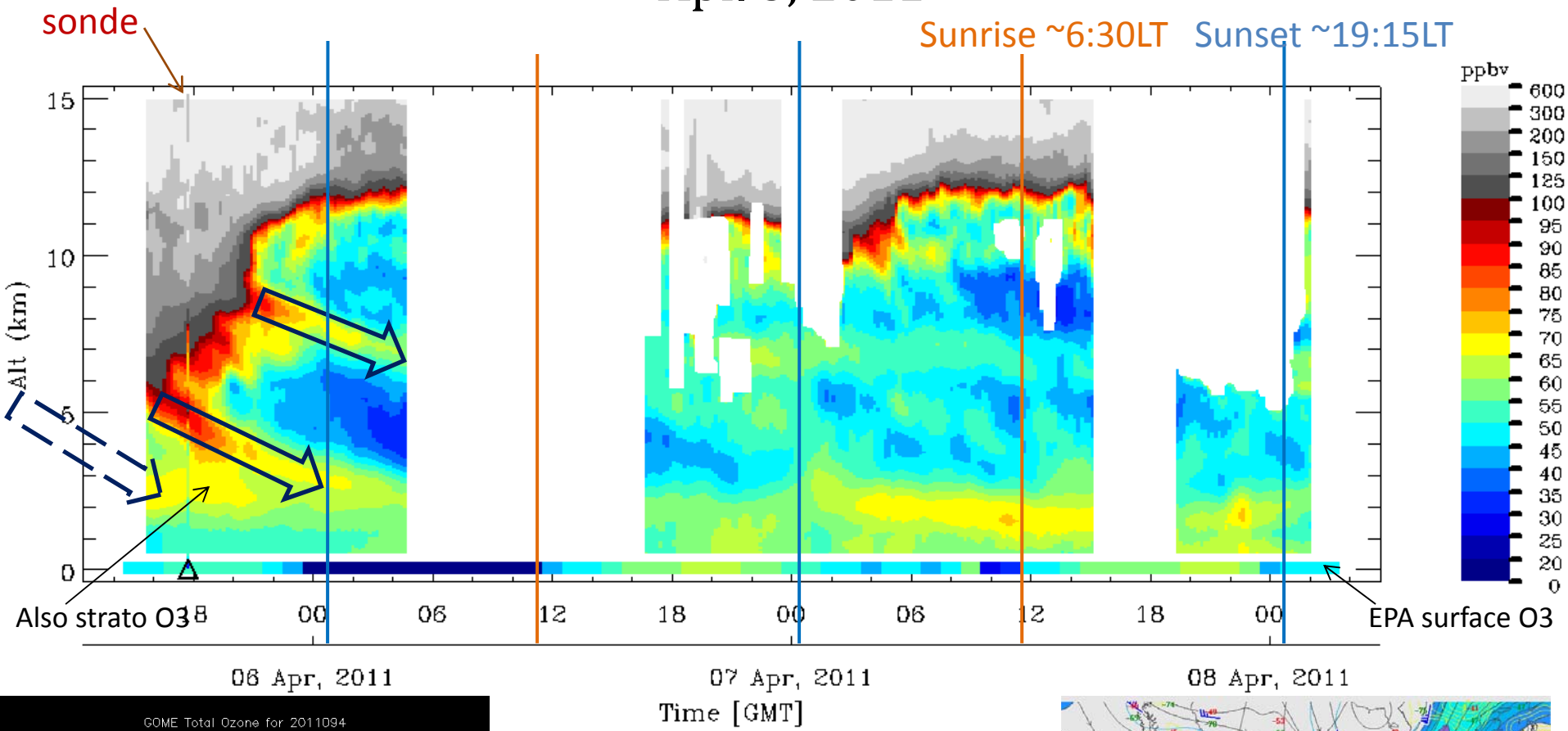

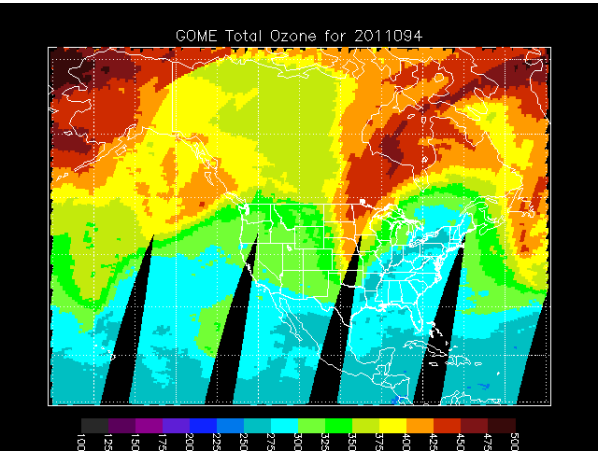

4/5 GOME

300hPa 12Z, Apr. 5

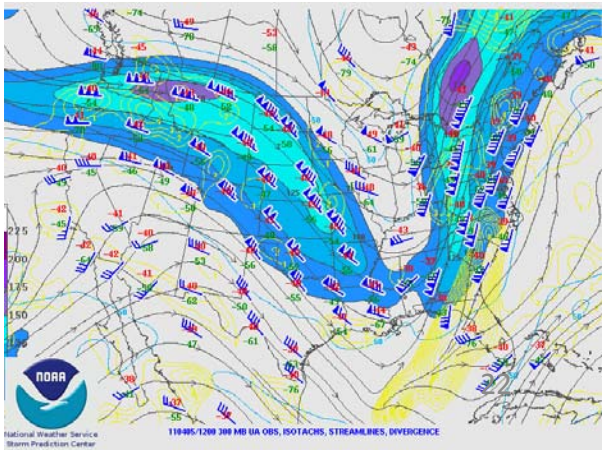

Evolution of the Boundary Layer Ozone Maximum

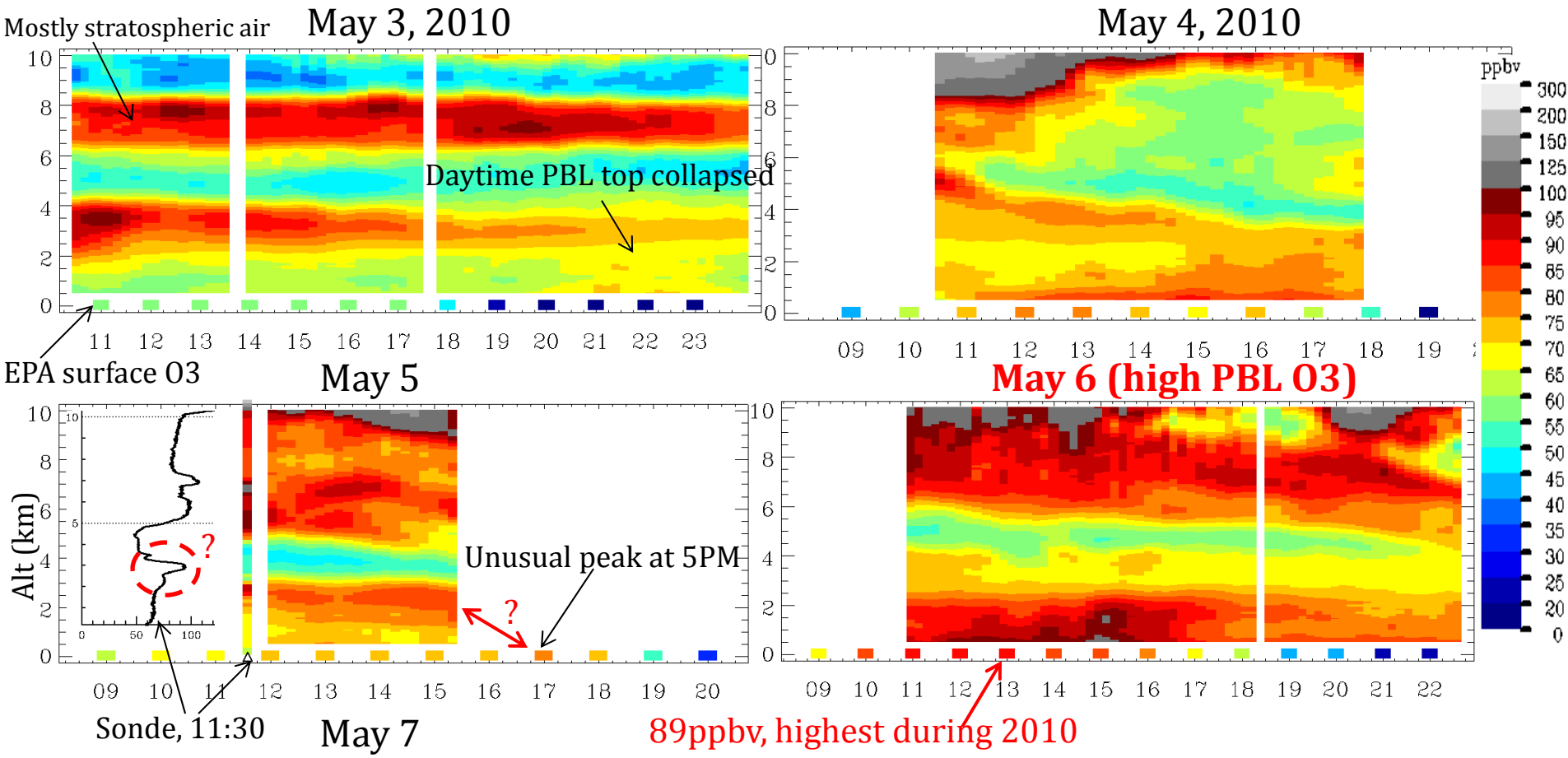

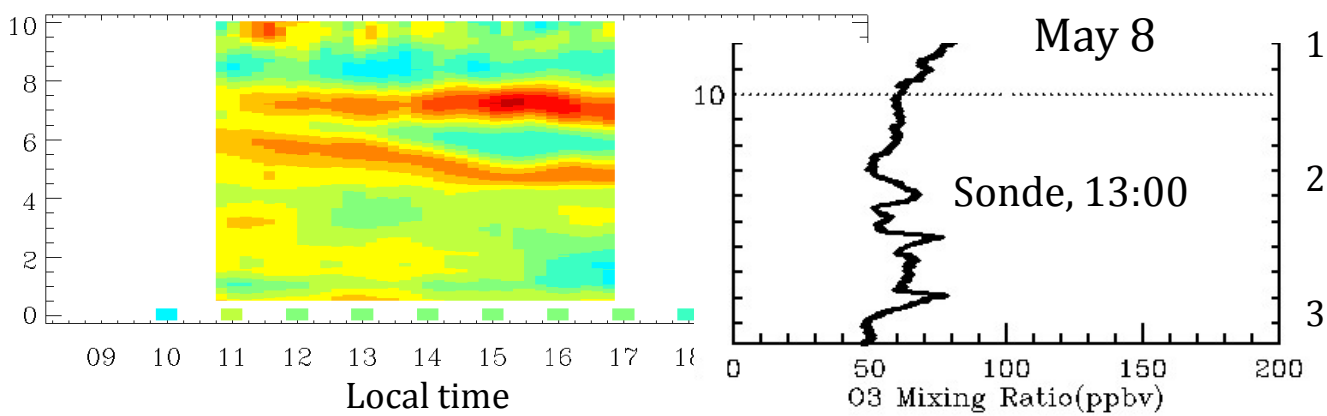

1. PBL O3 maximum on May 6 due to post-front air stagnation.
2. PBL ozone aloft generally agree with the daily surface maximum.
3. Decoupling of surface and upper-air O3 during nighttime.

Comparison of the lidar observation and RAQMS model simulation

RAQMS misses ozone layer at 2-4km

over estimates depth of 6-8km layer

shows collapse of PBL

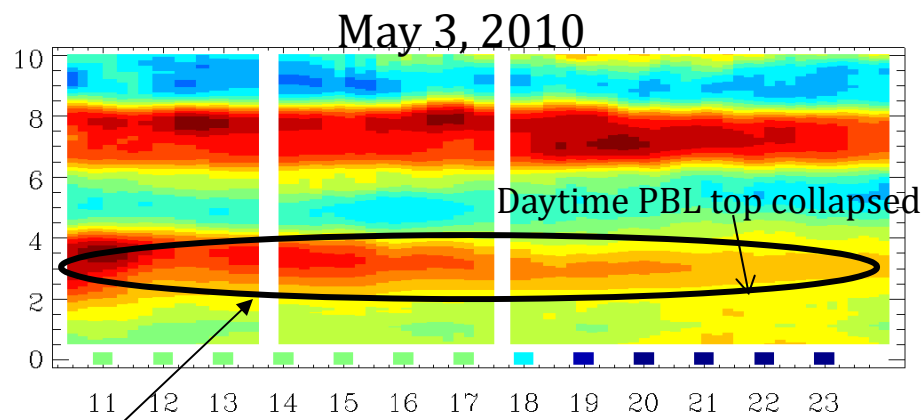

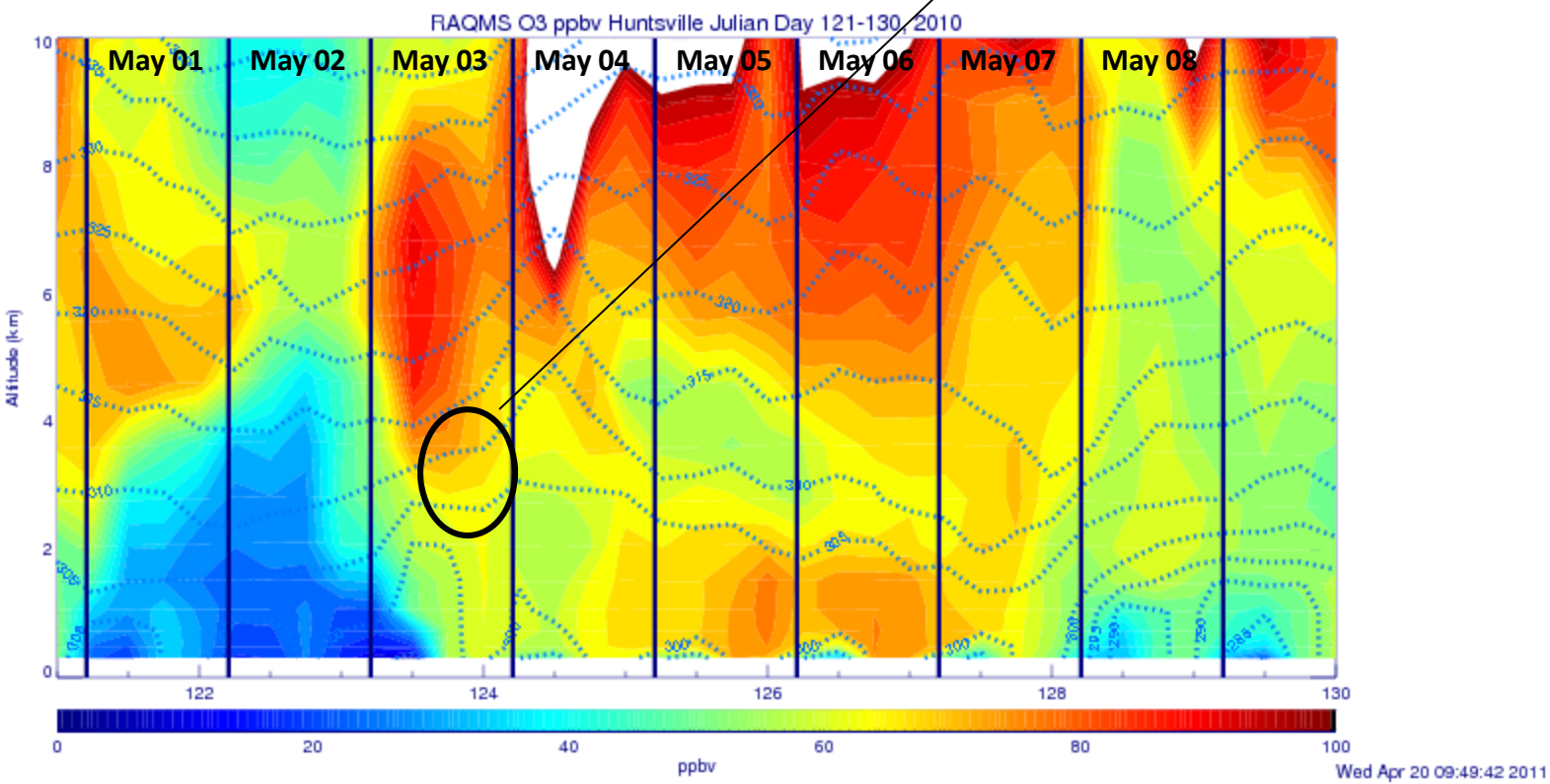

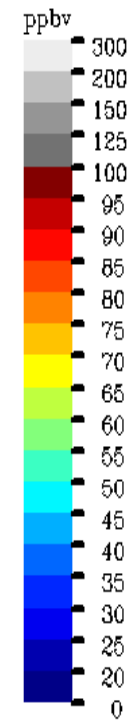

Timing of low upper tropospheric ozone minimum seems delayed (note RAQMS only every 6hrs)

doesn't show surface O3 enhancement

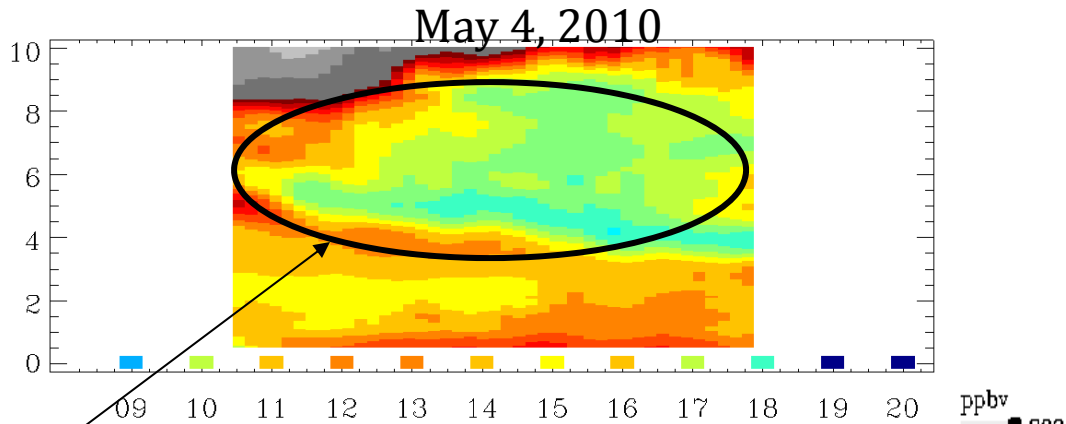

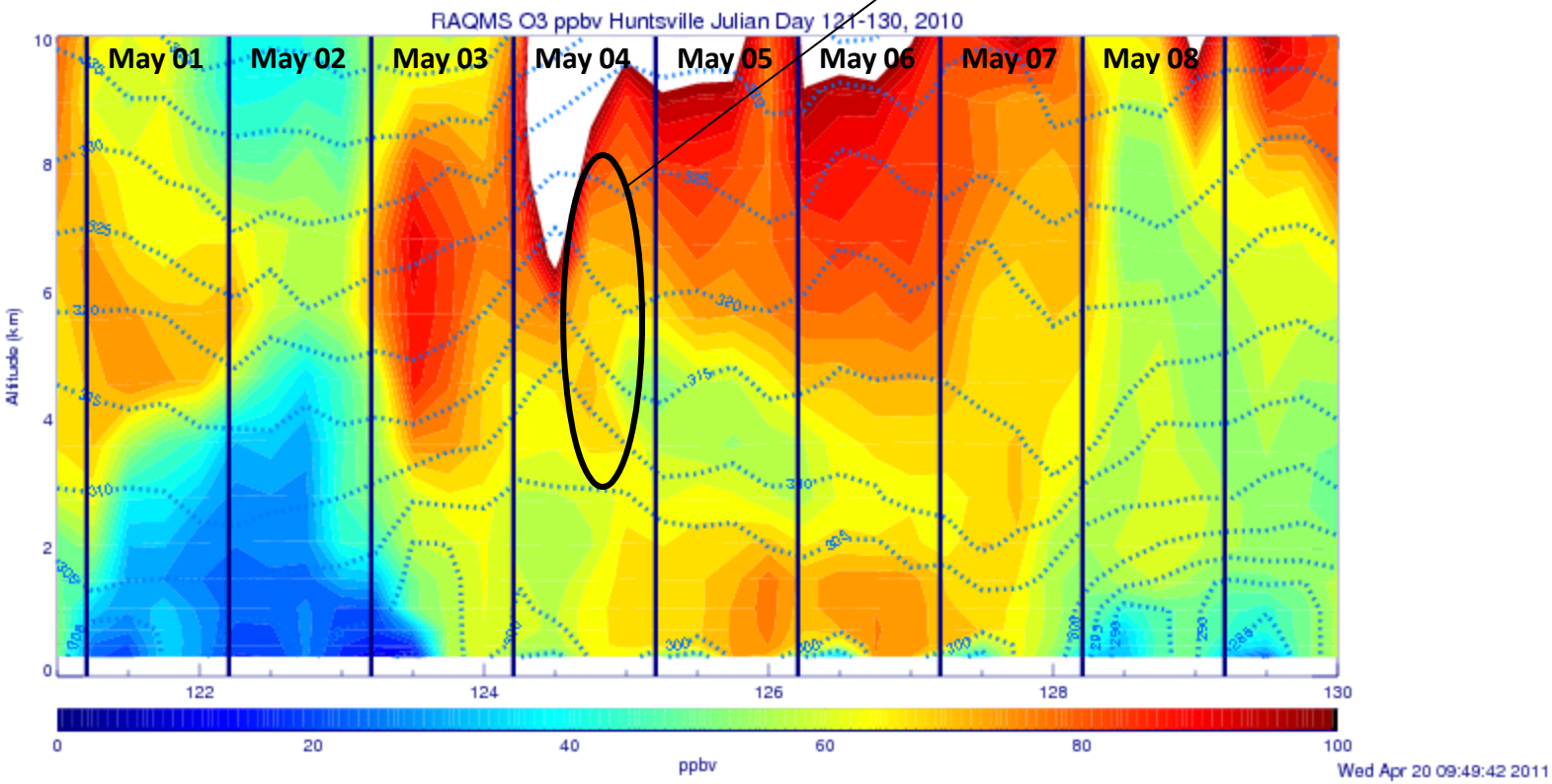

RAQMS is in good agreement with Huntsville Lidar above ~3km

under estimates low level ozone enhancement

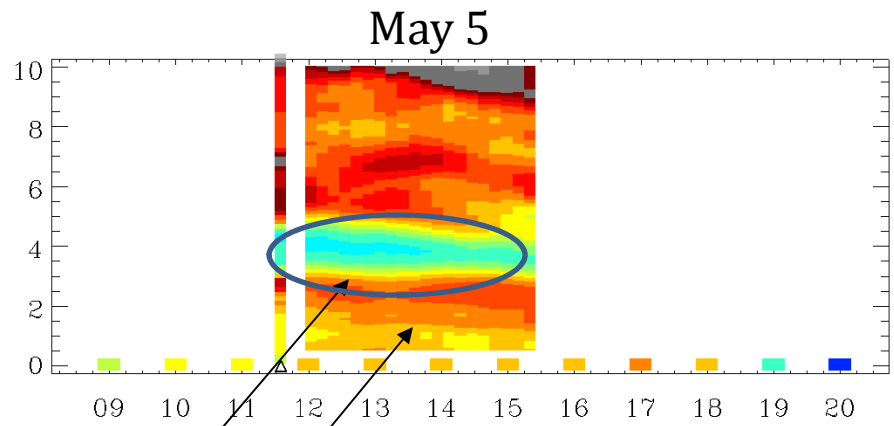

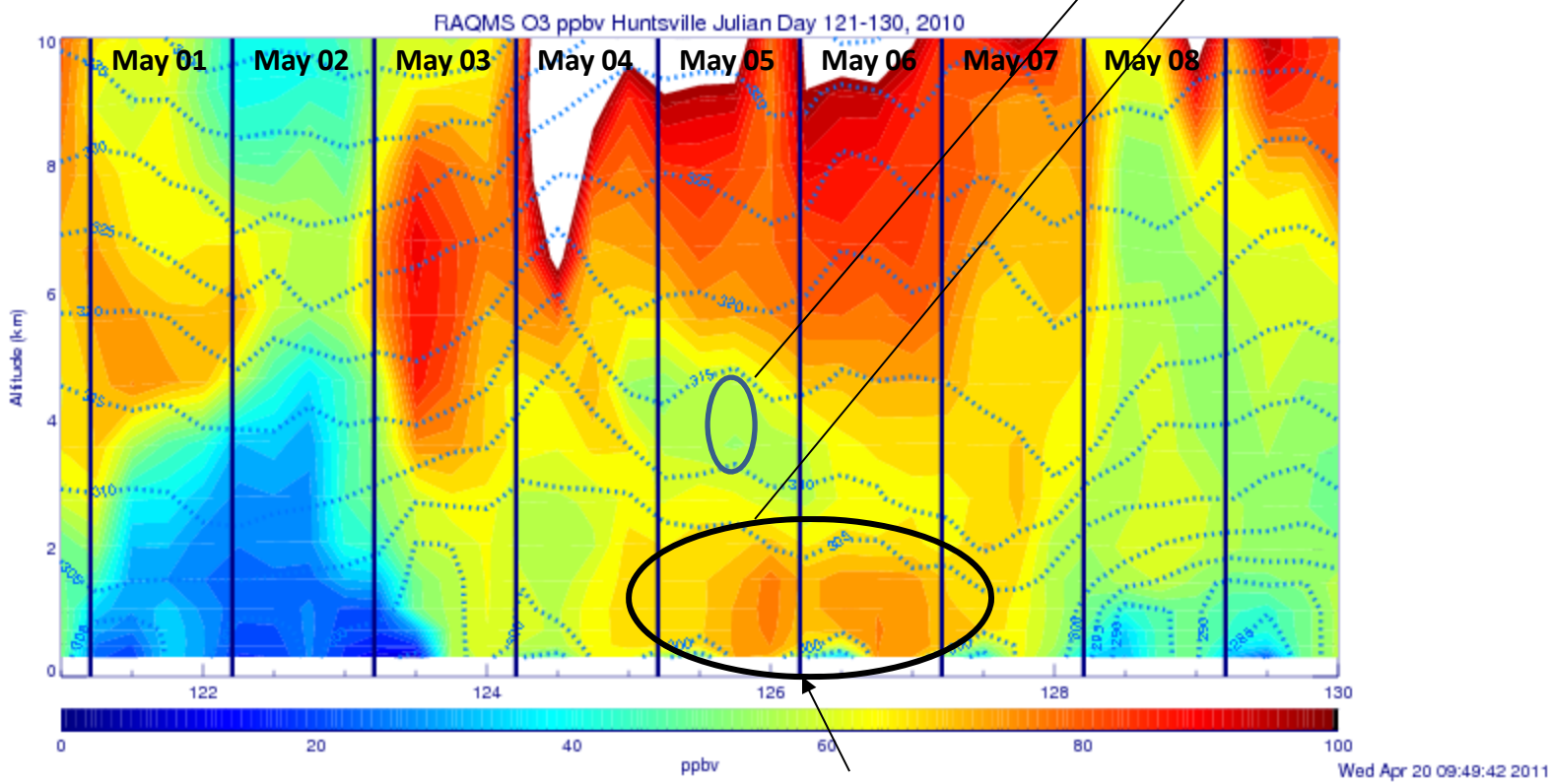

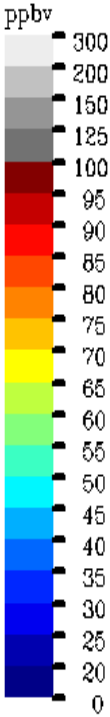

O3 AQ event

RAQMS is in good agreement with Huntsville Lidar above ~3km

under estimates low level ozone enhancement

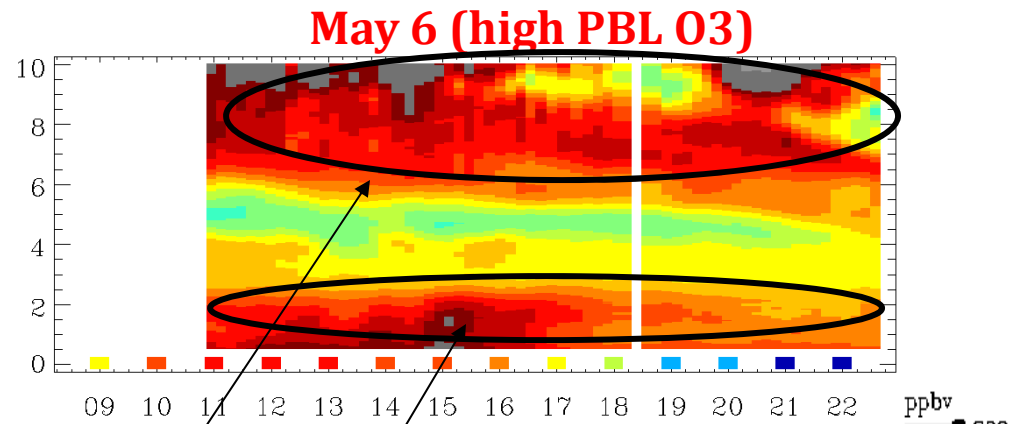

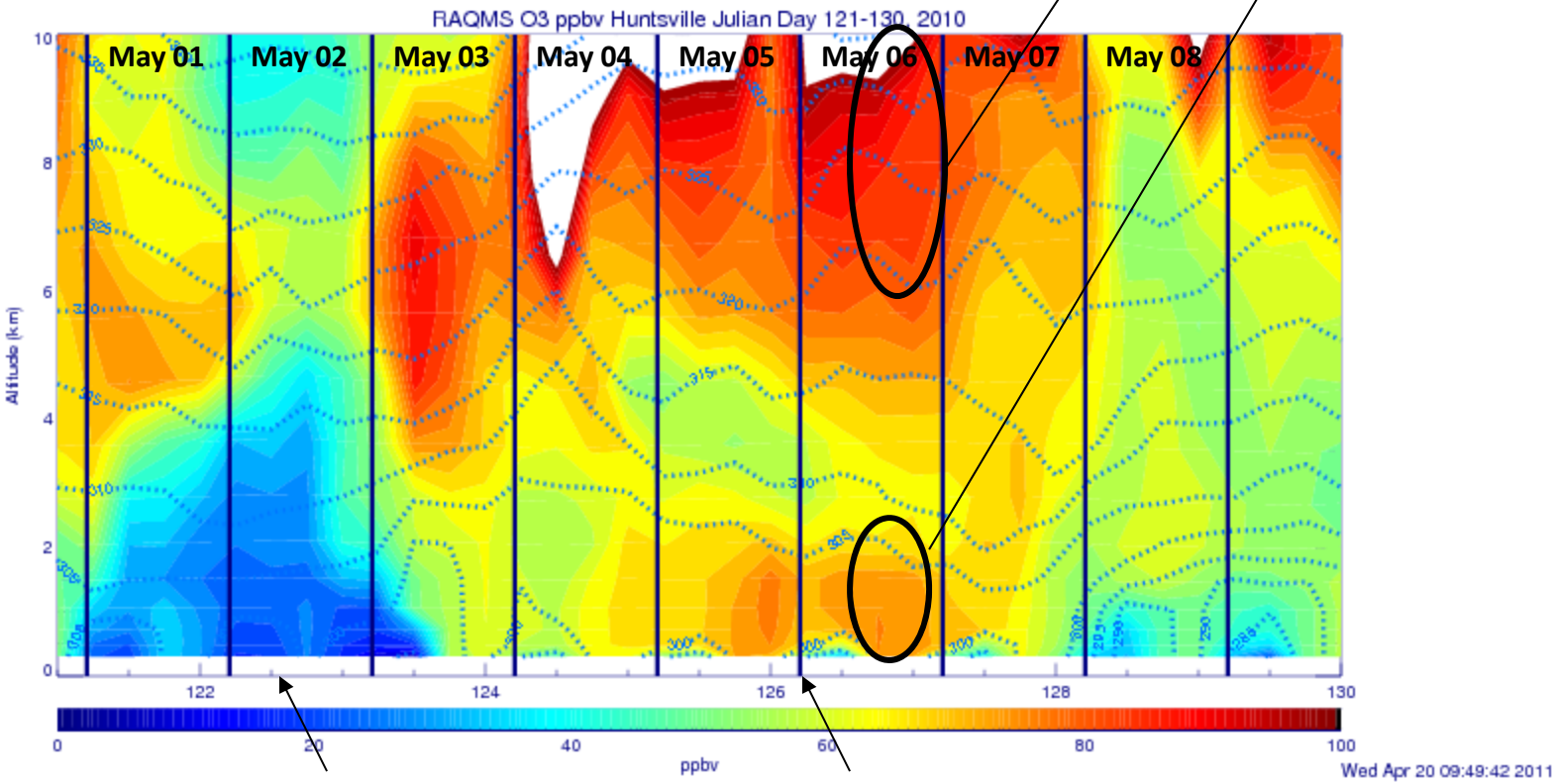

Saharan dust event

O3 AQ event

RAQMS shows diffuse free
Tropospheric ozone

Does not resolve thin filaments observed
By lidar

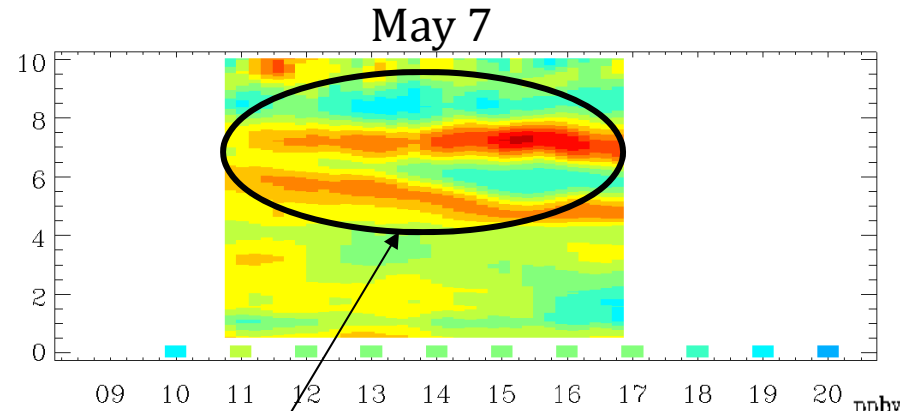

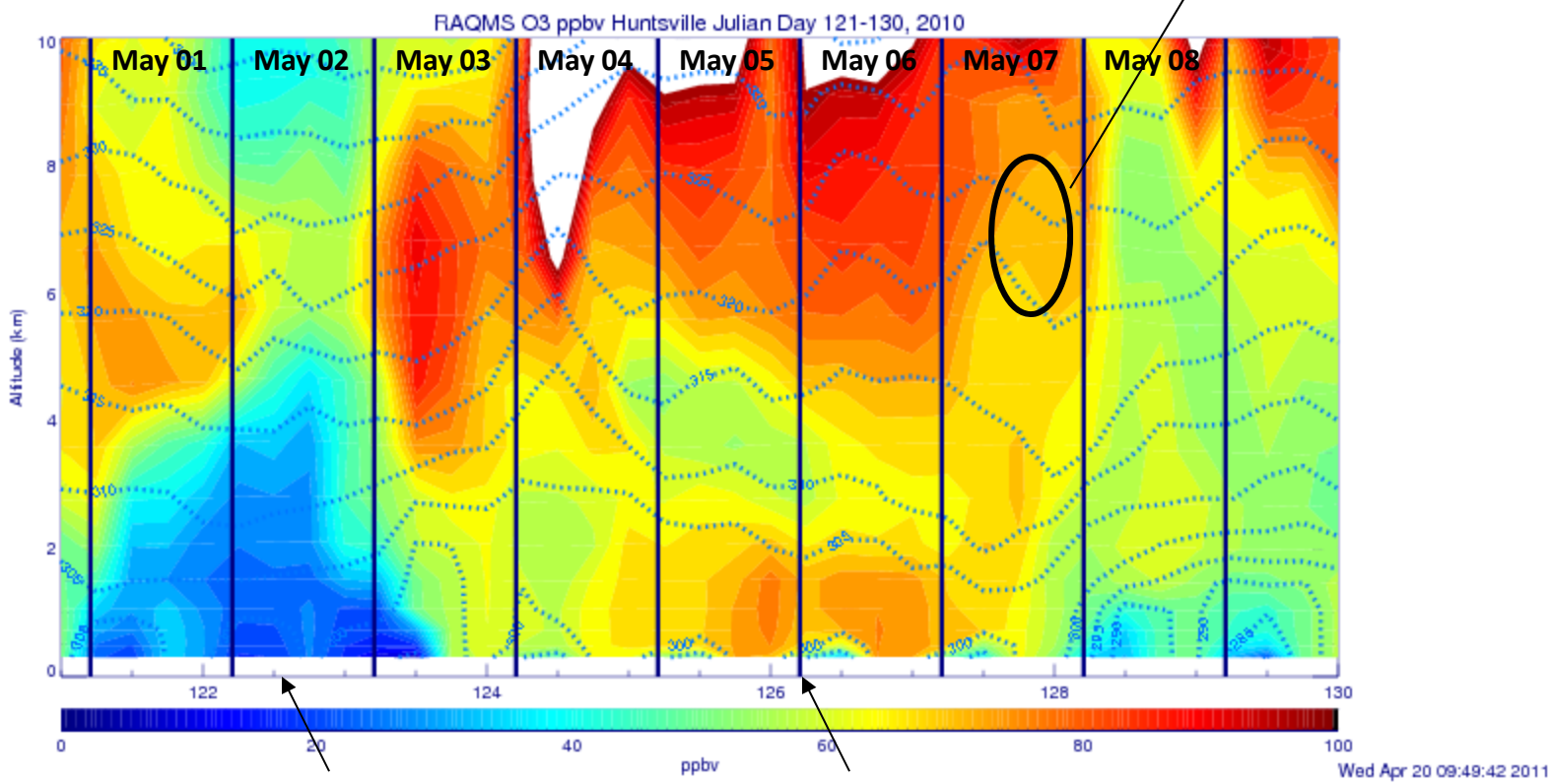

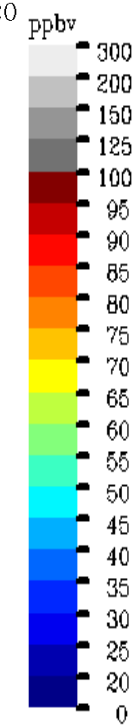

Saharan dust event

O3 AQ event

Nocturnal ozone enhancement associated with low-level jet

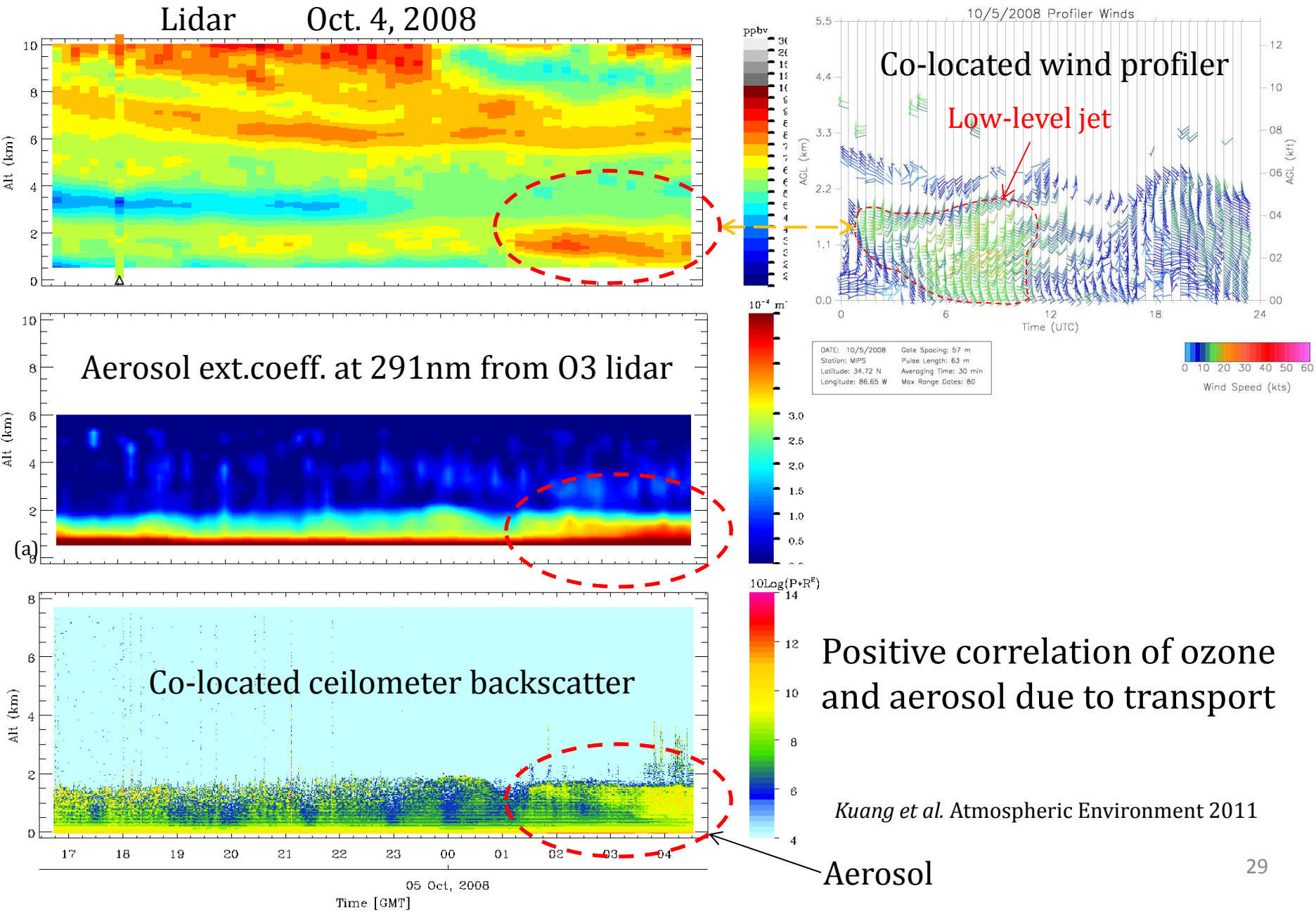

Positive correlation of ozone and aerosol due to transport

Kuang et al. Atmospheric Environment 2011

Higher increasing rate of the surface O3 before 10AM on Oct. 5 due to the low-level transport on the previous day

Surface O3 and convective boundary layer height

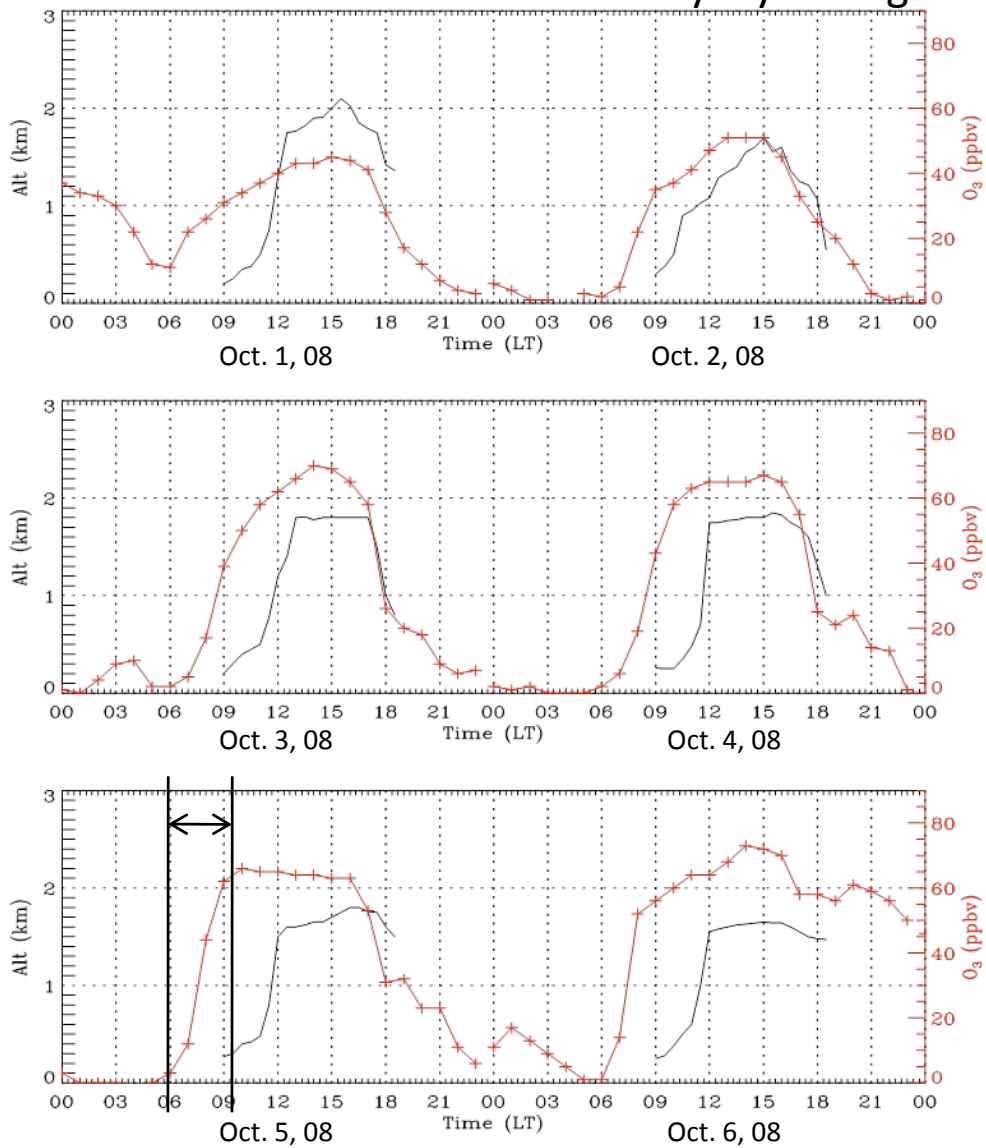

Oct. 4 O3 DIAL measurement

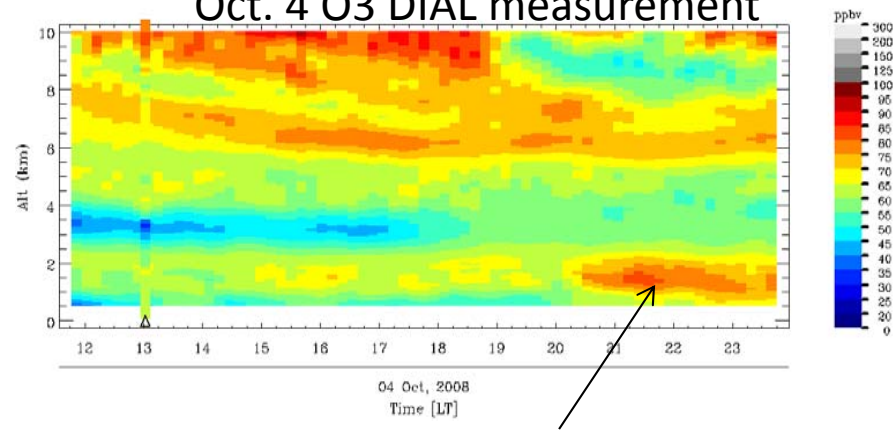

Due to southerly transport

Hourly surface-ozone measurement by EPA Huntsville station at airport road (http://www.airnow.gov) and the CBL height derived from the UAHuntsville 915MHz profiler measurement

High-resolution PBL lidar observation suggests both UV and Vis radiances required to capture significant PBL signal for satellite

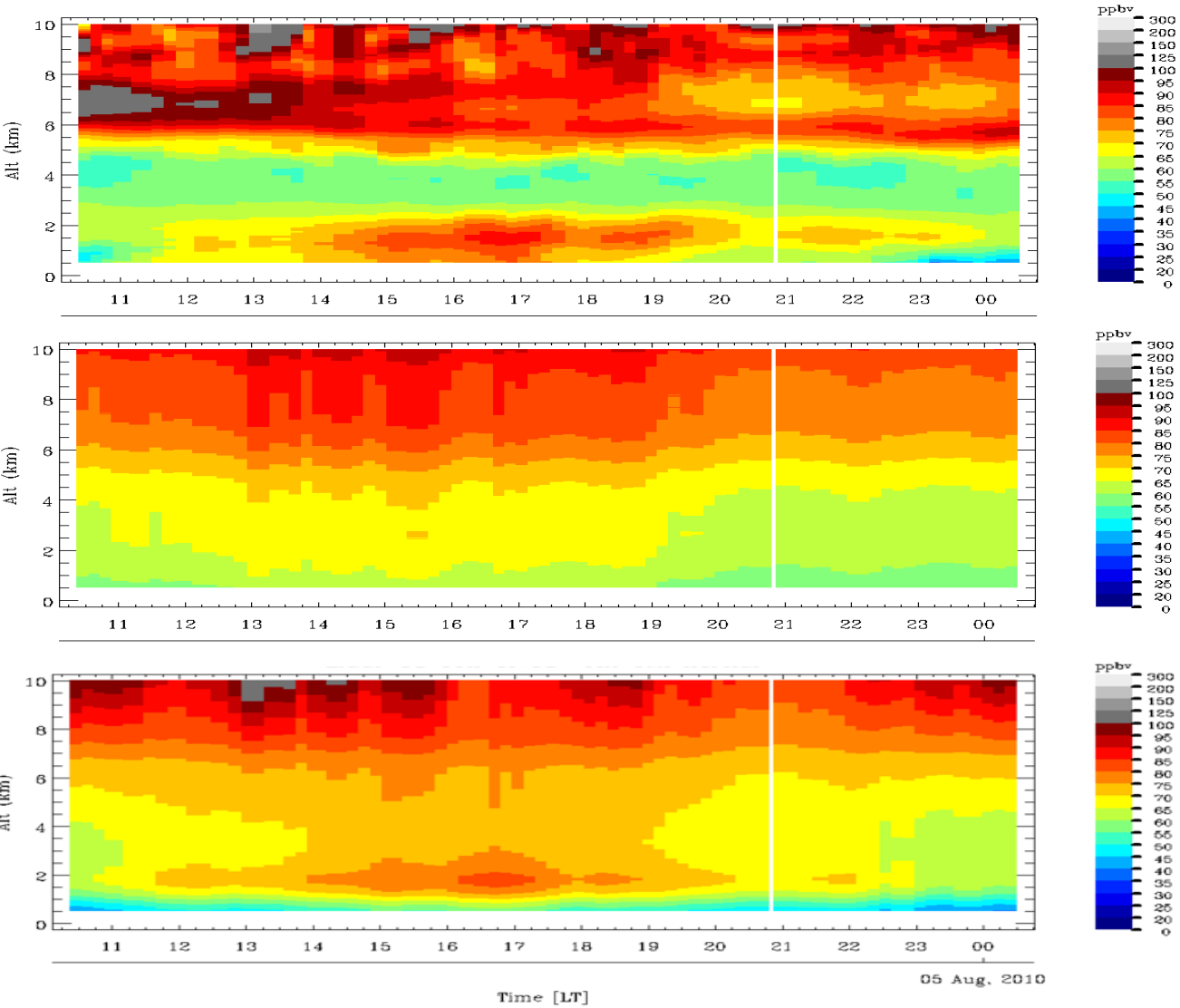

Huntsville lidar observation on Aug. 4, 2010

Lidar obs. convolved with OMI UV averaging kernel----unable to capture the highly variable ozone structure in PBL

Lidar obs. Convolved with OMI UV-Vis averaging kernel----Captures the PBL ozone structure. X. Liu et al.

10. O3 laminae detection

Fine structure in the temporal variations of layer attributes can be quantified by Wavelet and Gradient methods from Lidar observations.

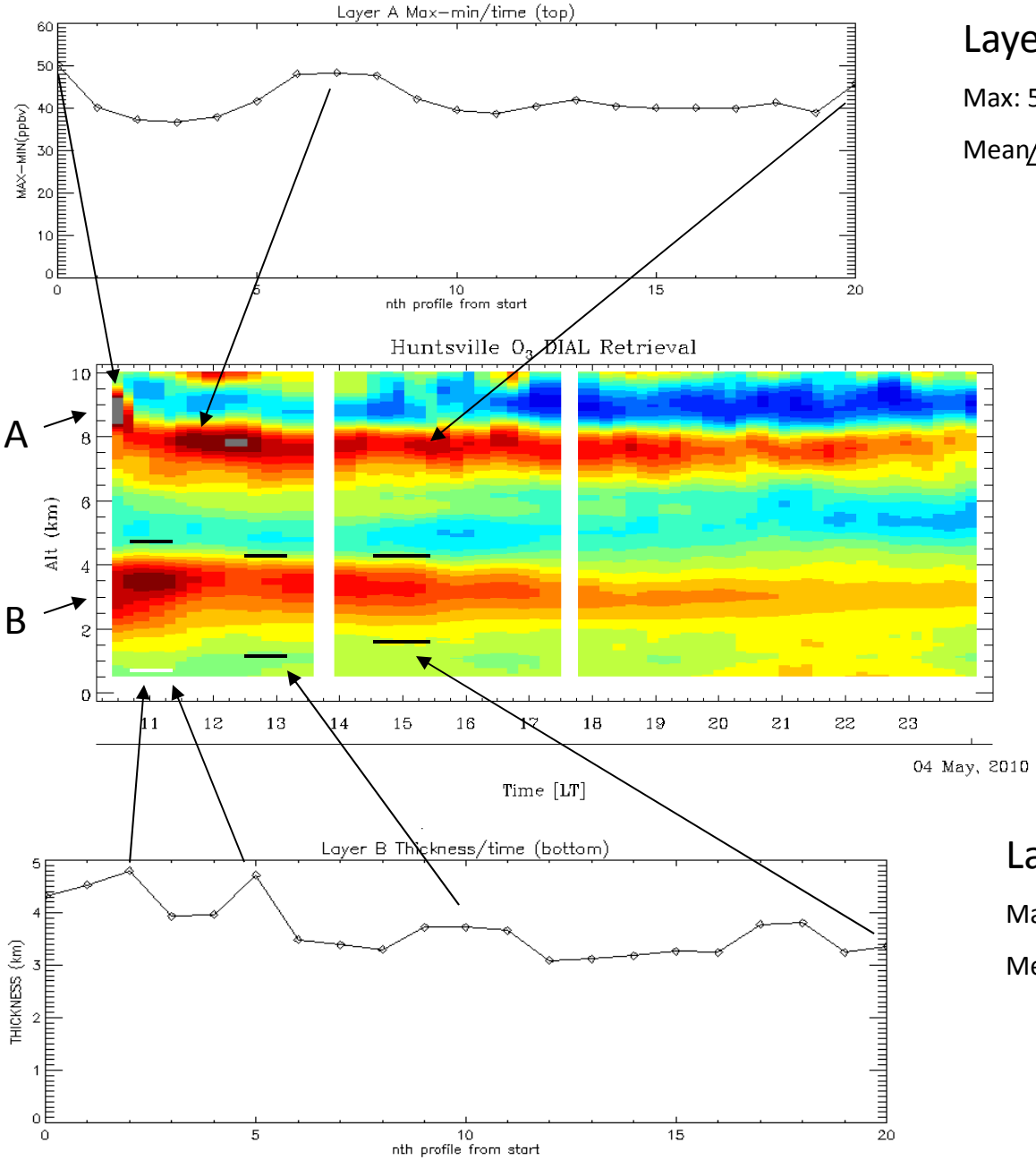

Layer A Max-Min

Max: 50.1 ppbv Min: 36.6 ppbv

Mean Δ max-min : 2.5 ppbv / 10min

+7.9 ppbv / 10min

-2.4 ppbv / 10min

- Temporal variability from other layer attributes can be similarly quantified.
- For example: O3 peak altitude, mixing ratio at peak.

Layer B Thickness

Max: 4.8 km Min: 3.0 km

Mean Δ Thickness: 0.3 km /10min

+0.9 km /10min

-0.3 km /10min

33

Ozone in the free troposphere is not correlated with surface ozone

Seasonal correlation of surface w/ ozone aloft

$$R^2 = \frac{SS_{\mathrm{reg}}}{SS_{\mathrm{tot}}}.$$

Huntsville 1999-2010 Ozonesonde Data

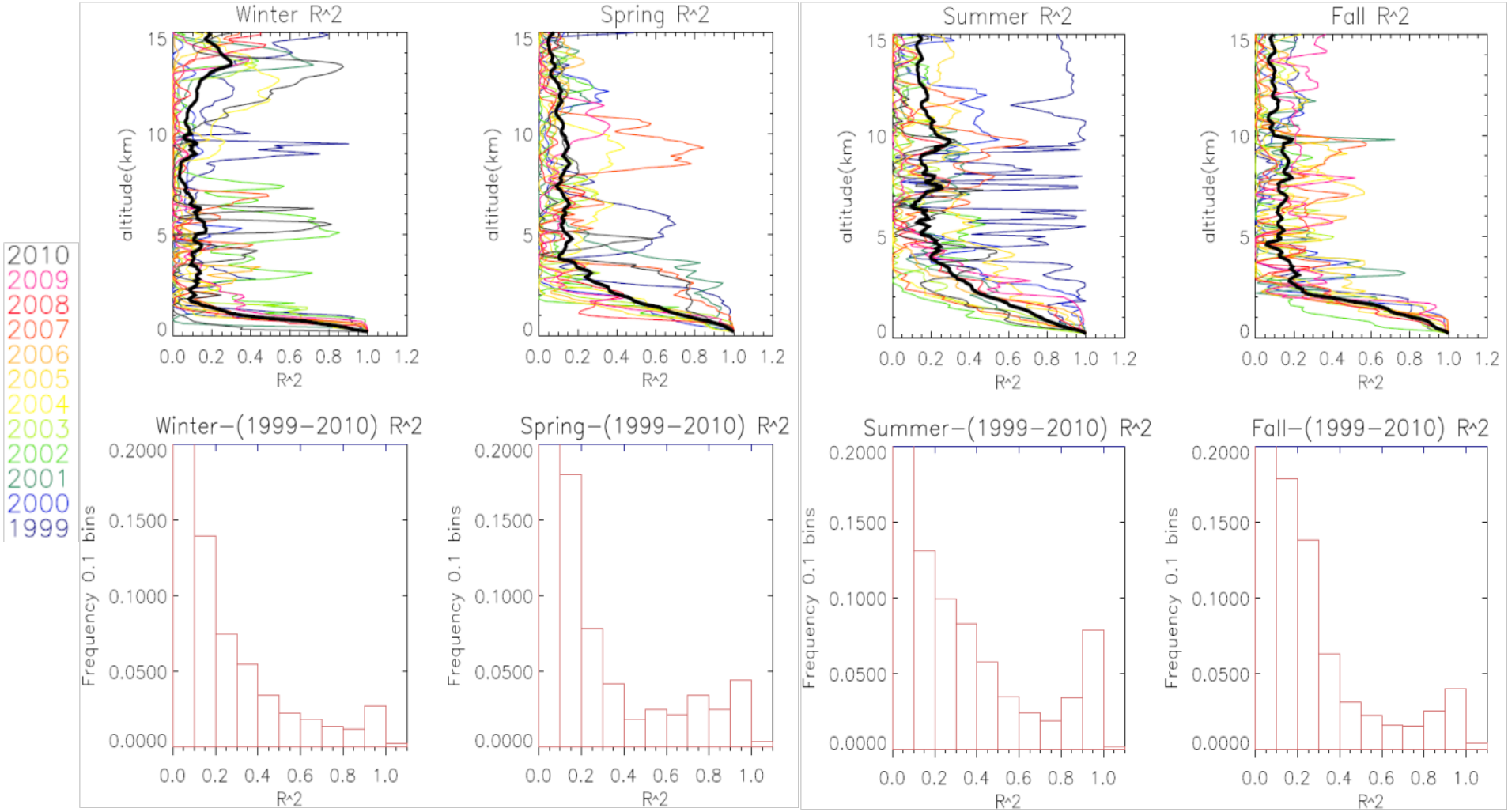

P(R^2>0.5)= 10% 15% 19%

12%

Laminar structures cause anomalous behavior in correlations

Huntsville Lidar Data

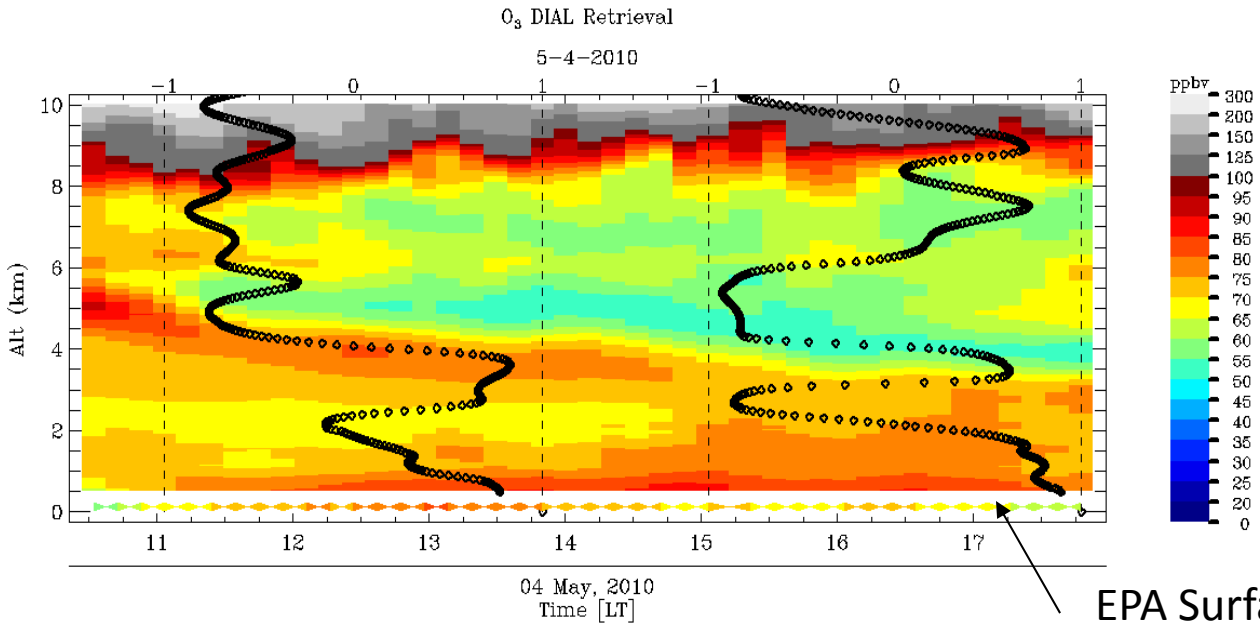

EPA Surface Data

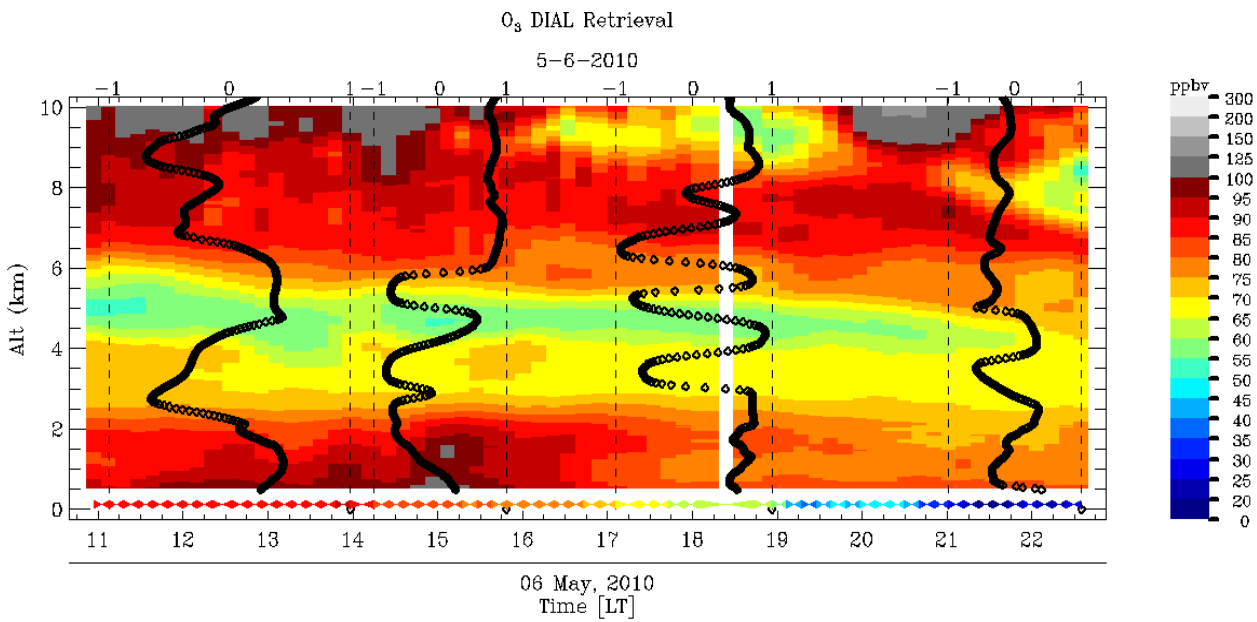

Correlation Lengths

Definition: the altitude over which R^2 decreases from 1 to 0.5.

•Each line is a regression through the correlations of at least 0.5.

•Correlations >0.5 above the first occurrence of a statistically insignificant value (<0.5) are not considered.

Conclusion:

•Measurements of ozone above correlation length carries no info about surface ozone.

Corollary: To determine surface ozone concentration, a measurement must contain info from within the correlation length.

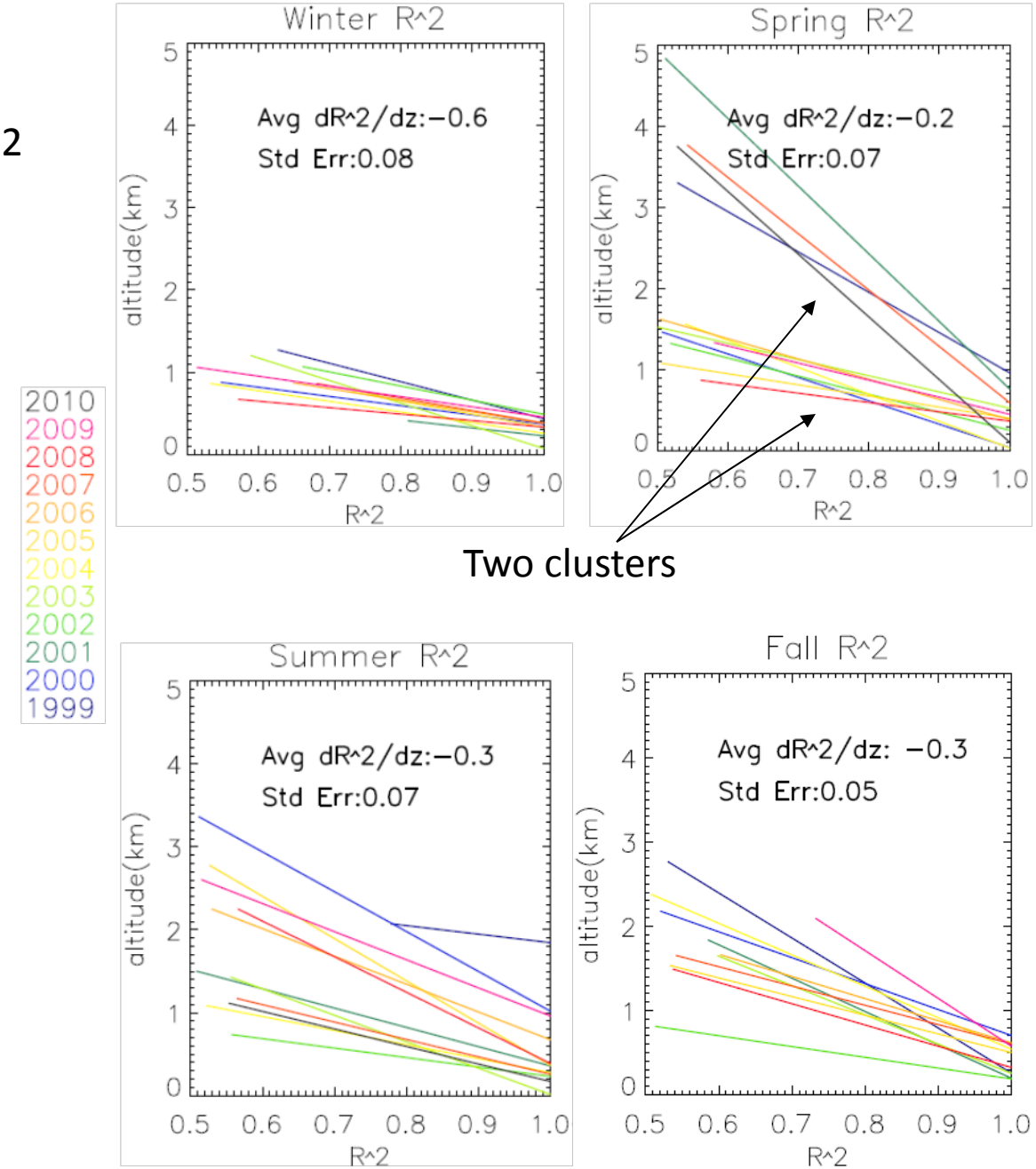

11. Micro-scale horizontal variability

27/8/2011

UAHuntsville Campus Ozone

Measured with ozonesonde

@ 12:30 P.M.

50 to 10 ppbv over ~1000 ft.

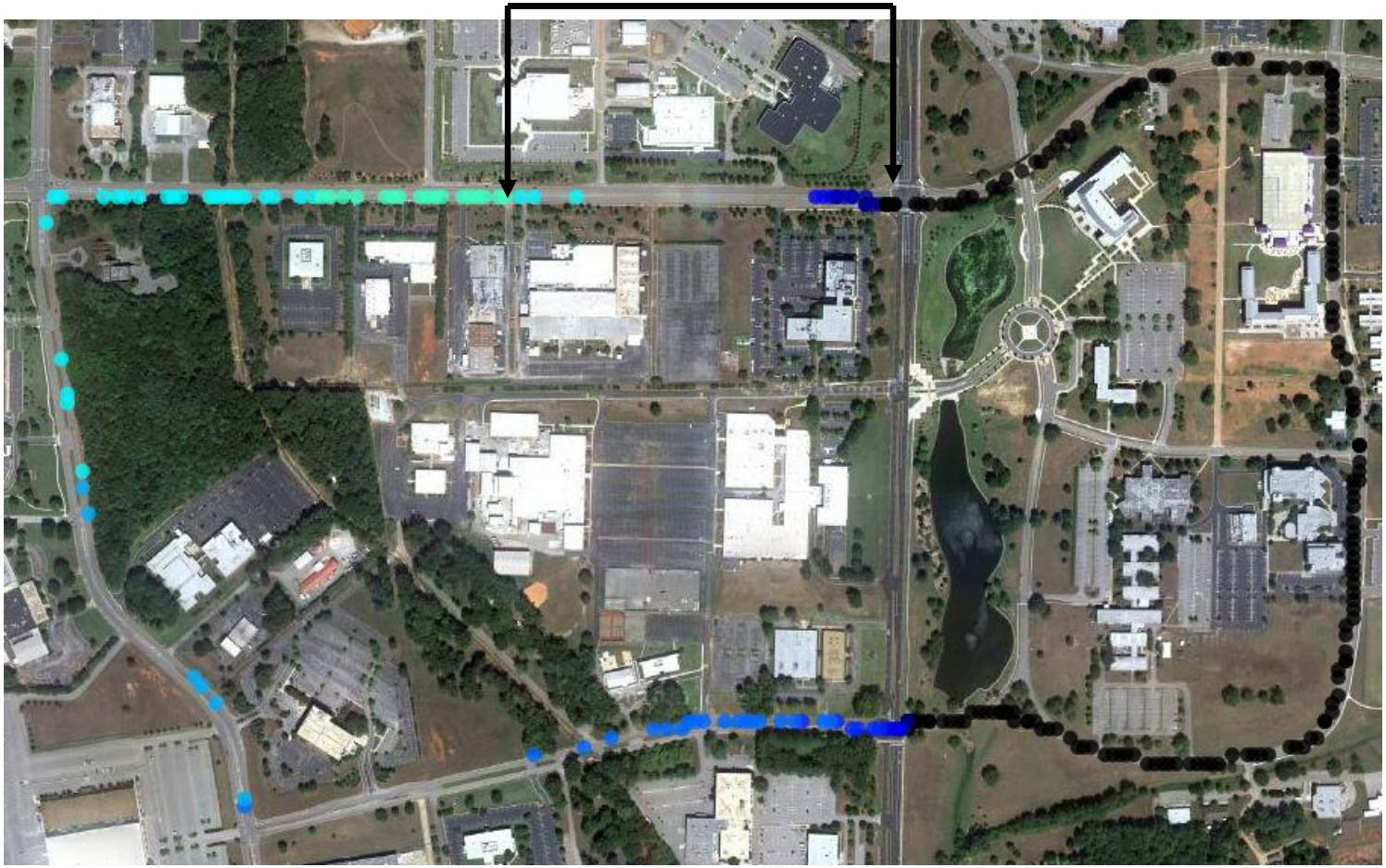

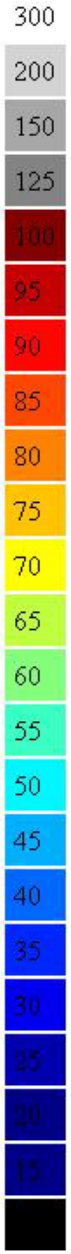

12. Ozone Variation 0-150 m above the Surface

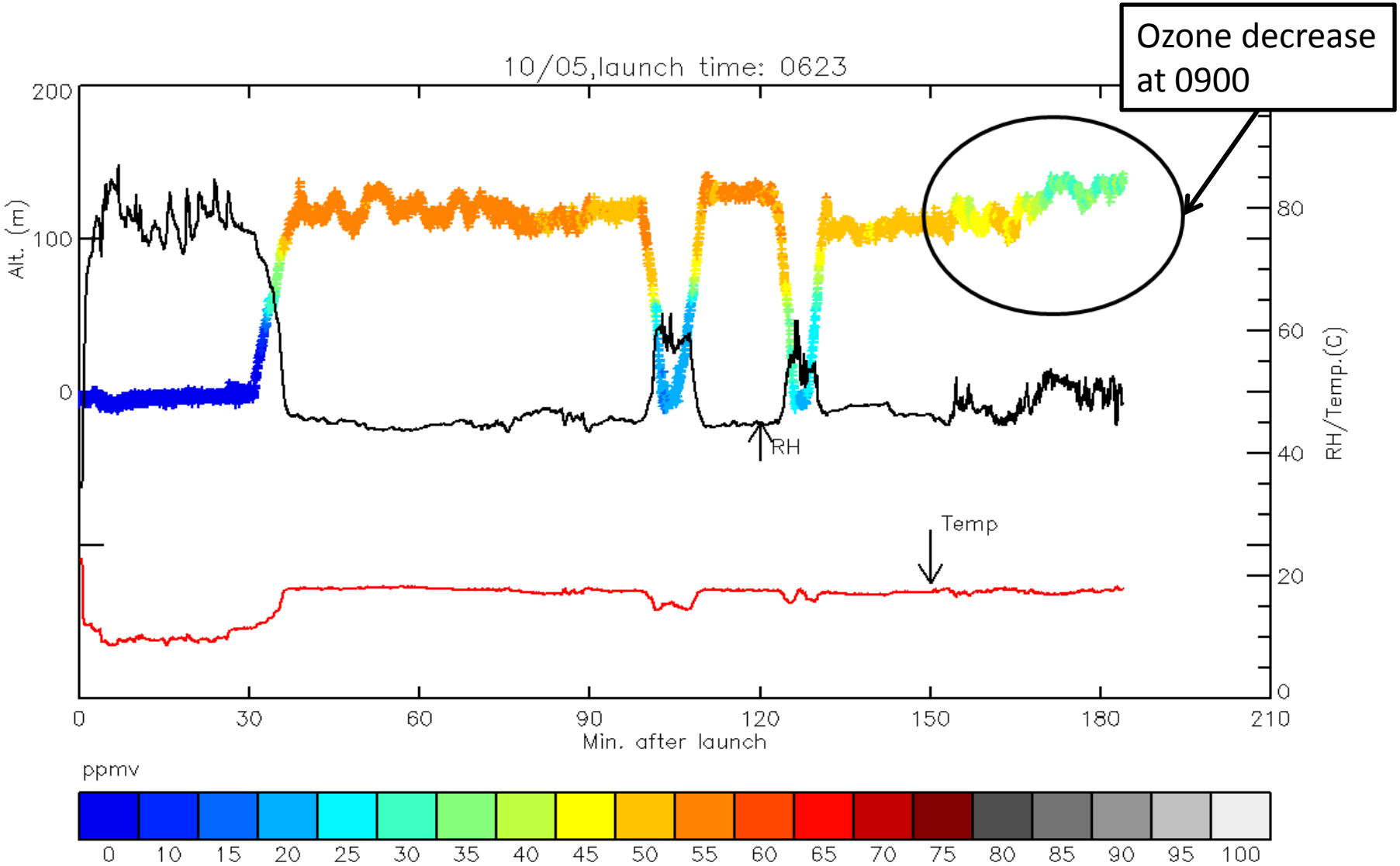

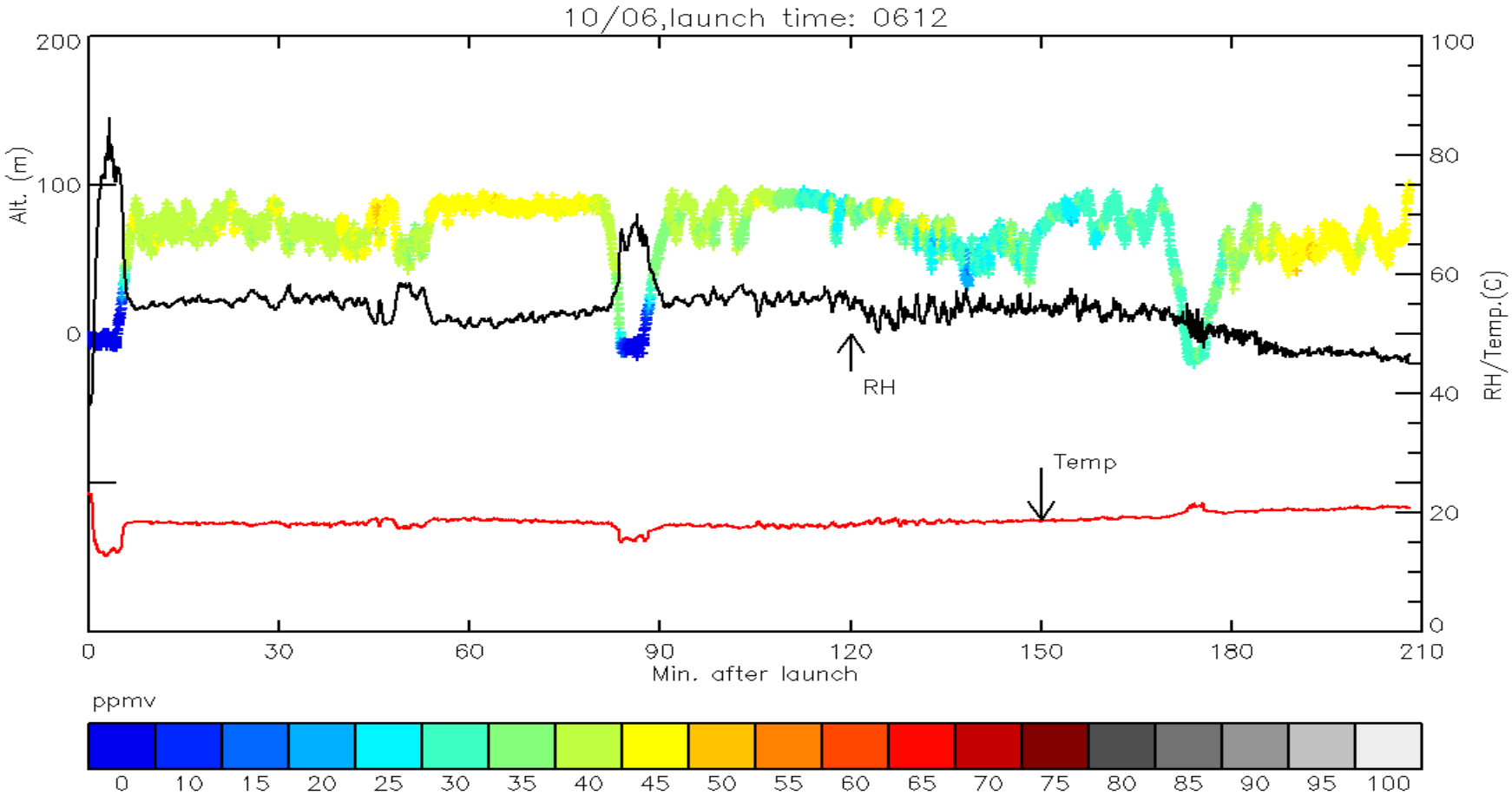

- Complex dynamical and chemical processes control the ozone in the near-surface layer.
- Ozone has strong vertical gradient at near-surface layer
- Water vapor is reverse proportional to ozone mixing ratio
- Temperature has insignificant impacts on ozone production near surface
- Need more experiments to study the ozone variation at near-surface layer.

13. O3 Lidar Network

Science Investigations Addressed by an AQ Lidar Network

1. Significantly complements satellite measurements by providing high spatial/temporal resolution measurements of atmospheric aerosols and ozone in the PBL and Free Troposphere.
2. Use these high-resolution ozone and aerosol observations to improve the processes in air-quality forecast and diagnostic models.
3. Improve our understanding of the relationship between ozone and aerosols aloft and surface ozone and PM values.< Szykman/AE, Fairlie 09 or 10, Thompson et al., 2008 ACP, Morris et al. 2010 AE>, (e.g., HSV-ATL).
4. Discover new structures and processes at the PBL/FT boundary, especially in the diurnal variation of that interface.
5. Exploit synergy with DISCOVER AQ, thermodynamic profilers, MOZAIC/IAGOS, other networks.
6. Advance our understanding of STE processes and their effect on surface ozone.
7. Explore the vertical distribution of NO2.

Lidar locations at the early stage

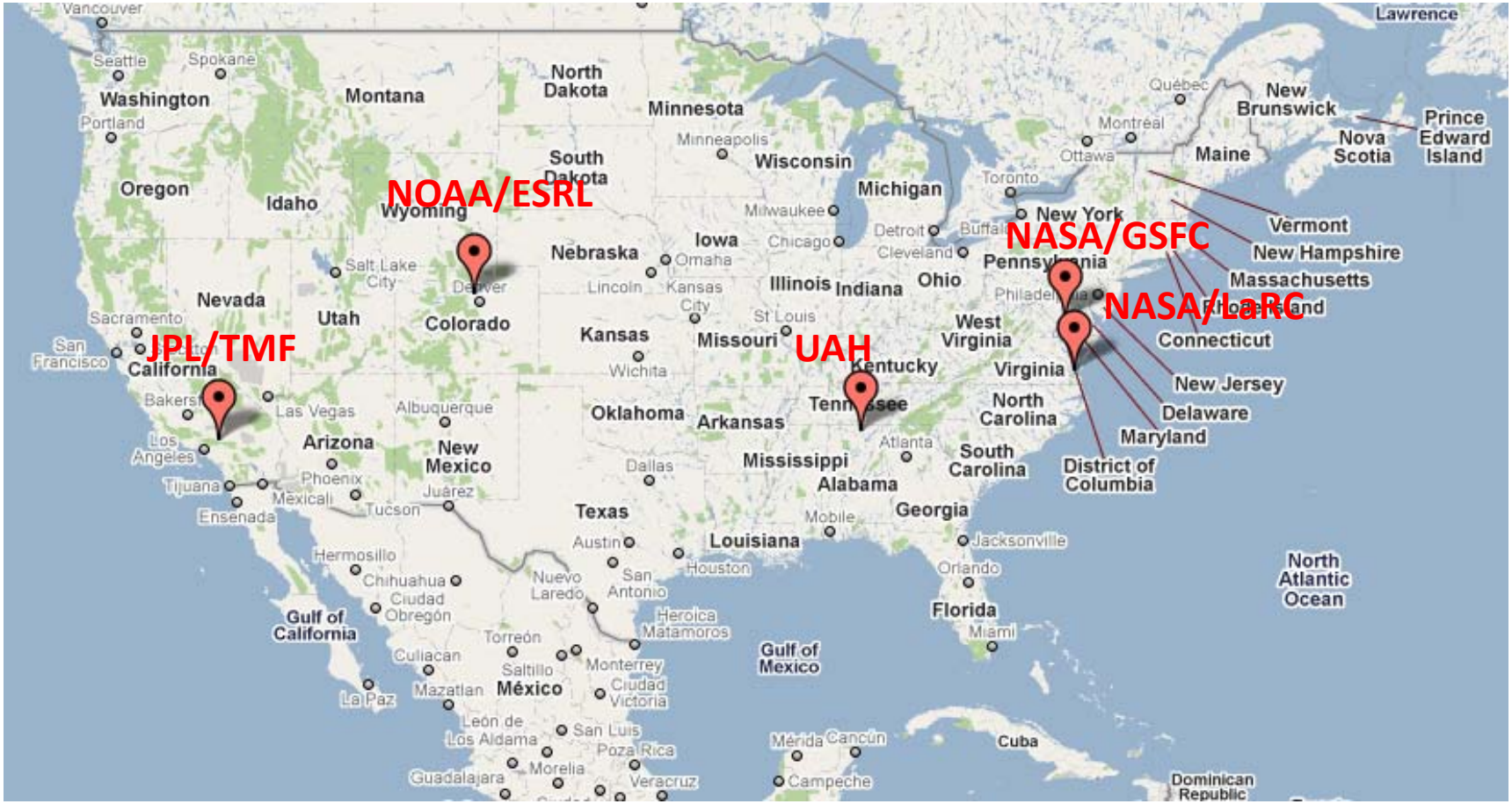

14. Future plan

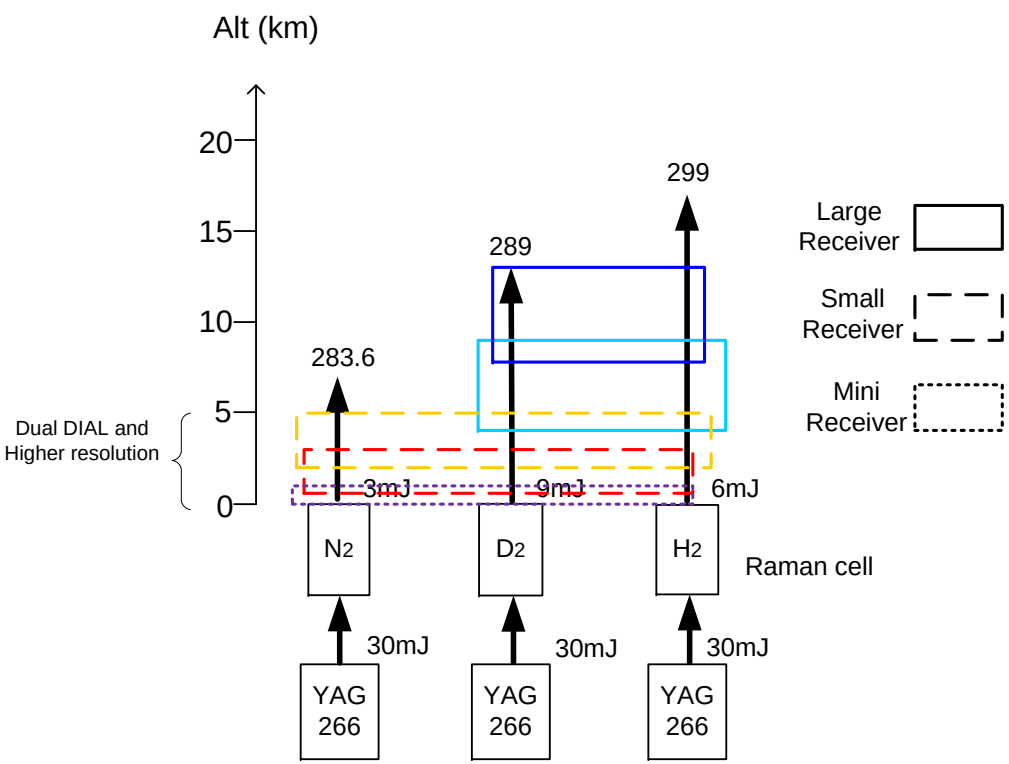

Schematic diagram of the future transmitters, wavelength pairs, and their measurement ranges. Different colors refer to the different PMT channels.

1. Replace the current 2-λ (285-291) transmitter with a 3- λ (284-289-299) system for applying dual-DIAL retrieval technique to remove aerosol interference and also extending the observations to tropopause
2. Add a mini receiver channel to reduce the lowest measurement altitude to ~100m from the current 500m

Diagram of the future receiving system
- 3 receiver channels covering 0.1-15km

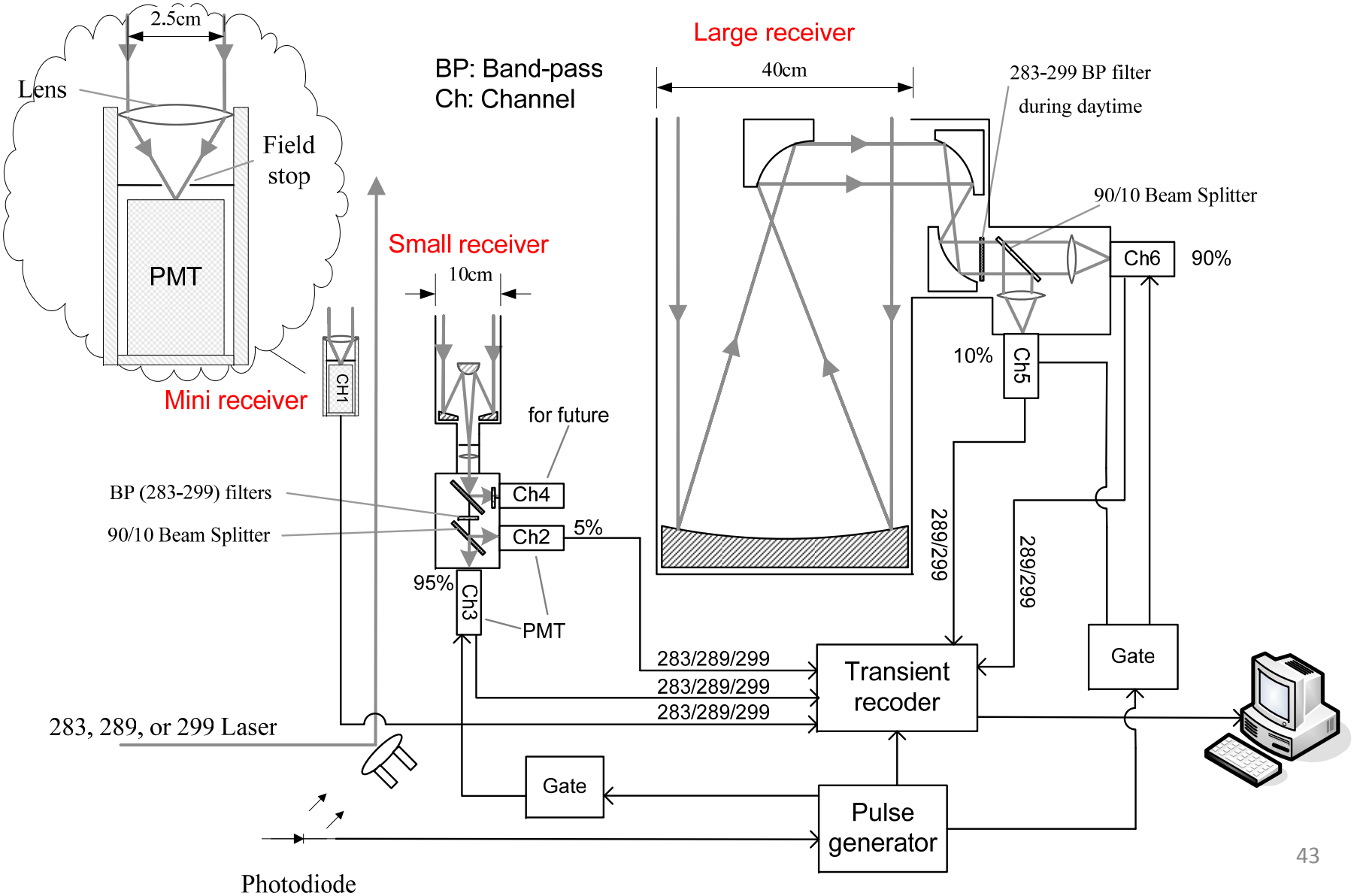

15. Summary

- Using measured ozone as initial and boundary conditions significantly improves model representation of mean vertical distributions.
- Free-tropospheric and nocturnal boundary layer laminae are frequently not well represented in regional models.
- UAHuntsville has developed a tropospheric ozone lidar system that provides high-resolution data for air-quality studies, model validation, and future GEO-CAPE mission. The future plan is to extend the observation down to the near the surface.
- We have developed a ozone laminar detection algorithm to characterize the ozone layers.
- The ozone lidar network will provide complementary lidar data for model and satellite, especially in the PBL.